People's Democratic Republic of Algeria

Ministry of Higher Education and Scientific Research

University of 20 Août 1955 Skikda
Faculty of Sciences
Department of Chemistry

Thesis

Submitted to the Department of Chemistry of

the Requirement for PhD Degree (LMD) in Chemistry

Specialty: Materials chemistry

Presented by

GRINE DJIHAD

Elaboration, functionalization and characterisation of modified titanium oxide thin films for antibacterial performance.

Presented publicly on: June 02nd 2024

Jury composed of :

Chiha Mahdi	Full Professor	President	University of Skikda.
Akkari Hocine	Full Professor	Supervisor	University of Batna-2.
Hassani Salim	Research Director	Co-supervisor	CDTA.
Chettah Abd Elhak	Full Professor	Examiner	University of Skikda.
Ayache Rachid	Full Professor	Examiner	University of Batna-2.
Lekoui Fouaz	MRA	Invited	CDTA.

2023/2024

République Algérienne Démocratique et Populaire

Ministère de l'enseignement supérieur et de la recherche scientifique

Université 20 Août 1955 Skikda

Faculté des Sciences

Département de Chimie

Thèse

Soumis au Département de Chimie

Pour l'obtention du diplôme de Doctorat (LMD) en Chimie

Spécialité : Chimie des matériaux

Présenté par :

GRINE DJIHAD

Elaboration, fonctionnalisation et caractérisation de couches minces d'oxyde de titanes modifiés pour des performances antibactériennes.

Soutenue le : 02/06/2024

Devant le jury :

Chiha Mahdi	Professeur	Président	Université de Skikda.
Akkari Hocine	Professeur	Directeur de thèse	Université de Batna-2.
Hassani Salim	Directeur de recherche	Co-directeur de thèse	CDTA.
Chettah Abd Elhak	Professeur	Examinateur	Université de Skikda.
Ayache Rachid	Professeur	Examinateur	Université de Batna-2.
Lekoui Fouaz	MRA	Invité	CDTA.

2023/2024

***I** dedicate this modest work to my dear parents Mr. Grine Abdelhamid and Mrs. Zeghbib Ouarda for their everlasting love and support. Our dream finally comes true. To the best maternal uncle in the whole world, Zeghbib Ali for his encouragements and support all the time, to my dear husband, Tazir Sabri for his never-ending love, patience, and motivation throughout my study. To my lovely kid Mouhamed Anes. To my sweet sisters Amira and Amina, to my grandparents and all member of my family for their continuous love and support that enabled me to achieve my goals. Finally, to all my friends and colleagues...*

Djihad

ACKNOWLEDGEMENTS

First of all, I am deeply grateful to Allah for blessing me health, patience, creativity, and the ability to complete this work. It has been a great honor to have the opportunity to live this scientific and life experience during these years, which has taught me a lot.

I would like to offer my complements to my supervisor Professor Akkari Houcine and my co-supervisor Professor Hassani Salim for their interest and guidance during my PhD studies.

I am pleased to express my sincere thanks to my reading committee members for their time to read my thesis and attend my defense meeting.

I wish to express my great gratitude to Doctor Lekoui Fouaz for his help, encouragements, and constructive feedback to continue my research towards the right direction.

I would also like to extend my sincere appreciation to Doctor Mekhalif Salim for his support and guidance throughout the duration of my PhD study and experimental work.

I would like to express my deepest gratitude to Professor Paloma Fernández from Complutense University of Madrid for her kindness, guidance and help in performing various crucial tasks and experiments associated to this work.

I would like to express my sincere gratitude to Professor Haladja Sabrina for her advice and guidance during my PhD study.

My other thanks are directed to the staff of Center for Development of Advanced Technologies (CDTA) Division of Ionized Media & Laser, Algiers for providing the deposition coating method for my samples elaboration.

From the bottom of my heart, I would like to express my gratitude to Dr. Bouzrara Moufida for her support and help in performing antibacterial tests, I

am also thankful to all the staff of microbiology laboratory at Abderrezak Bouhara Hospital, Skikda for their kindness, friendly environment and support, special thanks to my friends Ahlem at laboratory of El-Amel Skikda and Dr. Kihal Raouf at Aboulkasem clinic for their help and kind wishes.

I am pleased to express my warmest gratitude to all the administrative staff and teachers in the Department of Chemistry in particular and in the Faculty of Science in general specially Doctor Guedah Doria for her guidance and kidness with all PhD students.

I am deeply grateful to all my friends and colleagues at university of 20 Août 1955 Skikda for their support and encouragements, and I also thank my friend Pablo from the University of Granada, Spain **(**within the framework of the ERASMUS grant).

I would like to express my heartfelt gratitude to my marvelous family, who always believed in me and supported me to the end especially my great mother for her unconditional support, endless love and everlasting contributions into my life, I am deeply thankful to my dear father, my wonderful sisters Amira and Amina, my beloved husband and my darling uncle Ali for their never-ending love, immense patient, motivation, encouragements, financial and emotional support in every situation. I am very thankful to God for having them around me.

Finally, I would like to express my appreciation to everyone who helped me from near or far in my doctoral study, even with a kind word, without forgetting my special and huge thanks to every member of my big family, young and old for their support, love and prayers which keep me going. Words cannot describe my love and gratitude to them.

Table of Contents

Chapter II: Thin film deposition methods and antibacterial coatings

Chapter III: Materials and methods

Chapter IV: Results and discussion

List of Figures

List of Tables

List of Abbreviations

2D	Two dimensional
3D	Three dimensional
Å	Angstroms
A	Absorbance
Ag-TiO_2-Fe	Silver- titanium dioxide- iron
ALD	Atomic laser deposition
APCVD	Atmospheric-pressure chemical vapor deposition
ATCC	American type culture collection
BK	Bacteria killing percentage
CB	Conduction band
CDTA	Centre de développement des technologies avancées
CVD	Chemical vapor deposition
CFU	Colony forming units
℃	Degree celsius
D	Crystallite size
DC	Direct current
DNA	Deoxyribonucleic acid
Eg	Band gap energy
EDX	Energy dispersive x-rays
E. coli	*Escherichia coli*
eV	Electron volts
EVD	Electrochemical vapor deposition
$e^- – h^+$	Electron-hole
FCC	Face centred cubic
FVDM	Frank van der merwe
FWHM	Full width at half maximum
hν	Photon energy
HPCVD	Hybrid physical chemical vapor deposition
I_0	Incident intensity
I	Transmitted intensity

JCPDS	Joint Committee on Powder Diffraction Standards
LECVD	Laser-enhanced chemical vapor deposition
LPCVD	Low-pressure chemical vapor deposition
LPS	Lipopolysaccharides
LIBs	Lithium-ion batteries
MOCVD	Metal organic chemical vapor deposition
MWCNTs	Multi-walled carbon nanotubes
n	Refractive index
Nps	Nanoparticles
PACVD	Plasma-assisted chemical vapor deposition
P.aeruginosa	*Pseudomonas aeruginosa*
PECVD	Plasma-enhanced chemical vapor deposition
PGN	Peptidoglycan
PL	Photoluminescence
PLD	Pulsed laser deposition
PE	Phosphatidyl-ethanolcholine
PVD	Physical vapor deposition
RF	Radio frequency
RNA	Ribonucleic acid
ROS	Reactive oxygen species
S. aureus	*Staphylococcus aureus*
SEM	Scanning electron microscopy
SERS	Surface-enhanced Raman spectra
SK	Stranski-krastanov
SPA	Surface plasmon absorption
T	Transmission
UV	Ultraviolet

UV–vis–NIR	Ultraviolet-visible-near infrared
VB	Valance band
VW	Volmer-weber
wt%	Weight percent
XRD	X-ray diffraction
ν_0	Frequency
λ	Wave length

Introduction

Introduction

Microbial contamination and transmission remain a global public health concern, with the potential to cause infections and outbreaks in various settings. To address this issue, the development of surfaces and coatings as antimicrobial materials has emerged as a promising solution. These antibacterial coatings can be applied to a wide array of surfaces, from medical equipment and high-touch surfaces in public spaces to food packaging and drinking water systems, By integrating these coatings into our environment, we can create self-sanitizing and pathogen-resistant surfaces that can reduce the risk of infections and the spread of microorganisms. This innovation holds immense potential in environmental and healthcare settings, the ongoing research and development of antimicrobial coatings offer a proactive and effective strategy to combat bacterial contamination on a global scale, contributing to a safer and healthier world **[1-3]**.

Several materials with intrinsic antibacterial properties have been used in fabrication of antibacterial films. Recently, titanium dioxide is a versatile material known for its dual functionality as a photocatalyst and an antibacterial agent **[4]**. In photocatalysis, TiO_2 demonstrates exceptional effectiveness, particularly in the anatase form, when exposed to ultraviolet (UV) light. Under UV irradiation, TiO_2 generates electron-hole pairs, leading to the production of reactive oxygen species (ROS), which play a pivotal role in deactivating microbial organisms, including bacteria, viruses, and cancer cells. This photocatalytic activity has found diverse applications in air and wastewater purification, as well as various biomedical applications **[5]**.

Additionally, TiO_2 film has garnered attention as an antibacterial material, owing to its ability to hinder microbial adhesion and inhibit biofilm formation **[4, 5]**, when TiO_2 incorporated into surfaces and coatings, it acts as a potent antibacterial agent due to its unique properties such as strong oxidizing power **[6]**, nontoxicity **[7]**, and good chemical stability **[8]**, which makes it a promising candidate for addressing both environmental and healthcare challenges through its photocatalytic and antibacterial activity.

The modification of titanium dioxide (TiO_2) photocatalyst by transition and noble metals has emerged as a promising strategy to enhance their antibacterial activity. Transition metals like iron (Fe), cobalt (Co), and noble metals such as silver (Ag) and platinum (Pt) have been extensively explored for their ability to enhance TiO_2 performance

as an antibacterial agent. By incorporating these metals into the TiO_2 matrix, researchers aim to reduce the recombination rate of electron–hole pairs, a crucial factor affecting photocatalytic efficiency **[9, 10]**. This modification results in improved photocatalytic activity and extends antibacterial capabilities of TiO_2 beyond its native UV irradiation range, making it effective under visible light as well **[10]**.

Silver, in particular, is of significant interest due to its low toxicity, exceptional catalytic and antibacterial properties. The presence of these metals in TiO_2 not only expands its antibacterial potential but also introduces synergistic effects that lead to a more robust antibacterial response. As a result, modified TiO_2 materials with these metals exhibit increased efficacy in deactivating microbial organisms, ranging from bacteria to viruses, making them a vital component in various antimicrobial applications **[11, 12]**.

Furthermore, iron has shown its unique potential as an antibacterial agent in recent research, this transition metal has gained attention for its role in disrupting bacterial growth and pathogenicity **[13]**. Modifying TiO_2 with Fe under UV light may considerably enhance its antibacterial activity **[7, 14, 15]**, pure and modified TiO_2-based coatings are fabricated using numerous film deposition techniques **[16]** such as electron beam evaporation **[17]**, sputtering **[18]**, chemical vapor deposition **[19]**, spray pyrolysis **[20]**, and sol–gel method **[21]**.

The objectives of this research are to create novel and effective antibacterial coating based on the Ag-TiO_2-Fe system. In this study, we investigated the effects of incorporating Fe, and Ag on the structural, morphological, optical, and luminescent properties of TiO_2 film, as well as their relation with antibacterial activity. Additionally, we examined the antibacterial efficiency of pure and composite thin films with varying Ag content against *Escherichia coli* bacteria in both dark and under UV light.

The present thesis consists of four chapters:

In the first chapter, we present a comprehensive literature review that delves into the fundamentals, properties, and applications of the materials utilized in the creation of our thin films, including TiO_2, TiO_2-Fe, and Ag-TiO_2-Fe.

The second chapter focuses on the basics of thin films (or coatings) by presenting the different methods for fabricating thin films, the principle of antibacterial coatings, their classification, and their mechanisms of action.

The third chapter highlights the methodology of the study; including materials, experimental procedures employed for the preparation of our thin films and the different characterization techniques carried out in this work.

The fourth chapter is devoted to the interpretation and discussion of the results obtained in this study.

Finally, the general conclusion in which we highlight the main results of this work, as well as the future perspectives proposed for this work.

References

[1] G. E. Yılmaz, I. Göktürk, M. Ovezova, F. Yılmaz, S. Kılıç, and A. Denizli, "Antimicrobial Nanomaterials: A Review," *Hygiene*, vol. 3, no. 3, pp. 269–290, Jul. 2023, doi: 10.3390/hygiene3030020.

[2] M. Cloutier, D. Mantovani, and F. Rosei, "Antibacterial Coatings: Challenges, Perspectives, and Opportunities," *Trends in Biotechnology*, vol. 33, no. 11, pp. 637–652, Nov. 2015, doi: 10.1016/j.tibtech.2015.09.002.

[3] I. D. Akhidime *et al.*, "The antimicrobial effect of metal substrates on food pathogens," *Food and Bioproducts Processing*, vol. 113, pp. 68–76, Jan. 2019, doi: 10.1016/j.fbp.2018.09.003.

[4] I. De Pasquale *et al.*, "Photocatalytic TiO2-Based Nanostructured Materials for Microbial Inactivation," *Catalysts*, vol. 10, no. 12, p. 1382, Nov. 2020, doi: 10.3390/catal10121382.

[5] L. V. Suárez Murillo, A. Schärer, S. Giannakis, S. Rtimi, and C. Pulgarín, "Iron-coated polymer films with high antibacterial activity under indoor and outdoor light, prepared by different facile pre-treatment and deposition methods," *Applied Catalysis B: Environmental*, vol. 243, pp. 161–174, Apr. 2019, doi: 10.1016/j.apcatb.2018.10.035.

[6] B. Yu, K. M. Leung, Q. Guo, W. M. Lau, and J. Yang, "Synthesis of Ag–TiO_2 composite nano thin film for antimicrobial application," *Nanotechnology*, vol. 22, no. 11, p. 115603, Mar. 2011, doi: 10.1088/0957-4484/22/11/115603.

[7] S. M. H. AL-Jawad, A. A. Taha, and M. M. Salim, "Synthesis and characterization of pure and Fe doped TiO2 thin films for antimicrobial activity," *Optik*, vol. 142, pp. 42–53, Aug. 2017, doi: 10.1016/j.ijleo.2017.05.048.

[8] S. Veziroglu *et al.*, "Ag Nanoparticles Decorated TiO_2 Thin Films with Enhanced Photocatalytic Activity," *Phys. Status Solidi A*, vol. 216, no. 14, p. 1800898, Jul. 2019, doi: 10.1002/pssa.201800898.

[9] J. Moma and J. Baloyi, "Modified Titanium Dioxide for Photocatalytic Applications," in *Photocatalysts - Applications and Attributes*, S. Bahadar Khan and K. Akhtar, Eds., IntechOpen, 2019. doi: 10.5772/intechopen.79374.

[10] D. Jiang *et al.*, "A Review on Metal Ions Modified TiO2 for Photocatalytic Degradation of Organic Pollutants," *Catalysts*, vol. 11, no. 9, p. 1039, Aug. 2021, doi: 10.3390/catal11091039.

[11] S. Anees Ahmad *et al.*, "Bactericidal activity of silver nanoparticles: A mechanistic review," *Materials Science for Energy Technologies*, vol. 3, pp. 756–769, 2020, doi: 10.1016/j.mset.2020.09.002.

[12] H. B. Dias, M. I. B. Bernardi, T. M. Bauab, A. C. Hernandes, and A. N. De Souza Rastelli, "Titanium dioxide and modified titanium dioxide by silver nanoparticles as an anti biofilm filler content for composite resins," *Dental Materials*, vol. 35, no. 2, pp. e36–e46, Feb. 2019, doi: 10.1016/j.dental.2018.11.002.

[13] C. Huang *et al.*, "Insights into the antibacterial mechanism of iron doped carbon dots," *Journal of Colloid and Interface Science*, vol. 645, pp. 933–942, Sep. 2023, doi: 10.1016/j.jcis.2023.04.149.

[14] S. Naghibi, S. Vahed, O. Torabi, A. Jamshidi, and M. H. Golabgir, "Exploring a new phenomenon in the bactericidal response of TiO2 thin films by Fe doping: Exerting the antimicrobial activity even after stoppage of illumination," *Applied Surface Science*, vol. 327, pp. 371–378, Feb. 2015, doi: 10.1016/j.apsusc.2014.11.162.

[15] C. C. Trapalis *et al.*, "TiO2(Fe3+) nanostructured thin films with antibacterial properties," *Thin Solid Films*, vol. 433, no. 1–2, pp. 186–190, Jun. 2003, doi: 10.1016/S0040-6090(03)00331-6.

[16] D. Grine, H. Akkari, P. Fernández, T. Mekhalif, S. Hassani, and F. Lekoui, "Synthesis, Characterization, and Antibacterial Activity of Ag–TiO2–Fe Composite Thin Films," *Phys. Status Solidi A*, vol. 219, no. 11, p. 2200036, Apr. 2022, doi: 10.1002/pssa.202200036.

[17] C. Garlisi and G. Palmisano, "Radiation-free superhydrophilic and antifogging properties of e-beam evaporated TiO 2 films on glass," *Applied Surface Science*, vol. 420, pp. 83–93, Oct. 2017, doi: 10.1016/j.apsusc.2017.05.077.

[18] M. Sreedhar, I. Neelakanta Reddy, Ch. V. Reddy, J. Shim, and J. Brijitta, "Highly photostable Zn-doped TiO2 thin film nanostructures for enhanced dye degradation deposited by sputtering method," *Materials Science in Semiconductor Processing*, vol. 85, pp. 113–121, Oct. 2018, doi: 10.1016/j.mssp.2018.06.005.

[19] A. M. Alotaibi *et al.*, "Chemical Vapor Deposition of Photocatalytically Active Pure Brookite TiO $_2$ Thin Films," *Chem. Mater.*, vol. 30, no. 4, pp. 1353–1361, Feb. 2018, doi: 10.1021/acs.chemmater.7b04944.

[20] T. C. Paul, J. Podder, and M. H. Babu, "Optical constants and dispersion energy parameters of Zn-doped TiO2 thin films prepared by spray pyrolysis technique,"

Surfaces and Interfaces, vol. 21, p. 100725, Dec. 2020, doi: 10.1016/j.surfin.2020.100725.

[21] A. Fouzia and B. Rabah, "The influence of doping lead and annealing temperature on grown of nanostructures of TiO2 thin films prepared by a sol-gel method," *Materials Science and Engineering: B*, vol. 265, p. 114982, Mar. 2021, doi: 10.1016/j.mseb.2020.114982.

ChapterI

Literature review

I.1 Introduction

This chapter provides the essential information on the materials used to produce the desired thin films, which include TiO_2, Ag, and Fe, with a description of their varied properties and uses. We also go over the modification methods of TiO_2 photocatalyst, followed by state of the art of modified TiO_2 thin films with Ag and Fe metals (Ag-TiO_2-Fe) and their antibacterial effectiveness and applications.

I.2 Titanium dioxide

Titanium dioxide with a chemical formula TiO_2 (titania) was first discovered in 1791 from mineral ilmenite, It has been commercially manufactured as white pigments in building since 1916 **[1]**. TiO_2 belongs to the family of transition metal oxides. It is a semiconductor material that can be synthesized in various forms, e.g. nanoparticles, thick/thin films etc. TiO_2 is a functional material that promises a wide range of new and various technological application fields due to its advantageous features **[2]**.

I.2.1 Titanium dioxide properties

Titanium dioxide (TiO_2) has become one of the most studied semiconductor materials. It has attracted the attention of many researchers in numerous domains due to its extraordinary properties such as chemical stability, inexpensive material with high refractive index, non-toxicity, large band gap, and biocompatibility, etc **[3- 5]**.

I.2.1.1 Crystalline structure

Titanium dioxide naturally occurs in three main crystalline polymorphs anatase, rutile, and brookite **[5, 6]**. Rutile and anatase have a tetragonal structure; it consists of TiO_6 octahedron chains, where each Ti^{4+} ion is surrounded by an octahedron of six O^{2-} ions. In the rutile structure, each octahedron is surrounded by ten close octahedrons; instead, in the anatase phase, each octahedron is in contact with eight neighbors. Brookite TiO_2 belongs to the orthorhombic crystal system. Its unit cell is more complicated; it is composed of 8 formula units of TiO_2 and is formed by edge-sharing TiO_6 octahedron. The three crystalline phases differ from each other by the arrangement and the distortion of the octahedron **[7- 9]**. The crystal structures of the unit cell of anatase, rutile and brookite phases are shown in **figure I.1**

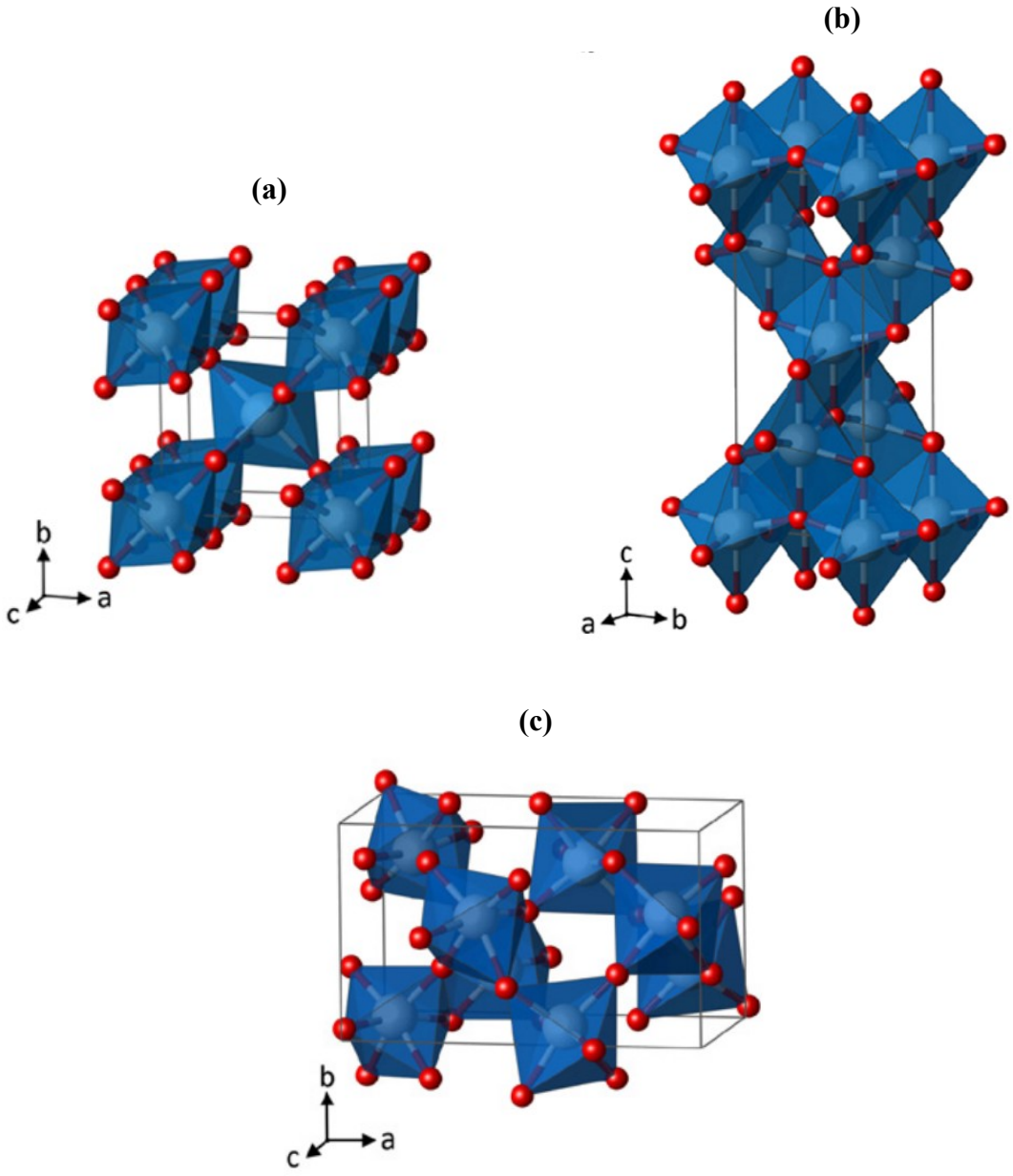

Figure I.1 Three different polymorphs of titanium dioxide (a) rutile phase, (b) anatase phase, and (c) brookite phase. (Ti (grey); O (red)), while the blue polyhedral shapes show the orientation in space of the TiO_6 octahedra **[10]**.

Among these structures, rutile is a thermodynamically stable phase, whereas anatase and brookite are metastable **[3]**. Annealing temperatures above 600 °C lead to an irreversible phase transformation from anatase to rutile **[11]** depending on particle size, ambient pressure, other factors, etc **[6, 8]**. Each crystalline form has practical applications, however, the anatase is the most studied and used phase in many applications due to its great

photocatalytic efficiency such as energy, environment, health and medicine, catalysts, etc **[12]**. Physical and structural properties of three main crystalline polymorphs of TiO_2 are summarized in **table I.1**

Table I.1 Comparison of the structural and physical data for rutile, anatase and brookite phases **[5, 9, 13, 14]**.

Chemical Formula	**TiO_2**		
Structure	**Rutile**	**Anatase**	**Brookite**
Molecular Weight ($g.mol^{-1}$)	79.88	79.88	79.88
Z	2	4	8
Crystal System	Tetragonal	Tetragonal	Orthorhombic
Space Group	P42/mnm	I41/amd	Pbca
Lattice constant (Å)	a=b= 4.5936 c= 2.9587	a=b= 3.784 c= 9.515	a= 9.184 b= 5.447 c= 5.154
Volume/ molecule ($Å^3$)	31.2160	34.061	32.172
Density [g/cm^3]	4.13	3.79	3.99
Band gap eV	3.0 ± 0.1	3.2 ±0.1	3.4 ± 0.1
Ti-O bond length (Å)	1.949 (4) 1.980 (2)	1.937(4) 1.965(2)	1.87–2.04
Refractive index	2.605–2.616, 2.890–2.903	2.561, 2.488	2.583, 2.700
Light absorption (nm)	<415	<390	–
Mohr's hardness	6.0 – 6.5	5.5 – 6.0	5.5 – 6.0
Bulk conductivity ($S\ cm^{-1}$)	$10^{-2} – 10^{-7}$	5×10^{-8}	3×10^{-7}
Static dielectric constant (ε_0 in MHz range)	173	48	–
Melting point °C	1855 °C	$A \xrightarrow{\sim 600\ ^\circ C} R$	$B \xrightarrow{\sim 700^\circ C} R$
Boiling point °C	2500– 3000	2500– 3000	2500– 3000
Solubility in H_2O	Insoluble	Insoluble	Insoluble
Solubility in HF	Insoluble	Soluble	Insoluble

I.2.1.2 Electronic and optical properties

The electronic structure of a semiconductor is a key factor in photocatalysis. Titanium dioxide is an n-type, it consists of a valance band (VB) and a conduction band (CB) levels, respectively. The energy difference between these two levels is known as the bandgap (E_g) **[8]**. The valence band (VB) of TiO_2 is formed by the hybridization of 2p orbitals of O_2 and 3d orbitals of Ti, while, the conduction band (CB) comprises pure 3d orbitals of Ti. When TiO_2 is exposed to UV light (photon energy $h\upsilon \geq E_g$), the UV light will be absorbed by TiO_2, and an electrons in the valence band are excited to the conduction band, leaving behind holes (h^+) in the valence band **[9, 15]**. The optical properties of semiconductors, such as the absorbance and emission, result from the excitonic transitions **[7]**. The anatase and rutile phases have band gap energy of 3.2 eV and 3.0 eV, respectively, that explains the transparency of TiO_2 when is pure and stoichiometric **[16]**. Oxygen and titanium vacancies in TiO_2 are intrinsic defects which influence the bandgap based on its phase of existence **[17]**. On the other hand, TiO_2 is unique because it combines a high refractive index ($n_{anatase} = 2.488$, $n_{rutile} = 2.609$) with a high degree of transparency in the visible region of the spectrum, which makes it very important in optical applications **[18]**. **Figure I.2** shows the light spectrum with TiO_2 action area.

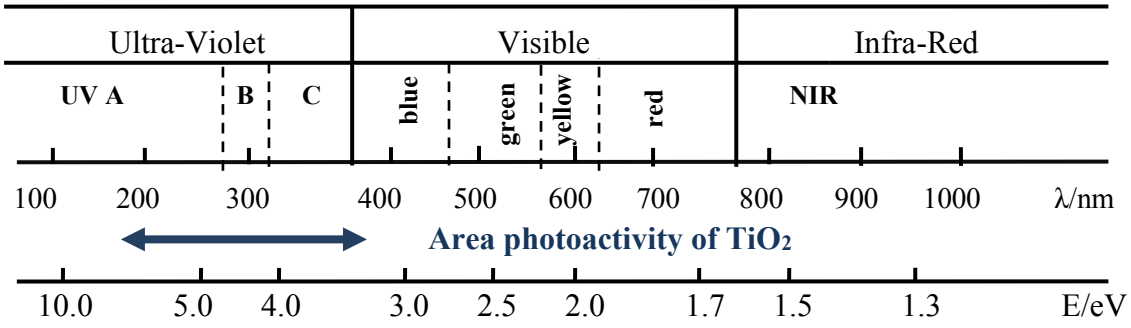

Figure I.2 Light spectrum with TiO_2 action area **[18]**.

I.2.2 TiO_2 as a Photocatalyst

Photocatalysis is an efficient process for the degradation of organic and inorganic contaminants through the generation of free radicals such as $HO^{\bullet}$ and $O_2^{\bullet -}$, this operation occurs through the use of light and semiconductors **[19]**. The photocatalytic properties of titanium dioxide (TiO_2) were discovered for the first time in 1972 by Fujishima and Honda **[20, 21]**. TiO_2 in the anatase form is considered as one of the most interesting photocatalyst,

and its photocatalytic performance strongly depends on the electronic band structure and band gap energy. The **table I.2** below provides a list of the most common photo-catalyst types with their energy bandgap **[8]**.

Table I.2 List of common photocatalyst and their bandgap energies at 0 K **[22]**.

Semiconductors	Bandgap energy (eV)	Drawbacks
TiO_2	3.03	Active in UV
ZnO	3.2	Unstable,corrodes, poisoning
ZnS	3.6	-
α-Fe_2O_3	2.8	-
WO_3	2.8	Expensive, production problems
$SrTiO_3$	3.2	-
CdS	2.42	Expensive, corrosion
CdSe	1.7	-
Si	1.17	-
Ge	0.74	Expensive

Photocatalysis using TiO_2 has been used in many applications including environmental problems **[3, 23]**. TiO_2 can produce free radicals on its surface when exposed to UV irradiation by promoting electrons to the conduction band **(figure I.3)**. The available hole which is very reactive and the electron can react with adsorbed water or oxygen to create free radicals and singlet oxygen, the contaminants (organic compounds, microorganisms) will react with hydroxyl radicals and undergo mineralization reactions to produce CO_2 and H_2O **[20]**. This process requires low energy requirements and relatively low cost **[19]**. The reaction mechanisms are widely known and can be resumed by (equations I.1-6) **[3, 24]**:

$$TiO_2 \xrightarrow{h\upsilon} e^-_{CB} + h^+_{VB} \quad \text{(eq.1)}$$

$$H_2O + h^+_{VB} \rightarrow {}^{\bullet}OH + H^+ \quad \text{(eq.2)}$$

$${}^{\bullet}OH + \text{pollutant} \rightarrow H_2O + CO_2 \quad \text{(eq.3)}$$

$$O_2 + e^-_{CB} \rightarrow O_2^{\bullet -} \quad \text{(eq.4)}$$

$$O_2^{\bullet -} + \text{pollutant} \rightarrow H_2O + CO_2 \quad \text{(eq.5)}$$

$$O_2^{\bullet -} + H^+ \rightarrow {}^{\bullet}OOH \quad \text{(eq.6)}$$

$$^{\bullet}OOH + pollutant \rightarrow H_2O_2 + CO_2 \quad \text{(eq.7)}$$

$$^{\bullet}OOH + {}^{\bullet}OOH \rightarrow H_2O_2 + CO_2 \quad \text{(eq.8)}$$

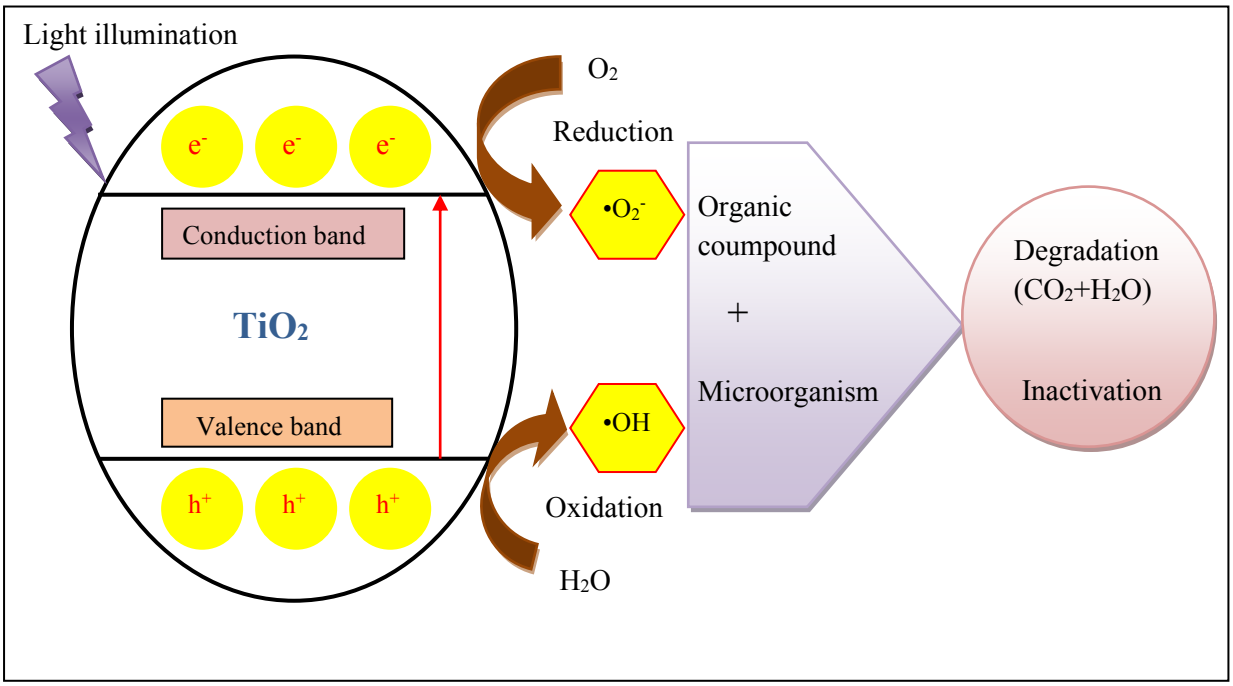

Figure I.3 Photocatalysis mechanism of TiO_2 **[25]**.

photocatalysis process is considered as significant disinfection approaches against a variety of pathogenic microorganisms **[26]**. Photocatalyst TiO_2 is one of the most potent antibacterial agents; it plays a vital role in minimizing environmental and health issues due to its a chemical stability, biocompatible and non-toxic. Recent studies have demonstrated that a human coronavirus (HCoV-NL63) was inactivated using TiO_2 nanoparticles coated film. TiO_2 is commonly used for disinfecting surfaces, water and air from bacteria, microbes and virus by producing highly reactive oxygen species (ROS), which damage microorganisms **[27, 28]**.

I.2.3 Applications of titanium dioxide

TiO_2 in its various forms (thin film, powder) has several advantages making it one of the most important and promising candidate in great domain of applications **[5] (figure I.4)** include solar cells, water purification, antibacterial coatings, sensing and biomedicine applications, etc. Some of these applications are detailed **[29]**.

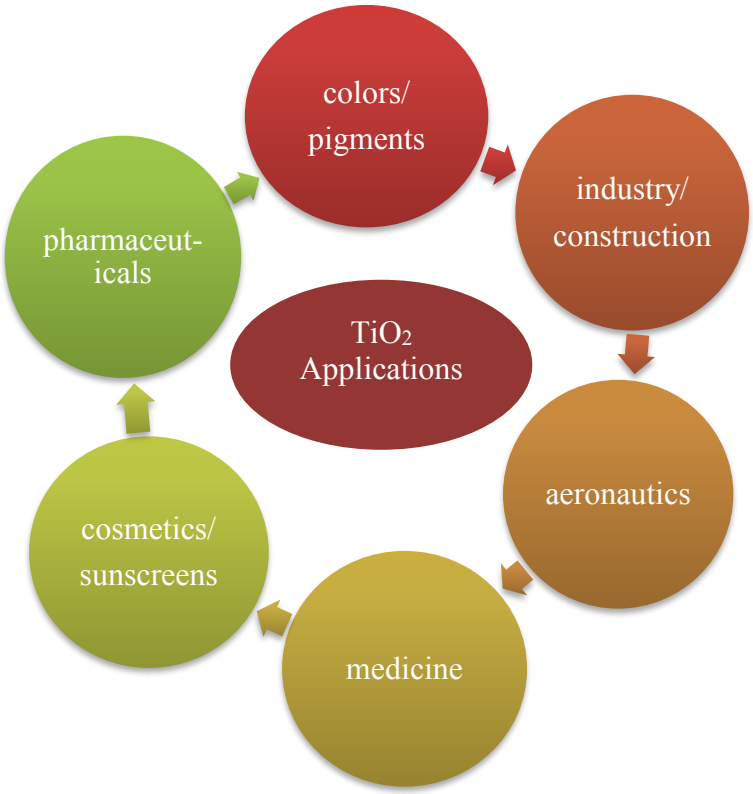

Figure I.4 Different application fields of TiO_2 **[30]**.

I.2.3.1 Application of TiO_2 in energy storage

Lithium-ion batteries are a type of rechargeable batteries and promising energy storage devices generally employed in electric vehicles and mobile electronics. TiO_2 has the potential to be a viable anode material for high-power lithium-ion batteries (LIBs) as replacement materials for carbonaceous anodes. TiO_2 offers many advantages such as charge transfer, high discharge voltage and excellent cycling stability making it good candidates in storage research **[12, 31]**.

I.2.3.2 Application of TiO_2 for environmental problems

Human activities are a major problem in polluting air and water resources. Nanostructured TiO_2 has raised a great deal of research interest due to its photocatalysis efficiency, which is an environmentally friendly technology. In recent years, nanostructured TiO_2 has been considered as the ideal choice for water-treatment. It is frequently used for decomposing organic pollutants and harmful microorganisms in water by producing free radicals ($HO^{\bullet}$) and superoxide ions ($O_2^{\bullet -}$), with strong oxidizing properties under UV light. This process improves water quality **[32, 33, 12]**.

I.2.3.3 Antibacterial applications of TiO_2

Various investigations have been reported on the use of TiO_2 in healthcare and biomedicine owing to its active role in damaging many harmful pathogens, such as bacteria, viruses, and fungi, which are found in the human body, water and on varied surfaces. TiO_2 in anatase form has higher photocatalytic and cytotoxic activity, it has been noticed as effective antibacterial agent, which has the ability to generate reactive oxygen species (ROS) such as $O_2^{\bullet -}$, $HO^{\bullet}$ and H_2O_2 during the photocatalysis process making TiO_2 as one of the preferred for antibacterial applications, including the photodynamic therapy for cancer treatment, water purification, self cleaning, air-conditioning filters, medical devices, orthopedic implants, sterilizing surfaces, etc **[8, 34, 35]**.

I.2.4 Modification of TiO_2 photocatalyst

The UV light activity and high electron – hole recombination rate are drawbacks that hinder practical application of TiO_2 in visible light and the photocatalytic efficacy, respectively. Many efforts have been performed to amend these difficulties. Modification of TiO_2 with various materials can enhance its photocatalytic efficiency and antibacterial performance. These modifications have been performed using many different strategies including metal and non-metals doping, codoping, fabrication of composites with other materials and immobilization of TiO_2 particles supported on different substrate materials **[36 – 38, 7]**.

I.2.4.1 Metal doping

Many studies have demonstrated that adding metal doping to the TiO_2 structure can improve the photocatalytic efficiency of TiO_2 in the visible light region by creating donor or acceptor levels in the band gap of semiconducting TiO_2 **(figure I.5)**. The visible light activity of semiconductor materials is influenced by the type of doping elements, the

doping amount, the doping method, the doping position (substitution or clearance), and the doping distribution **[39]**. Doping TiO_2 with transition metals such as Ce, Co, Fe, Ni, Cu, and Zn **[40- 45]** produces favorable changes in its electronic structure. The introduction of these metals into TiO_2 structure causes a red shift in absorption edge and a decrease in band gap energy **[46]**, which extends the visible light response of TiO_2 and thus enhances the photocatalytic activity **[36, 9]**. The use of noble metals such as Ag **[47]**, Pt **[48]** , Pd **[49]**, Rh **[50]** and Au **[51]** is another approach for modifying TiO_2 photocatalysts **[36]**. The incorporation of noble metals (micro or nanoparticles) into TiO_2 lattice promotes the electron-hole separation by forming impurity and defect energy levels that act as electron traps, reducing the recombination of light generated e^-– h^+ at the TiO_2 surface and consequently raising TiO_2 photocatalytic performance under visible light **[52, 38]**.

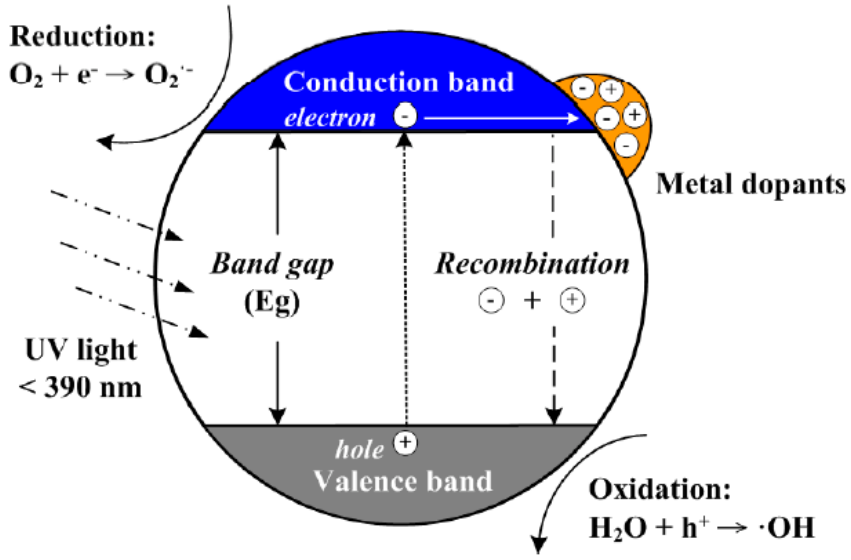

Figure I.5 Schematic of metal-TiO_2 photocatalytic mechanism **[3]**.

I.2.4.2 Non-metal doping

TiO_2 can be doped with non-metal materials (N, S ,C etc.) as a substitute for oxygen in the TiO_2 lattice and thus creating new defect energy levels and narrowing the band gap energy of TiO_2, however, they do not act as charge carriers, and their role as recombination centers and thus, they are considered to be more effective in improving the photocatalytic performance of TiO_2 **[9, 46]**.

I.2.4.3 Codoped TiO_2

Co-doping is a successful method to modify pure TiO_2 properties based on the doping of two kinds of atoms into TiO_2 (metal-metal, nonmetal-nonmetal and metal-nonmetal), it has attracted much interest owing to its high photocatalytic activity and low side effects (such as instability, recombination of photoexcited electron- hole pairs, and mobility reduction) in comparison to single-elements doping. In this case, the codoped TiO_2 material exhibits synergistic effects that significantly improve the charge separation by facilitating the transfer of photogenerated charge carriers, redshifting in the adsorption edge, and high absorbance under visible light. Consequently, the photocatalytic activity is greatly increased as well as the antibacterial efficiency **[9, 53]**. several researchers have demonstrated that doped , codoped and composites TiO_2 exhibit very high bactericidal effect and a visible light activated photocatalyst, as well as strong antibacterial properties without light activation against various bacteria **(table I.3)**.

Table I.3 Antibacterial activity with modified TiO_2 photocatalyst **[13]**.

Metal	**Non-metal**	**Nobel**	**Composite**	**Bacteria**	**Ref**
Fe-TiO_2				*Escherichia coli* K12	**[54]**
			Fe_3O_4/TiO_2	*Edwardsiella tarda* (BCRC 10670)	**[55]**
		Pt-TiO_2		*Escherichia coli*	**[56]**
			CNT-TiO_2	*Escherichia coli*	**[57]**
Cu-TiO_2				*Escherichia coli* and *Staphylococcus aureus*	**[58]**
	S-TiO_2			*Micrococcus lylae*	**[59]**
			Ag-N-TiO_2	*Escherichia coli*	**[60]**
	N-TiO_2			*Lactobacillus acidophilus* and *Candida albicans*	**[61]**
Sn-TiO_2				*Escherichia coli (ATCC 23282)* and *Staphylococ-cus aureus*	**[62]**

			Ag-TiO_2	*Escherichia coli*	**[63]**
			Au-TiO_2	*Escherichia coli* (DH 5α) and *Bacillus megat-erium (QM B1551)*	**[64]**
Co-TiO_2				*Staplylococcus aureus* and *Salmonella typhimurium*	**[65]**
		Au-TiO_2		*Escherichia coli MTCC 40* and *S. aureus ATCC 6633*	**[66]**
	S-TiO_2			*hepatocellular carcinoma (Huh-7)*	**[67]**
			Cu/TiO_2/CS	*Escherichia coli* and *Staphylococcus aureus*	**[68]**
		Ag-TiO_2		*Escherichia Coli Pseudomonas aeruginosa, Klebsiella pneumoniae* and *Enterobacter Cloacae*	**[69]**

I.2.4.4 Immobilized TiO_2

A variety of studies have proven that photocatalyst activity is more effective when the TiO_2 catalytic is immobilized on support materials. The immobilization of a TiO_2 photocatalyst onto different surfaces, including glass, silica gel, metals, ceramics, polymers, thin films, fibers, clays, activated carbon, cellulose, etc can expand TiO_2 absorption range and greatly affects the photocatalytic properties. Moreover, the modification of TiO_2 on support materials does not need additional treatment of the final purification process because it does not produce a catalyst suspension. This makes it a very desirable way in many different applications especially water purification **[70, 71]**.

I.3 Modification materials

I.3.1 Silver (Ag)

Silver with the chemical symbol "Ag" is a precious metal. It belongs to the family of noble (rare) chemical elements. The name silver is derived first from the Greek, argyros, and later from the Latin, argentum **[72]**. Silver crystallizes in face centred cubic (fcc) crystal structure and it has an atomic radius of 0.144 nm. Silver has been used for many thousands of years owing to its unique chemical and physical properties **(table I.4)**; it is white metal with a shiny surface, ductile and malleable transition metal. This metal has the greatest electrical and thermal conductivity of any other metal **[73-76]**.

Table I.4 Physical and chemical properties of silver **[73-76]**.

Parameters	Ag
Atomic number	47
Atomic weight	107.868
Group	11
Period	5
Melting point	961.78 °C
Boiling point	2162 °C
Density	10.49 g/cm^3
Atomic radius	0.144 nm
Oxidation states	$^{+1}$, $^{+2}$, $^{+3}$
Electron configuration	[Kr] $4d^{10}\,5s^1$
Thermal conductivity	429 W/(m·K)

The primary use of this metal was the fabrication of jewellery and decorative items, but nowadays, silver is key material in industry and in new innovations **[77] (Figure I.6)**. On the other hand, It is also known as great antibacterial agent since ancient times **[78]**. Recently, it is combined with a broad range of materials, under various forms (salts, immobilized ions or metallic nanoparticles) to produce an effective disinfection system that reduces pathogenic bacterial strains, as well as silver has low toxicity towards humans, making it an ideal candidate for healthcare and biomedical uses **[77, 79]**.

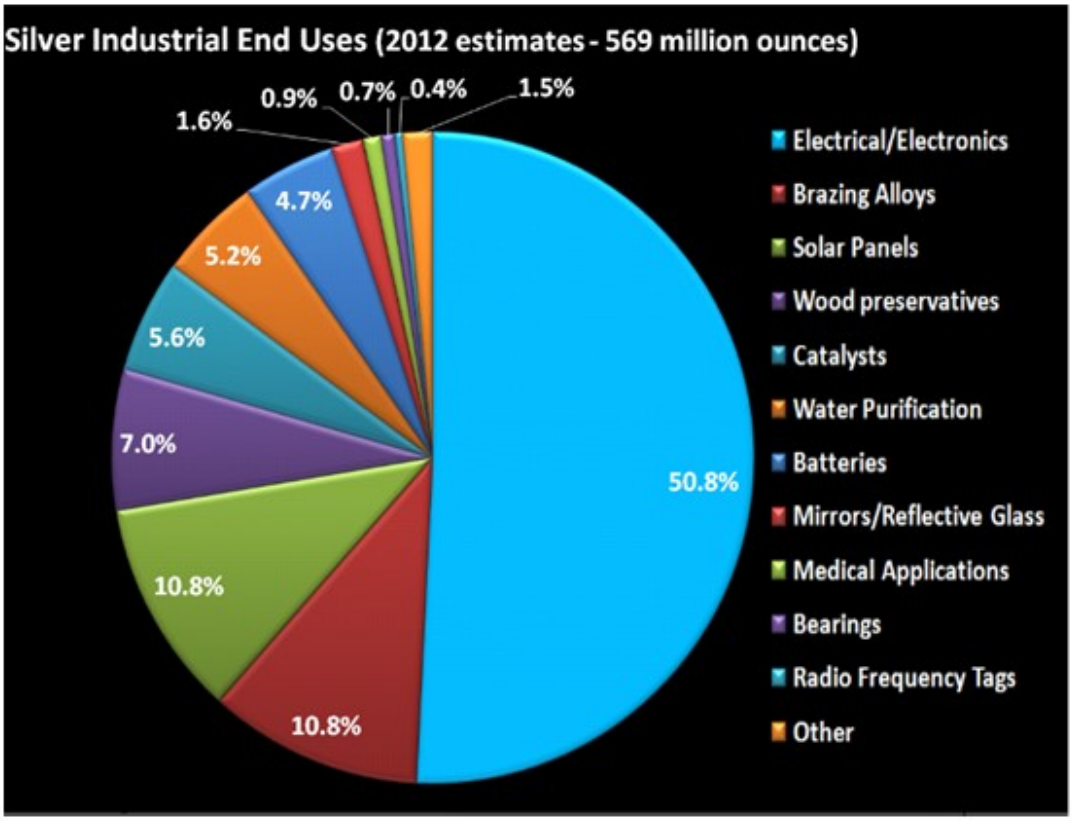

Figure I.6 Estimating industrial demand for various uses (source Thomson Reuters, 2012) **[80]**.

Silver use is currently growing due to its importance in a variety of applications include **[73-76, 81]**:

- **Electronics**: Silver is an important element in electronics applications, it is used in battery manufacturing, cavity filters, cell phones, etc.
- **Energy**: In the field of energy, silver is the preferable choice for many researchers in developing various technologies such as the manufacturing of solar panels, photovoltaic cells, and the production of nuclear energy.
- **Medicine**: Silver is promising material in medicine because of its outstanding features such as antimicrobial activity and non-toxicity, it has the ability to kill bacteria and prevent its adhesion on many surfaces. Therefore, it is applied in hospitals as an antibacterial coating for medical devices and for different surfaces such as doors, walls, windows, etc to prevent infection and bacteria adhesion, furthermore, silver nanoparticles is used to kill cancer cells in human body.

- **Catalysis**: Silver is used as a catalyst for oxidation reactions in water purification to oxidize organic compounds and to prevent the growth of algae and bacteria in filters.

I.3.2 Iron (Fe)

Iron is a chemical element that belongs to the group of transition metals. The name comes from the old English word iren while the symbol of iron comes from the Latin word Ferrum **[82]**. Iron is classified as the second most abundant metal in the Earth's crust after aluminum. It is the most commonly used metal, making about 95% of all the metal tonnage produced around the world **[83]**. **Figure I.7** represents a representative graph of the geographical distribution of iron production and consumption in the world.

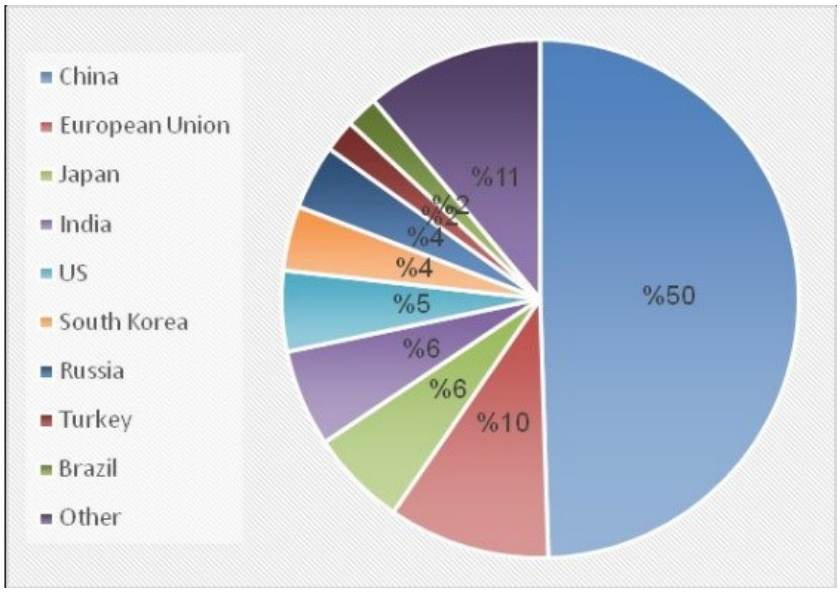

Figure I.7 Representative diagram of the geographical distribution of iron production and consumption world **[84]**.

Iron is a grey or silvery-white metal, lustrous, ductile, malleable and chemically active. Moreover, it is one of the three elements (iron, nickel and cobalt) found in nature that possess magnetic properties **[85, 86]**, Iron can form iron oxides when it comes into contact with air and water. Generally, iron is found in the form of magnetite (Fe_3O_4), hematite (Fe_2O_3), goethite (FeO(OH)), limonite (FeO(OH).n(H_2O), etc. On the other hand, iron is combined with carbon and other elements to produce different types according to human needs, such as: cast iron, wrought iron, pig iron, carbon steel, and alloy steel. Due to its unique properties such as multiple oxidation states, non-toxicity, and redox potential, iron

acts as a catalyst and plays essential role in chemical and biological reactions (Fenton reaction, photo-Fenton) in the presence of H_2O_2 to generate highly reactive hydroxyl radicals for the oxidation of a wide range of pollutants **[86-89]**.**Table I.5** shows some characteristics of iron (Fe).

Table I.5 Characteristics of Fe **[90, 91]**.

Parameters	Fe
Atomic number	26
Atomic weight	55.845
Group	8
Period	4
Melting point	1538 °C
Boiling point	2861°C
Density	7.86 g/cm^3
Ionic radius	0.076 nm (+2) ; 0.064 nm (+3)
Oxidation states	$^{+2}$, $^{+3}$, $^{+4}$, $^{+6}$
Electron configuration	[Ar] 3d^6 4s^2
Thermal conductivity	80.4 W/(m·K)

Iron is an attractive and useful material for different purposes owing to its specific characteristics and enormous potential. The following are the application areas of iron and iron oxides:

- Production of building tools, materials and industrial machinery **[87]**.
- Fabrication of iron batteries for renewable energy storage **[92]**.
- It is used in medicinal surgical instruments **[85]**, and as antibacterial coatings of implants for medical applications **[93]**.
- Iron and its compounds are considered basic materials in the field of water treatment through the oxidation process by removing many harmful contaminants from water resources including dyes, pesticides, microorganisms, heavy metals, discharge of pharmaceuticals, etc **[94, 95]**.

I.4 Ag, Fe modified TiO_2 composite thin films

The development of antibacterial materials has received a great deal of interest in recent years due to their potential use in photocatalysis, microbial disinfection, medical and environmental applications. Antibacterial coating based TiO_2 semiconductor–metals composites thin films can be an effective way to kill microorganisms and prevent microbial adhesion. Ag-TiO_2 composite thin film possess strong antibacterial performance against variety of bacterial strains due to the combination of the biocidal properties of silver and the generation of highly reactive species such as hydroxyl radical, hydrogen peroxide and superoxide by the photocatalysis of TiO_2 **[96]**. The antibacterial effect of Ag introduced in TiO_2 matrix has been shown by many researchers **[96, 97, 63]**. Wahyuni and Roto reported the inactivation of *Escherichia coli (E.coli)* bacteria by Ag nanoparticles incorporated in TiO_2 matrix **[98]**. Binyu Yu et al. synthesized Ag-TiO_2 composite nano thin films on silicon substrate using sol–gel method; the composite films exhibited better bactericidal activities both in the dark and under UV illumination than the pure TiO_2 film **[38]**. Significant enhancement in visible-light response and the durability of antibacterial system composed of silver nanoparticles impregnated in TiO_2:(N) thin films against pathogens like *E.coli, Streptococcus pyogenes, S.aureus* and *Acinetobacter baumanii* were reported by Wong et al. **[99]**. Fe modified TiO_2 can improve photocatalytic inactivation of microorganisms through redox reactions, making it prominent disinfection system for environmental pollution applications **[100, 101]**. U. Arellano et al. **[102]** prepared Fe-TiO_2 thin film deposited on sodium glass by the spin-coating method and studied the antimicrobial photocatalytic performance of the films toward *E. coli* bacteria. The Fe-TiO_2 film with high Fe content showed complete elimination of *E. coli* after 60 min under visible radiation. S.M.H. AL-Jawad et al. studied the inactivation of *S. aureus* and *E. coli* under UV light using Fe-TiO_2 photocatalysts **[42]**. Excellent antibacterial effects of TiO_2 modified with Ag and Cu nanocomposite thin coatings prepared by radiofrequency magnetron sputter technique against Pseudomonas putida were reported by I.A. Ivanova et al. **[96]**.

Ag-TiO_2-Fe composite thin film is a novel antibacterial coating. There is no detailed studies have been reported for antibacterial activity of TiO_2 thin films modified with Ag and Fe and deposited through thermal evaporation method. This is the reason to investigate the antibacterial properties of these coating materials. Ag-modified TiO_2-Fe composite thin film with different Ag contents is a new antibacterial coating prepared via thermal

evaporation technique **[103]**. It is considered as a promising antibacterial coating to protect human health and their environment from contamination with harmful pathogens (bacteria, viruses, fungi, etc).

I.4.1 Applications of Ag-TiO_2-Fe composite thin films

Fabrication of modified TiO_2 based composite thin films has become widely favored study topics, and these types of materials can be synthesized using physical and chemical techniques. Each method will be briefly explained in the next chapter, with a detailed discussion of the thermal evaporation process, which is the principal technique employed in this study to produce thin films **[32, 8]**. The prepared Ag-TiO_2-Fe composite thin film is a novel antibacterial coating with special properties. This disinfection system is important for healthy living; it can be applied in a wide range of uses particularly in the environmental and healthcare fields.

I.4.1.1 Medical devices

Ag-TiO_2-Fe surface coating is a highly effective strategy to protect medical devices against infections in clinics and hospitals. This antibacterial coating can be applied for preventing bacterial growth on the surfaces of medical devices including sterile needles in self-monitoring device for blood glucose in diabetes, urinary tract devices and can also be used on surgical equipment (such as catheters, lancets and scissors, etc) **[96, 34, 104]**.

I.4.1.2 Touch surfaces

Ag-TiO_2-Fe composite antimicrobial coating is the greatest approaches for removing pathogenic organisms (viruses, bacteria and fungi) from touched surfaces in various parts of our environment (in hospitals, home, industrial buildings, etc). Furthermore, it can provide safe usage of the frequently used surfaces such as commercial touch screens, mobile phones and ceramics by inhibiting bacterial contamination **[28, 105, 106]**.

I.4.1.3 Water purification

One of the main issues we currently face is water pollution. Ag-TiO_2-Fe composite coating offers the possibility for efficient disinfection of polluted water due to the unique photocatalytic and antibacterial properties by eliminating toxic substances and harmful microorganisms to make water safe for use and drinking **[107, 108]**.

I.5 Conclusion

In this first chapter, we have presented a bibliographic study about materials and thin films based on the Ag-TiO_2-Fe system. Moreover, the prepared Ag-TiO_2-Fe composite thin films have great antibacterial efficiency which makes it promising candidate as antibacterial coating for medical devices, environmental surfaces disinfection, and water purification field.

References

[1] Y. Lan, Y. Lu, and Z. Ren, "Mini review on photocatalysis of titanium dioxide nanoparticles and their solar applications," *Nano Energy*, vol. 2, no. 5, pp. 1031–1045, Sep. 2013, doi: 10.1016/j.nanoen.2013.04.002.

[2] S. Demirci, T. Dikici, M. Yurddaskal, S. Gultekin, M. Toparli, and E. Celik, "Synthesis and characterization of Ag doped TiO2 heterojunction films and their photocatalytic performances," *Applied Surface Science*, vol. 390, pp. 591–601, Dec. 2016, doi: 10.1016/j.apsusc.2016.08.145.

[3] Y.-H. Wang, K. H. Rahman, C.-C. Wu, and K.-C. Chen, "A Review on the Pathways of the Improved Structural Characteristics and Photocatalytic Performance of Titanium Dioxide (TiO2) Thin Films Fabricated by the Magnetron-Sputtering Technique," *Catalysts*, vol. 10, no. 6, p. 598, May 2020, doi: 10.3390/catal10060598.

[4] A. A. Yousif, K. A. Aadim, and N. A. Hamzah, "Influence of Ag doping on Optical Properties of Nanocrystalline Titanium Dioxide prepared by PLD," *IOSR*, vol. 08, no. 05, pp. 50–56, May 2016, doi: 10.9790/4861-0805025056.

[5] I. Ali, M. Suhail, Z. A. Alothman, and A. Alwarthan, "Recent advances in syntheses, properties and applications of TiO_2 nanostructures," *RSC Adv.*, vol. 8, no. 53, pp. 30125–30147, 2018, doi: 10.1039/C8RA06517A.

[6] K.-R. Zhu, M.-S. Zhang, J.-M. Hong, and Z. Yin, "Size effect on phase transition sequence of TiO2 nanocrystal," *Materials Science and Engineering: A*, vol. 403, no. 1–2, pp. 87–93, Aug. 2005, doi: 10.1016/j.msea.2005.04.029.

[7] J. Vargas Hernandez, "Structural and Morphological modification of TiO2 doped metal ions and investigation of photo-induced charge transfer processes," thesis, University of Maine, 2017.

[8] Y. Faheem Joya, "Titanium Dioxide Films Prepared by Sol-Gel/Laser-Induced Technique for Inactivation of Bacteria," thesis, University of Manchester, Manchester, 2011.

[9] S. M. Gupta and M. Tripathi, "A review of TiO2 nanoparticles," *Chin. Sci. Bull.*, vol. 56, no. 16, pp. 1639–1657, Jun. 2011, doi: 10.1007/s11434-011-4476-1.

[10] M. Landmann, E. Rauls, and W. G. Schmidt, "The electronic structure and optical response of rutile, anatase and brookite TiO_2," *J. Phys.: Condens. Matter*, vol. 24, no. 19, p. 195503, May 2012, doi: 10.1088/0953-8984/24/19/195503.

[11] A. A. Cavalheiro, L. C. S. D. Oliveira, and S. A. L. D. Santos, "Structural Aspects of Anatase to Rutile Phase Transition in Titanium Dioxide Powders Elucidated by the Rietveld Method," in *Titanium Dioxide*, M. Janus, Ed., InTech, 2017. doi: 10.5772/intechopen.68601.

[12] X. Wu, "Applications of Titanium Dioxide Materials," in *Titanium Dioxide - Advances and Applications*, H. Muhammad Ali, Ed., IntechOpen, 2022. doi: 10.5772/intechopen.99255.

[13] H. Mahipati Yadav, "Antibacterial studies with metal-doped TiO2 nanoparticles," D. Y. Patil University, Kolhapur, India, 2014.

[14] X. Yan and X. Chen, "Titanium Dioxide Nanomaterials," in *Encyclopedia of Inorganic and Bioinorganic Chemistry*, 2nd ed., R. A. Scott, Ed., Wiley, 2015, pp. 1–38. doi: 10.1002/9781119951438.eibc2335.

[15] W. M. Omymen, "Photoelectrochemical cell based on titanium dioxide nanotubes modified by iron oxide," thesis, University of Belgrade, Belgrade, 2018.

[16] R. S. Pessoa, M. A. Fraga, L. V. Santos, M. Massi, and H. S. Maciel, "Nanostructured thin films based on TiO2 and/or SiC for use in photoelectrochemical cells: A review of the material characteristics, synthesis and recent applications," *Materials Science in Semiconductor Processing*, vol. 29, pp. 56–68, Jan. 2015, doi: 10.1016/j.mssp.2014.05.053.

[17] R. V. Nair, V. S. Gummaluri, M. V. Matham, and V. C, "A review on optical bandgap engineering in TiO $_2$ nanostructures via doping and intrinsic vacancy modulation towards visible light applications," *J. Phys. D: Appl. Phys.*, vol. 55, no. 31, p. 313003, Aug. 2022, doi: 10.1088/1361-6463/ac6135.

[18] H.-J. Yen, C.-L. Tsai, P.-H. Wang, J.-J. Lin, and G.-S. Liou, "Flexible, optically transparent, high refractive, and thermally stable polyimide–TiO2 hybrids for anti-reflection coating," *RSC Adv.*, vol. 3, no. 38, pp. 17048–17056, 2013, doi: 10.1039/c3ra42180e.

[19] G. Sujatha, S. Shanthakumar, and F. Chiampo, "UV Light-Irradiated Photocatalytic Degradation of Coffee Processing Wastewater Using TiO2 as a Catalyst," *Environments*, vol. 7, no. 6, p. 47, Jun. 2020, doi: 10.3390/environments7060047.

[20] M. Nuño, R. J. Ball, and C. R. Bowen, "Photocatalytic Properties of Commercially Available TiO2 Powders for Pollution Control," in *Semiconductor Photocatalysis - Materials, Mechanisms and Applications*, W. Cao, Ed., InTech, 2016. doi: 10.5772/62894.

[21] A. Fujishima and K. Honda, "Electrochemical Photolysis of Water at a Semiconductor Electrode," *Nature*, vol. 238, no. 5358, pp. 37–38, Jul. 1972, doi: 10.1038/238037a0.

[22] N. Serpone and E. Pelizzetti, Eds., *Photocatalysis: fundamentals and applications*. New York: Wiley, 1989.

[23] C. Chen, W. Ma, and J. Zhao, "Semiconductor-mediated photodegradation of pollutants under visible-light irradiation," *Chem. Soc. Rev.*, vol. 39, no. 11, p. 4206, 2010, doi: 10.1039/b921692h.

[24] M. Pelaez *et al.*, "A review on the visible light active titanium dioxide photocatalysts for environmental applications," *Applied Catalysis B: Environmental*, vol. 125, pp. 331–349, Aug. 2012, doi: 10.1016/j.apcatb.2012.05.036.

[25] J. Prakash, B. S. Kaith, S. Sun, S. Bellucci, and H. C. Swart, "Recent Progress on Novel Ag–TiO2 Nanocomposites for Antibacterial Applications," in *Microbial Nanobionics*, R. Prasad, Ed., in Nanotechnology in the Life Sciences. , Cham: Springer International Publishing, 2019, pp. 121–143. doi: 10.1007/978-3-030-16534-5_7.

[26] P. Ganguly, C. Byrne, A. Breen, and S. C. Pillai, "Antimicrobial activity of photocatalysts: Fundamentals, mechanisms, kinetics and recent advances," *Applied Catalysis B: Environmental*, vol. 225, pp. 51–75, Jun. 2018, doi: 10.1016/j.apcatb.2017.11.018.

[27] C. López De Dicastillo, M. Guerrero Correa, F. B. Martínez, C. Streitt, and M. José Galotto, "Antimicrobial Effect of Titanium Dioxide Nanoparticles," in *Antimicrobial Resistance - A One Health Perspective*, M. Mareș, S. Hua Erin Lim, K.-S. Lai, and R.-T. Cristina, Eds., IntechOpen, 2021. doi: 10.5772/intechopen.90891.

[28] V. Kumaravel *et al.*, "Antimicrobial TiO2 nanocomposite coatings for surfaces, dental and orthopaedic implants," *Chemical Engineering Journal*, vol. 416, p. 129071, Jul. 2021, doi: 10.1016/j.cej.2021.129071.

[29] A. J. Haider, Z. N. Jameel, and I. H. M. Al-Hussaini, "Review on: Titanium Dioxide Applications," *Energy Procedia*, vol. 157, pp. 17–29, Jan. 2019, doi: 10.1016/j.egypro.2018.11.159.

[30] N. Lagopati *et al.*, "Nanomedicine: Photo-activated nanostructured titanium dioxide, as a promising anticancer agent," *Pharmacology & Therapeutics*, vol. 222, p. 107795, Jun. 2021, doi: 10.1016/j.pharmthera.2020.107795.

[31] Z. Weng, H. Guo, X. Liu, S. Wu, K. W. K. Yeung, and Paul. K. Chu, "Nanostructured TiO2 for energy conversion and storage," *RSC Adv.*, vol. 3, no. 47, pp. 24758–24775, 2013, doi: DOI https://doi.org/10.1039/C3RA44031A.

[32] H. Yang, B. Yang, W. Chen, and J. Yang, "Preparation and Photocatalytic Activities of TiO2-Based Composite Catalysts," *Catalysts*, vol. 12, no. 10, p. 1263, Oct. 2022, doi: 10.3390/catal12101263.

[33] W. Selmi, N. Hosni, J. Ben Naceur, H. Maghraoui-Meherzi, and R. Chtourou, "Titanium Dioxide Thin Films for Environmental Applications," in *Titanium Dioxide - Advances and Applications*, H. Muhammad Ali, Ed., IntechOpen, 2022. doi: 10.5772/intechopen.99726.

[34] S. Jafari, B. Mahyad, H. Hashemzadeh, S. Janfaza, T. Gholikhani, and L. Tayebi, "Biomedical Applications of TiO_2 Nanostructures: Recent Advances," *IJN*, vol. 15, pp. 3447–3470, May 2020, doi: 10.2147/IJN.S249441.

[35] Z. Fei Yin, L. Wu, H. Gui Yang, and Y. Hua Su, "Recent progress in biomedical applications of titanium dioxide," *Phys. Chem. Chem. Phys.*, vol. 15, no. 14, pp. 4844–4858, 2013, doi: 10.1039/c3cp43938k.

[36] J. Moma and J. Baloyi, "Modified Titanium Dioxide for Photocatalytic Applications," in *Photocatalysts - Applications and Attributes*, S. Bahadar Khan and K. Akhtar, Eds., IntechOpen, 2019. doi: 10.5772/intechopen.79374.

[37] Md. A. Hossain *et al.*, "Synthesis of Fe- or Ag-doped TiO2–MWCNT nanocomposite thin films and their visible-light-induced catalysis of dye degradation and antibacterial activity," *Res Chem Intermed*, vol. 44, no. 4, pp. 2667–2683, Apr. 2018, doi: 10.1007/s11164-018-3253-z.

[38] B. Yu, K. M. Leung, Q. Guo, W. M. Lau, and J. Yang, "Synthesis of Ag–TiO_2 composite nano thin film for antimicrobial application," *Nanotechnology*, vol. 22, no. 11, p. 115603, Mar. 2011, doi: 10.1088/0957-4484/22/11/115603.

[39] S. Wang, Z. Ding, X. Chang, J. Xu, and D.-H. Wang, "Modified Nano-TiO2 Based Composites for Environmental Photocatalytic Applications," *Catalysts*, vol. 10, no. 7, p. 759, Jul. 2020, doi: 10.3390/catal10070759.

[40] P. Sun, L. Liu, S.-C. Cui, and J.-G. Liu, "Synthesis, Characterization of Ce-doped TiO2 Nanotubes with High Visible Light Photocatalytic Activity," *Catal Lett*, vol. 144, no. 12, pp. 2107–2113, Dec. 2014, doi: 10.1007/s10562-014-1377-3.

[41] B. Choudhury and A. Choudhury, "Luminescence characteristics of cobalt doped TiO2 nanoparticles," *Journal of Luminescence*, vol. 132, no. 1, pp. 178–184, Jan. 2012, doi: 10.1016/j.jlumin.2011.08.020.

[42] S. M. H. AL-Jawad, A. A. Taha, and M. M. Salim, "Synthesis and characterization of pure and Fe doped TiO2 thin films for antimicrobial activity," *Optik*, vol. 142, pp. 42–53, Aug. 2017, doi: 10.1016/j.ijleo.2017.05.048.

[43] B. Gao *et al.*, "Synthesis of yellow mesoporous Ni-doped TiO_2 with enhanced photoelectrochemical performance under visible light," *Inorg. Chem. Front.*, vol. 4, no. 5, pp. 898–906, 2017, doi: 10.1039/C6QI00609D.

[44] C. Karunakaran, G. Abiramasundari, P. Gomathisankar, G. Manikandan, and V. Anandi, "Cu-doped TiO2 nanoparticles for photocatalytic disinfection of bacteria under visible light," *Journal of Colloid and Interface Science*, vol. 352, no. 1, pp. 68–74, Dec. 2010, doi: 10.1016/j.jcis.2010.08.012.

[45] K. T. Merin, K. Athira, T. Raguram, and K. S. Rajni, "Effect of Zinc concentration in TiO2 nanoparticles synthesized by Sol-Gel technique for Photocatalytic Applications," *Materials Today: Proceedings*, vol. 33, pp. 2315–2320, 2020, doi: 10.1016/j.matpr.2020.04.516.

[46] G. Bahman Rokh, "Fabrication of Photocatalytic Ce- and Fe-Doped and Codoped TiO2 Thin Films," thesis, UNSW Sydney, 2019.

[47] X. Hou *et al.*, "Synthesis of Ag ion-implanted TiO2 thin films for antibacterial application and photocatalytic performance," *Journal of Hazardous Materials*, vol. 299, pp. 59–66, Dec. 2015, doi: 10.1016/j.jhazmat.2015.05.014.

[48] J. F. Guayaquil-Sosa, B. Serrano-Rosales, P. J. Valadés-Pelayo, and H. De Lasa, "Photocatalytic hydrogen production using mesoporous TiO2 doped with Pt," *Applied Catalysis B: Environmental*, vol. 211, pp. 337–348, Aug. 2017, doi: 10.1016/j.apcatb.2017.04.029.

[49] B. Rusinque, S. Escobedo, and H. De Lasa, "Photoreduction of a Pd-Doped Mesoporous TiO2 Photocatalyst for Hydrogen Production under Visible Light," *Catalysts*, vol. 10, no. 1, p. 74, Jan. 2020, doi: 10.3390/catal10010074.

[50] C. Jin, Y. Dai, W. Wei, X. Ma, M. Li, and B. Huang, "Effects of single metal atom (Pt, Pd, Rh and Ru) adsorption on the photocatalytic properties of anatase TiO 2," *Applied Surface Science*, vol. 426, pp. 639–646, Dec. 2017, doi: 10.1016/j.apsusc.2017.07.065.

[51] L. A. Al-Hajji *et al.*, "Construction of Au/TiO2 Heterojunction with high photocatalytic performances under UVA illumination," *Ceramics International*, vol. 46, no. 12, pp. 20155–20162, Aug. 2020, doi: 10.1016/j.ceramint.2020.05.093.

[52] C.-H. Liang *et al.*, "The effect of erbium on the adsorption and photodegradation of orange I in aqueous Er3+-TiO2 suspension," *Journal of Hazardous Materials*, vol. 138, no. 3, pp. 471–478, Dec. 2006, doi: 10.1016/j.jhazmat.2006.05.066.

[53] M. Ghaedi, Ed., *Photocatalysis: fundamental processes and applications*. in Interface science and technology, no. volume 32. London, United Kingdom ; San Diego, CA: Academic Press, 2021.

[54] G. Veréb *et al.*, "Comparison of the photocatalytic efficiencies of bare and doped rutile and anatase TiO2 photocatalysts under visible light for phenol degradation and E. coli inactivation," *Applied Catalysis B: Environmental*, vol. 129, pp. 566–574, Jan. 2013, doi: 10.1016/j.apcatb.2012.09.045.

[55] N. Yeh, Y. C. Lee, C. Y. Chang, and T. C. Cheng, "Anti-fish bacterial pathogen effect of visible light responsive Fe3O4@TiO2 nanoparticles immobilized on glass using TiO2 sol–gel," *Thin Solid Films*, vol. 549, pp. 93–97, Dec. 2013, doi: 10.1016/j.tsf.2013.09.092.

[56] B. Pal, I. Singh, K. Angrish, R. Aminedi, and N. Das, "Rapid photokilling of gram-negative Escherichia coli bacteria by platinum dispersed titania nanocomposite films," *Materials Chemistry and Physics*, vol. 136, no. 1, pp. 21–27, Sep. 2012, doi: 10.1016/j.matchemphys.2012.06.001.

[57] O. Akhavan, R. Azimirad, S. Safa, and M. M. Larijani, "Visible light photo-induced antibacterial activity of CNT–doped TiO2 thin films with various CNT contents," *J. Mater. Chem.*, vol. 20, no. 35, p. 7386, 2010, doi: 10.1039/c0jm00543f.

[58] H. M. Yadav *et al.*, "Preparation and characterization of copper-doped anatase TiO2 nanoparticles with visible light photocatalytic antibacterial activity," *Journal of Photochemistry and Photobiology A: Chemistry*, vol. 280, pp. 32–38, Apr. 2014, doi: 10.1016/j.jphotochem.2014.02.006.

[59] J. C. Yu, W. Ho, J. Yu, H. Yip, P. K. Wong, and J. Zhao, "Efficient Visible-Light-Induced Photocatalytic Disinfection on Sulfur-Doped Nanocrystalline Titania," *Environ. Sci. Technol.*, vol. 39, no. 4, pp. 1175–1179, Feb. 2005, doi: 10.1021/es035374h.

[60] A. A. Ashkarran, H. Hamidinezhad, H. Haddadi, and M. Mahmoudi, "Double-doped TiO2 nanoparticles as an efficient visible-light-active photocatalyst and

antibacterial agent under solar simulated light," *Applied Surface Science*, vol. 301, pp. 338–345, May 2014, doi: 10.1016/j.apsusc.2014.02.074.

[61] S. Cao, B. Liu, L. Fan, Z. Yue, B. Liu, and B. Cao, "Highly antibacterial activity of N-doped TiO2 thin films coated on stainless steel brackets under visible light irradiation," *Applied Surface Science*, vol. 309, pp. 119–127, Aug. 2014, doi: 10.1016/j.apsusc.2014.04.198.

[62] F. Sayılkan, M. Asiltürk, N. Kiraz, E. Burunkaya, E. Arpaç, and H. Sayılkan, "Photocatalytic antibacterial performance of Sn4+-doped TiO2 thin films on glass substrate," *Journal of Hazardous Materials*, vol. 162, no. 2–3, pp. 1309–1316, Mar. 2009, doi: 10.1016/j.jhazmat.2008.06.043.

[63] L. Mai, D. Wang, S. Zhang, Y. Xie, C. Huang, and Z. Zhang, "Synthesis and bactericidal ability of Ag/TiO2 composite films deposited on titanium plate," *Applied Surface Science*, vol. 257, no. 3, pp. 974–978, Nov. 2010, doi: 10.1016/j.apsusc.2010.08.003.

[64] G. Fu, P. S. Vary, and C.-T. Lin, "Anatase TiO_2 Nanocomposites for Antimicrobial Coatings," *J. Phys. Chem. B*, vol. 109, no. 18, pp. 8889–8898, May 2005, doi: 10.1021/jp0502196.

[65] T. Amna, M. Shamshi Hassan, M. Pandurangan, M.-S. Khil, H.-K. Lee, and I. H. Hwang, "Characterization and potent bactericidal effect of Cobalt doped Titanium dioxide nanofibers," *Ceramics International*, vol. 39, no. 3, pp. 3189–3193, Apr. 2013, doi: 10.1016/j.ceramint.2012.10.003.

[66] S. Mahboob *et al.*, "Facile synthesis of gold and platinum doped titanium oxide nanoparticles for antibacterial and photocatalytic activity: A photodynamic approach," *Photodiagnosis and Photodynamic Therapy*, vol. 33, p. 102148, Mar. 2021, doi: 10.1016/j.pdpdt.2020.102148.

[67] F. Tariq *et al.*, "Enhanced antibacterial activity of visible light activated sulfur-doped TiO2 nanoparticles against Vibrio cholerae," *Materials Science in Semiconductor Processing*, vol. 147, p. 106731, Aug. 2022, doi: 10.1016/j.mssp.2022.106731.

[68] S. Chen *et al.*, "Facile preparation and synergistic antibacterial effect of three-component Cu/TiO2/CS nanoparticles," *J. Mater. Chem.*, vol. 22, no. 18, p. 9092, 2012, doi: 10.1039/c2jm00063f.

[69] T. Ali, A. Ahmed, U. Alam, I. Uddin, P. Tripathi, and M. Muneer, "Enhanced photocatalytic and antibacterial activities of Ag-doped TiO2 nanoparticles under

visible light," *Materials Chemistry and Physics*, vol. 212, pp. 325–335, Jun. 2018, doi: 10.1016/j.matchemphys.2018.03.052.

[70] A. Y. Shan, T. I. Mohd. Ghazi, and S. A. Rashid, "Immobilisation of titanium dioxide onto supporting materials in heterogeneous photocatalysis: A review," *Applied Catalysis A: General*, vol. 389, no. 1–2, pp. 1–8, Dec. 2010, doi: 10.1016/j.apcata.2010.08.053.

[71] Y. Indriani, A. S. A. P. Sutanti, M. Ayuningtyas, and H. Widiyandari, "A Brief Review: Immobilization of TiO_2 Photocatalyst Materials on Supporting Surfaces for Degradation of Organic Pollutants," *MSF*, vol. 1044, pp. 153–161, Aug. 2021, doi: 10.4028/www.scientific.net/MSF.1044.153.

[72] M. Atanassova, "Naming of chemical elements," *Chemistry: Bulgarian J. of Science Education*, vol. 24, no. 1, pp. 125–144, 2015.

[73] Britannica, "Silver.Encyclopedia Britannica." The Editors of Encyclopaedia, 2023. Available: https://www.britannica.com/science/silver

[74] "Silver Element Properties and Information." Chemical Engineering World. Available: https://chemicalengineeringworld.com/silver-element-properties-and-information/

[75] "Silver." Available: https://en.wikipedia.org/wiki/Silver

[76] A. Reti, "Silver: Alloying, Properties and Applications," in *Encyclopedia of Materials: Science and Technology*, Elsevier, 2001, pp. 8618–8621. doi: 10.1016/B0-08-043152-6/01536-9.

[77] B. Le Ouay and F. Stellacci, "Antibacterial activity of silver nanoparticles: A surface science insight," *Nano Today*, vol. 10, no. 3, pp. 339–354, Jun. 2015, doi: 10.1016/j.nantod.2015.04.002.

[78] J. Lalley, D. D. Dionysiou, R. S. Varma, S. Shankara, D. J. Yang, and M. N. Nadagouda, "Silver-based antibacterial surfaces for drinking water disinfection—an overview," *Current Opinion in Chemical Engineering*, vol. 3, pp. 25–29, Feb. 2014, doi: 10.1016/j.coche.2013.09.004.

[79] J. W. Alexander, "History of the Medical Use of Silver," *Surgical Infections*, vol. 10, no. 3, pp. 289–292, Jun. 2009, doi: 10.1089/sur.2008.9941.

[80] A. Goren, "Is It Time To Buy Silver? Part 3." 2012. Available: https://seekingalpha.com/article/908321-is-it-time-to-buy-silver-part-3

[81] R. Chokkareddy, N. Thondavada, B. Kabane, and G. G. Redhi, "Current Advances in Biosynthesis of Silver Nanoparticles and Their Applications," in *Green Metal*

Nanoparticles, 1st ed., S. Kanchi and S. Ahmed, Eds., Wiley, 2018, pp. 165–198. doi: 10.1002/9781119418900.ch6.

[82] S. Das and C. Ranjan Patra, "Green synthesis of iron oxide nanoparticles using plant extracts and its biological application," in *Handbook of Greener Synthesis of Nanomaterials and Compounds*, Elsevier, 2021, pp. 139–170. doi: 10.1016/B978-0-12-822446-5.00006-X.

[83] "Iron." New World Encyclopedia. Available: https://www. newworldencyclopedia .org/entry/Iron

[84] F. Elamin, H. Elderrat, and S. Abushaala, "The role of iron and steel industry for achieving the industrial development in libya," *Journal of engineering research and applied sciences*, vol. 1, no. 7, pp. 22–30, 2019.

[85] "Iron Element, History, Properties, Facts, Uses, Function." Available: https://www.priyamstudycentre.com/2020/12/iron.html

[86] P. Mondal, A. Anweshan, and M. K. Purkait, "Green synthesis and environmental application of iron-based nanomaterials and nanocomposite: A review," *Chemosphere*, vol. 259, no. 10, p. 127509, Nov. 2020, doi: 10.1016/j.chemosphere.2020.127509.

[87] "Uses of Iron." Available: https://unacademy.com/content/neet-ug/study-material/chemistry/uses-of-iron

[88] P. Gupta, A. Lakes, and T. Dziubla, "A Free Radical Primer," in *Oxidative Stress and Biomaterials*, Elsevier, 2016, pp. 1–33. doi: 10.1016/B978-0-12-803269-5.00001-2.

[89] M. MAT, "Iron (Fe) Ore." Available: https://geologyscience.com/ore-minerals /iron-ore/

[90] "Iron (Fe) - Chemical properties, Health and Environmental." Available: https://www.lenntech.com/periodic/elements/fe.htm

[91] "Iron." Available: https://en.wikipedia.org/wiki/Iron

[92] N. Yensen and P. B. Allen, "Open source all-iron battery for renewable energy storage," *HardwareX*, vol. 6, p. e00072, Oct. 2019, doi: 10.1016/j.ohx.2019.e00072.

[93] Y. Tian, H. Cao, Y. Qiao, F. Meng, and X. Liu, "Antibacterial activity and cytocompatibility of titanium oxide coating modified by iron ion implantation," *Acta Biomaterialia*, vol. 10, no. 10, pp. 4505–4517, Oct. 2014, doi: 10.1016/j.actbio.2014.06.002.

[94] P. Saharan, G. R. Chaudhary, S. K. Mehta, and A. Umar, "Removal of Water Contaminants by Iron Oxide Nanomaterials," *j. nanosci. nanotech.*, vol. 14, no. 1, pp. 627–643, Jan. 2014, doi: 10.1166/jnn.2014.9053.

[95] A. Guðmundsson and J.-E. Bäckvall, "On the Use of Iron in Organic Chemistry," *Molecules*, vol. 25, no. 6, p. 1349, Mar. 2020, doi: 10.3390/molecules25061349.

[96] I. A. Ivanova, E. L. Pavlova, D. S. Stoyanova, and O. I. Angelov, "Antibacterial effect of TiO_2:Cu:Ag thin coatings on *Pseudomonas* strain measured by microbiological and ATP assays," *J Basic Microbiol*, vol. 59, no. 12, pp. 1165–1172, Dec. 2019, doi: 10.1002/jobm.201900427.

[97] S. Uhm, D. Song, J. Kwon, S. Lee, J. Han, and K. Kim, "Tailoring of antibacterial Ag nanostructures on TiO_2 nanotube layers by magnetron sputtering," *J Biomed Mater Res*, vol. 102, no. 3, pp. 592–603, Apr. 2014, doi: 10.1002/jbm.b.33038.

[98] E. T. Wahyuni and R. Roto, "Silver Nanoparticle Incorporated Titanium Oxide for Bacterial Inactivation and Dye Degradation," in *Titanium Dioxide - Material for a Sustainable Environment*, D. Yang, Ed., InTech, 2018. doi: 10.5772/intechopen.75918.

[99] M.-S. Wong, C.-W. Chen, C.-C. Hsieh, S.-C. Hung, D.-S. Sun, and H.-H. Chang, "Antibacterial property of Ag nanoparticle-impregnated N-doped titania films under visible light," *Sci Rep*, vol. 5, no. 1, p. 11978, Dec. 2015, doi: 10.1038/srep11978.

[100] P. Makvandi, C. Wang, E. N. Zare, A. Borzacchiello, L. Niu, and F. R. Tay, "Metal-Based Nanomaterials in Biomedical Applications: Antimicrobial Activity and Cytotoxicity Aspects," *Adv Funct Materials*, vol. 30, no. 22, p. 1910021, May 2020, doi: 10.1002/adfm.201910021.

[101] C. A. Castro-López, A. Centeno, and S. A. Giraldo, "Fe-modified TiO2 photocatalysts for the oxidative degradation of recalcitrant water contaminants," *Catalysis Today*, vol. 157, no. 1–4, pp. 119–124, Nov. 2010, doi: 10.1016/j.cattod.2010.04.050.

[102] U. Arellano, M. Asomoza, and F. Ramírez, "Antimicrobial activity of Fe–TiO2 thin film photocatalysts," *Journal of Photochemistry and Photobiology A: Chemistry*, vol. 222, no. 1, pp. 159–165, Jul. 2011, doi: 10.1016/j.jphotochem.2011.05.016.

[103] D. Grine, H. Akkari, P. Fernández, T. Mekhalif, S. Hassani, and F. Lekoui, "Synthesis, Characterization, and Antibacterial Activity of Ag–TiO2–Fe Composite Thin Films," *Phys. Status Solidi A*, vol. 219, no. 11, p. 2200036, Apr. 2022, doi: 10.1002/pssa.202200036.

[104] L. Visai *et al.*, "Titanium Oxide Antibacterial Surfaces in Biomedical Devices," *Int J Artif Organs*, vol. 34, no. 9, pp. 929–946, Sep. 2011, doi: 10.5301/ijao.5000050.

[105] S. Omar Elfakhri, "Antibacterial Activity of Novel Self-Disinfecting Surface Coatings," thesis, University of Salford, 2014.

[106] J. Kiwi, S. Rtimi, R. Sanjines, and C. Pulgarin, "TiO_2 and TiO_2 -Doped Films Able to Kill Bacteria by Contact: New Evidence for the Dynamics of Bacterial Inactivation in the Dark and under Light Irradiation," *International Journal of Photoenergy*, vol. 2014, pp. 1–17, 2014, doi: 10.1155/2014/785037.

[107] L. Matoh *et al.*, "Photocatalytic sol-gel/P25 TiO2 coatings for water treatment: Degradation of 7 selected pharmaceuticals," *Ceramics International*, vol. 49, no. 14, pp. 24395–24406, Jul. 2023, doi: 10.1016/j.ceramint.2022.09.204.

[108] S. J. Armaković, M. M. Savanović, and S. Armaković, "Titanium Dioxide as the Most Used Photocatalyst for Water Purification: An Overview," *Catalysts*, vol. 13, no. 1, p. 26, 2023, doi: doi.org/10.3390/catal13010026.

ChapterII

Thin film deposition methods and antibacterial coatings

II.1 Introduction

The present chapter highlights the different techniques used to fabricate pure and modified TiO_2 thin film coatings, including a presentation of each technique as well as a detailed description of the thermal evaporation process as the main technique employed throughout our research. We further explore the concept of antibacterial coatings and their importance, in addition to the classification of antibacterial coated surfaces and their modes of action.

II.2 Thin film technology

Thin films or coatings are a new field of materials science which have a significant influence on a great deal of technologies in recent years, a thin film is a layer of material with a thickness ranging from fractions of a nanometer to several micrometers, thin films can have an amorphous or polycrystalline structure depending on the preparation conditions and the type of material used **[1]**. Surface coatings are employed to modify or enhance the surface of a material or to produce functional devices in various areas of advanced applications such as energy, semiconductors, optoelectronics, medical and environmental applications. Many techniques are used to deposit thin film coatings onto different types of substrates (glass, metallic, semiconducting, polymers, etc). These deposition techniques and their working principles will be discussed in this section **[1, 2]**.

II.3 Thin film deposition techniques

There are two main categories of deposition processes for making high quality thin film coatings: chemical and physical depositions **(figure II.1)**. These methods provide the fabrication of a single material, or multiple materials in a layered structure.

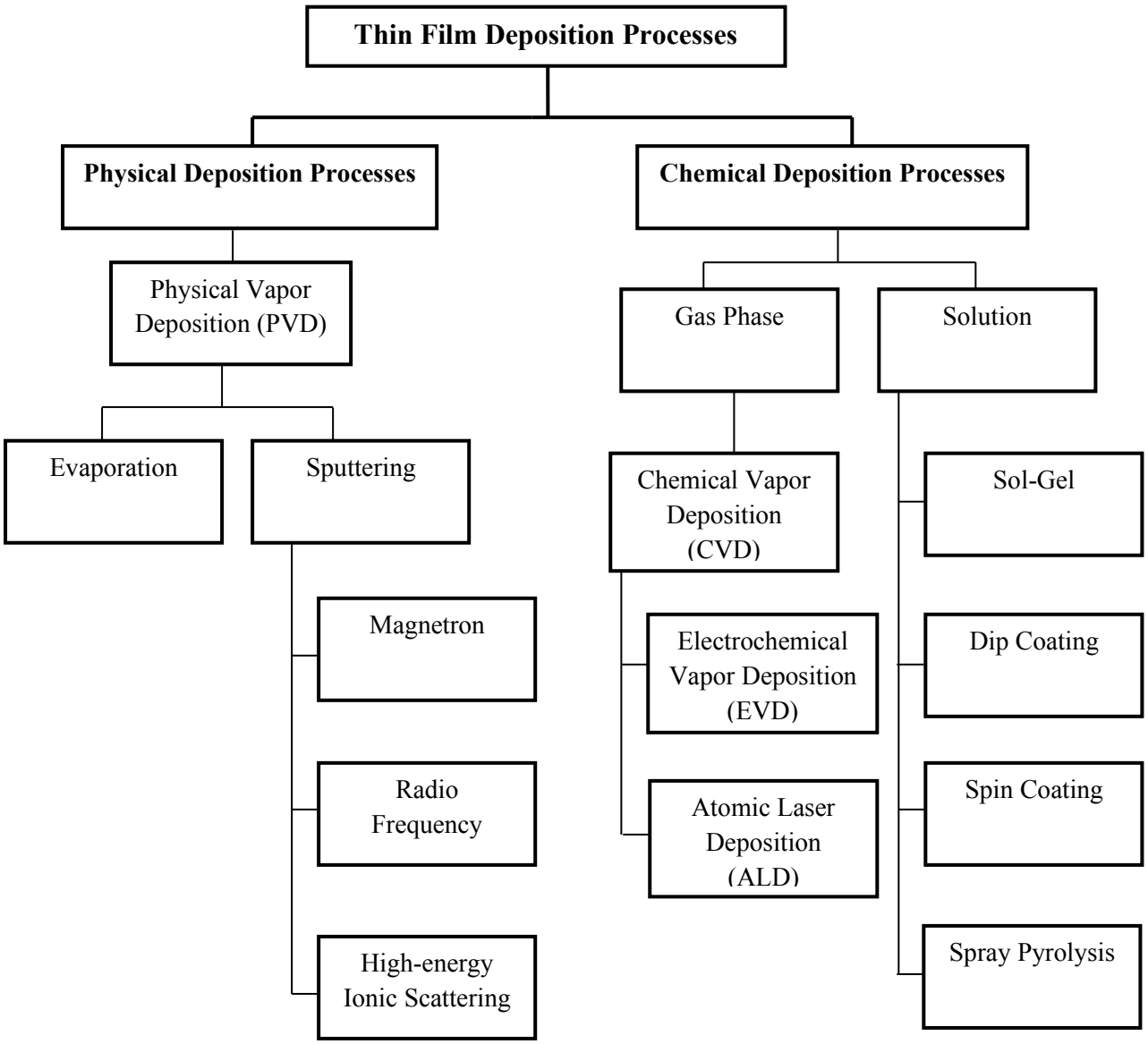

Figure II.1 Classification of thin film deposition techniques **[3]**.

II.3.1 Chemical deposition techniques

II.3.1.1 Spray pyrolysis

Spray pyrolysis technique involves the pulverization of a precursor solution as fine droplets onto a heated substrate, where the chemical constituents react to form a desired thin film **(figure II.2)**. In this process, many parameters affect the formation of deposited coating such as the flow rate, composition of the carrier gas, nature of the sol precursor, deposition temperature, substrate-nozzle distance, etc **[4]**. Spray pyrolysis is very efficient method for the fabrication of doped and undoped TiO_2 films. M. O. Abou-Helal et al. **[5]** have deposited TiO_2 on glass substrates. The solution was prepared by dissolving titanium (IV) isobutoxide $[Ti((CH_3)_2CHCH_2O)_4]$ **[6]**, A. Arunachalam et al. synthesized Zn-doped TiO_2 thin films on glass substrates using spray pyrolysis method **[7]**. This technique is used by many researchers because of its simplicity, low-cost, and effectiveness **[4, 8]**.

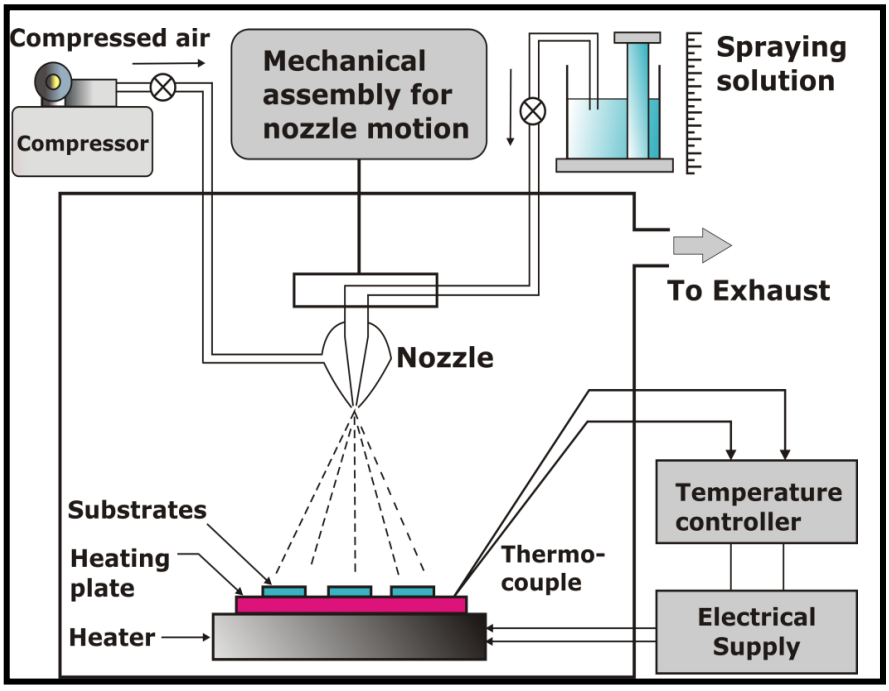

Figure II.2 Schematic diagram of the spray pyrolysis method **[9]**.

II.3.1.2 Sol-gel method

The sol-gel method is a traditional technique based on the hydrolysis of a precursor **(figure II.3)** which is usually a metal alkoxide followed by polycondensation reactions to create a colloidal suspension (sol), which is subsequently converted into a solid gel **[1, 10]**. The sol-gel method is significant method (wet-chemical technique) for producing powders, thin films and coatings of metal oxides, in particular silicon, zinc and titanium oxides **[1, 11]**. This method has many benefits, including low cost, facile setup, improved uniformity, and potential for large-scale manufacture **[4]**. However, the main drawback with this technique is the extended process duration. The two best-known sol-gel processes for fabricating thin films are dip-coating and spin-coating **[12]**, both methods can be used under ordinary conditions (ambient temperature and atmospheric pressure).

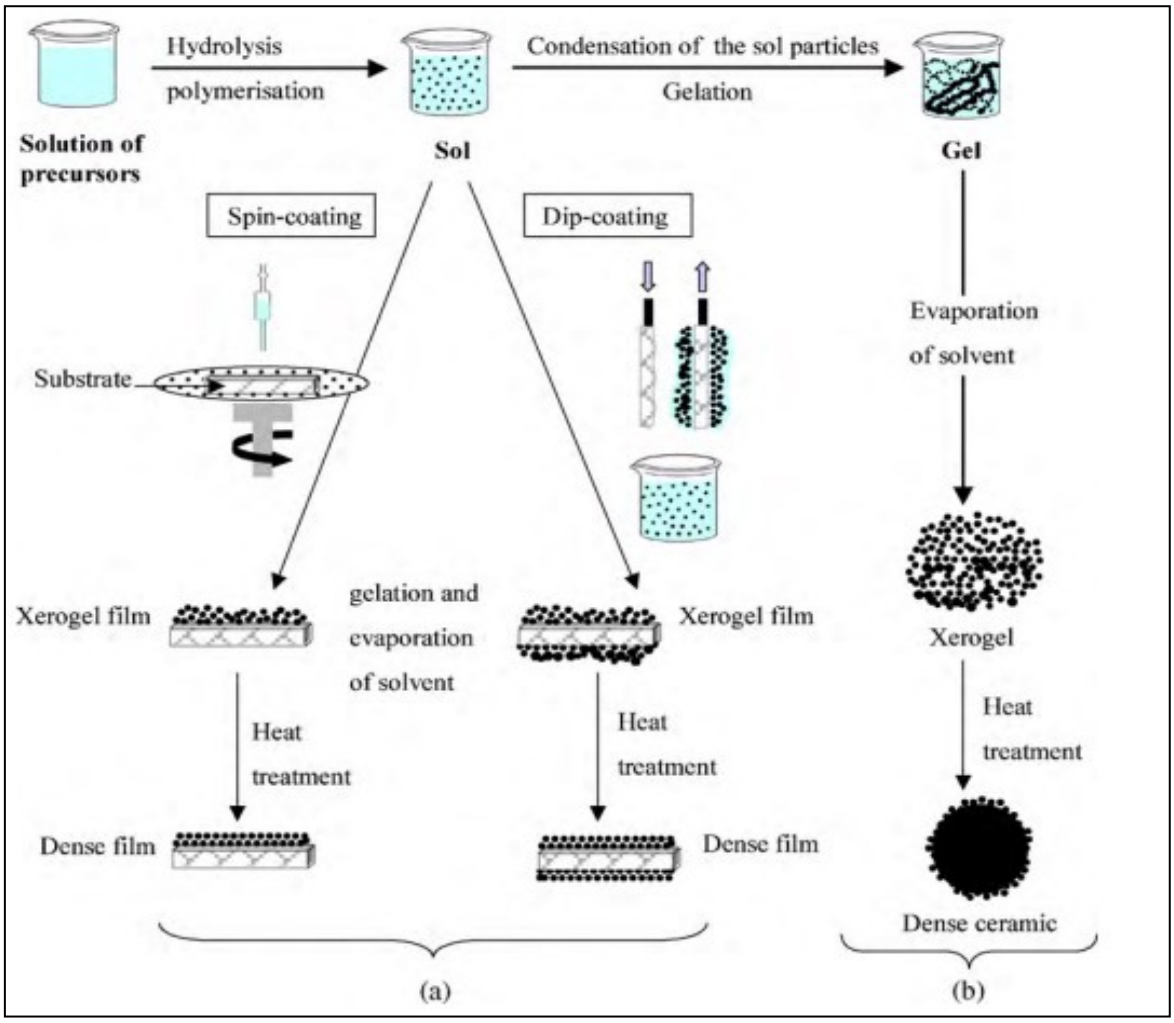

Figure II.3 Synthesis steps for: (a) films, (b) powder using the sol–gel method **[13]**.

II.3.1.3 Spin coating

Spin coating has been applied for a long time for the application of thin films. In this technique, a small quantity of a solution is deposited on the center of a circular surface, which rotates at a controlled speed to spread the coating material using centrifugal force, The coating material is created during the spinning process when the solvent rapidly evaporates **[4, 6, 14]**. This technique has been adopted by many researchers. CC Chang et al. **[15]** have prepared TiO_2/Ag thin film by sol-gel spin coating technique for photocatalytic applications. The thickness of the film is determined by the spinning speed, surface tension, and viscosity of the solution and they have a significant effect on the quality of the films **[14]**. **Figure II.4** shows the three distinct stages of the spin coating process.

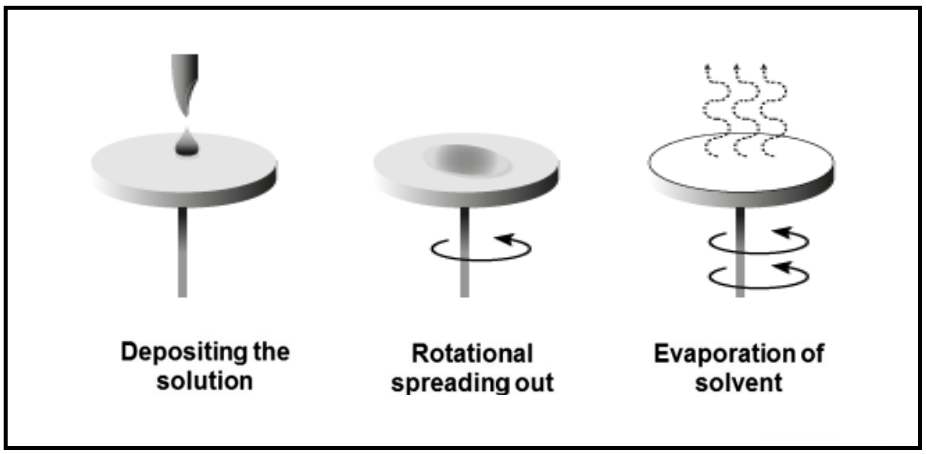

Figure II.4 Schematics of the spin-coating process **[16]**.

II.3.1.4 Dip coating

The dip coating is the best known sol gel coating techniques for producing a uniform thin films; it can be described as a process where the substrate is immersed in the solution and then withdrawing at a certain rate for the formation of a coating on the substrate surface. Compared to other deposition techniques, the dip coating offers some intriguing advantages, including a facile approach, low cost and processing at room temperature, but it also has its drawbacks including thickness variation across the surface of the material and slow process **[4]**. This method has been employed in numerous research works. K. Ubonchonlakate et al. prepared TiO_2 and TiO_2-Ag composites films coated on

glass fibre roving using dip coating method for photocatalytic disinfection of P.aeruginosa bacterial **[17]**. Many factors in dip coating method such as dipping time, withdrawal speed, the sol composition, and evaporation of the solvent during the emersion have key roles in the successful fabrication of thin films **[4, 18]**. The different steps of dip-coating method are schematically presented in **figure II.5**.

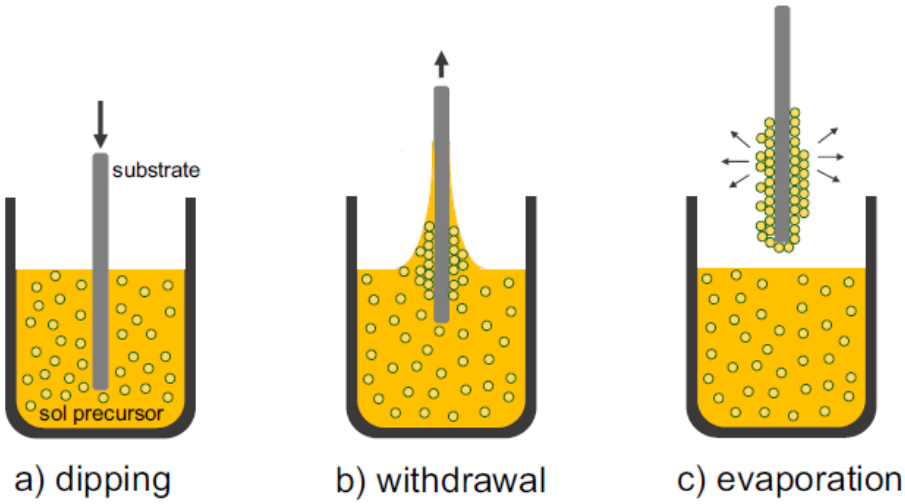

Figure II.5 Schematics of the dip coating process **[4]**.

II.3.1.5 Chemical vapor deposition

Chemical vapor deposition (CVD) is a potent process in which a solid coating is formed by a chemical reaction of gaseous compounds on a heated substrate **(figure II.6)**. This technique is widely employed in industry to fabricate semiconductors, ceramics, metals, organic, and inorganic films due to its distinct advantages, including high quality production of homogeneous and dense films **[19, 20]**. Hongfu Sun et al. investigated the photocatalytic efficacy of TiO_2 films synthesized through chemical vapor deposition (CVD) method **[21]**. The CVD technique can be categorized into: the atmospheric-pressure chemical vapor deposition (APCVD), low-pressure chemical vapor deposition (LPCVD), plasma-enhanced chemical vapor deposition (PECVD), or plasma-assisted CVD (PACVD), and laser-enhanced chemical vapor deposition (LECVD), metal-organic chemical vapor deposition (MOCVD) and hybrid physical chemical vapor deposition (HPCVD) **[20]**.

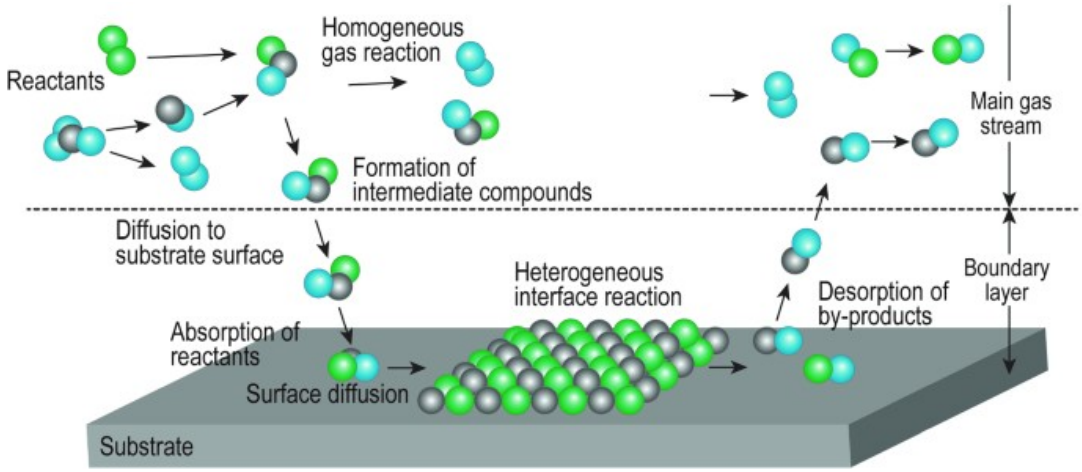

Figure II.6 Principle of a CVD process **[22]**.

II.3.2 Physical deposition techniques

II.3.2.1 Sputtering deposition

Sputtering deposition is a very common PVD technique for depositing thin films for various application fields such as antibacterial coatings, semiconductor industry, decorative coatings and protective coatings for sensitive metal oxides. The sputtering is the ejection of atoms from the target material (cathode) by bombardment with energetic ions of the plasma gas, usually Ar^+, and then the ejected atoms are deposited onto a substrate (anode) **[23]**. This approach has a number of advantages: an efficient way to create materials with a high melting point, dense films with extraordinarily high adhesion; On the other hand, the major disadvantages of this method are: difficult deposition of thick coats, non-uniform erosion of the target, which slows down the rate of deposition during time. There are different types of sputtering system. Direct current (DC) and radio frequency (RF) sputtering are the two most prevalent types of sputtering technique. The first one uses DC power, which is typically applied to targets made of electrically conductive materials, it is an inexpensive options and simple control. While for the majority of dielectric materials, RF power is applied in RF sputtering **[1, 24]**. D. Gospodonova et al. reported that TiO_2/Ag/Cu composite coatings produced by magnetron cosputtering method provided strong antimicrobial activity against different microbial strains **[25]**. **Figure II.7** illustrates the working principle of sputter process.

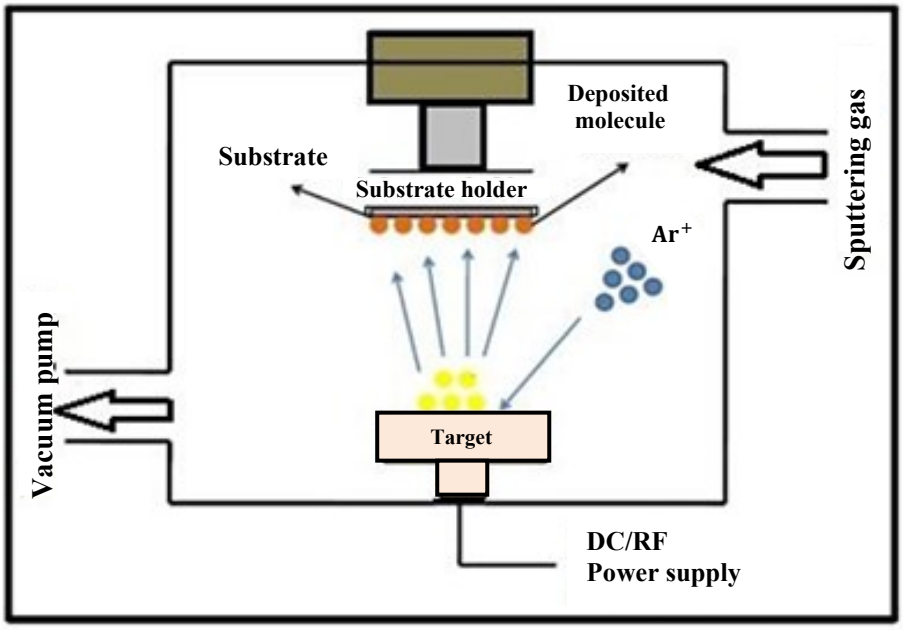

Figure II.7 Working principle of the sputter process **[1]**.

II.3.2.2 Pulsed laser deposition

Pulsed laser deposition (PLD) is a thin film deposition method based on the laser-matter interaction **(figure II.8)**, the deposition process occurs in vacuum chamber when an intensive pulsed laser used for removing target material to be vaporized. The ablated particles (plasma plume) escape from the target will then be condensed on the substrate **[23, 26]**. The successful performance of PLD process depends on a number of factors, including the laser wavelength, gas pressure, pulse energy, repetition rate, pulsed duration, and the target-substrate distance **[1]**. PLD method provides fast and highly uniform films deposition; furthermore it is a useful process for fabricating a wide variety of materials (pure and modified oxides, multilayer films, semiconductor films, ceramic and metallic layers) **[26]**. Lei Zhao et al. used the pulsed laser deposition (PLD) technique to synthesize TiO_2 films with mixed anatase and rutile structures that exhibited better photocatalytic activity than those of films with just anatase structures **[27]**.

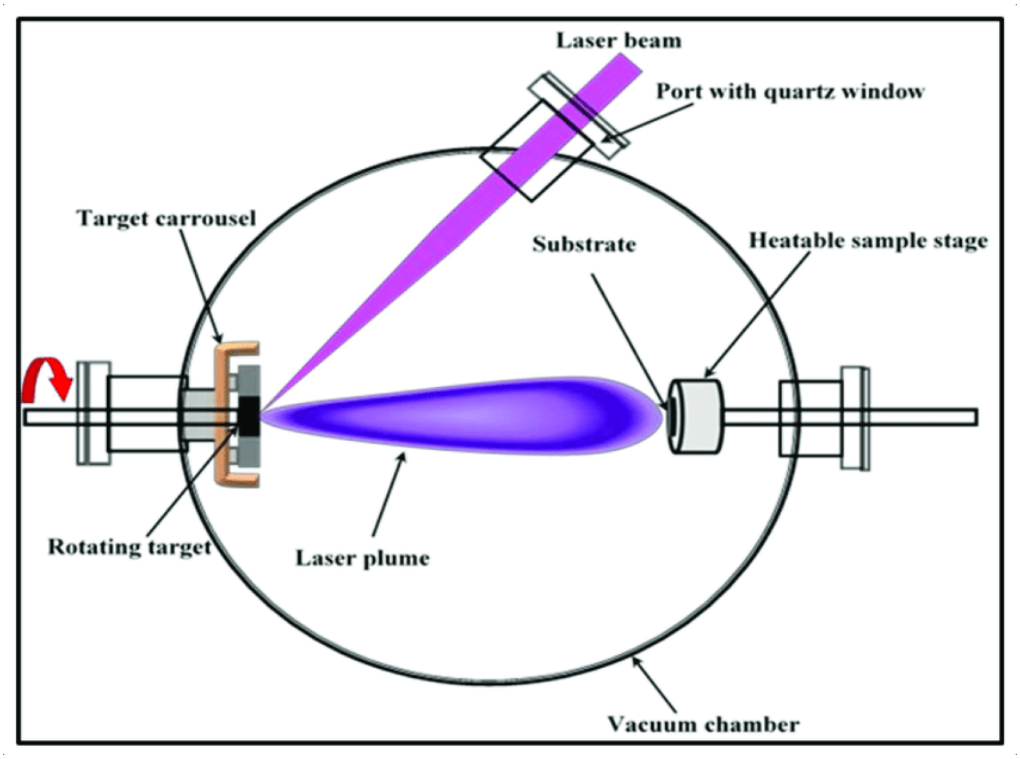

Figure II.8 Principle of pulsed laser process **[28]**.

II.3.2.3 Vacuum thermal evaporation technique

Thermal evaporation or vacuum evaporation is the process of heating a source material until evaporation under vacuum of ~10^{-6} Torr. This allows the vapor particles to solidify and condense once more into substrate surface **[29, 30]**. Investigations on thermal evaporation under vacuum started in the latter part of the 19th century. In 1887, Nahrwold detailed the creation of platinum thin films in a vacuum by subliming platinum evaporation materials. He is considered as the first person who employed thermal evaporation method to produce thin films under vacuum **[31]**. In the vacuum thermal evaporation technique, the materials to be coated can be metals, non-metals, oxides, etc deposited on different types of substrates such as glass, ceramics and metals. Thermal evaporation is a typical and effective technique that has been used by many researchers **[32-34]**. In addition, it has become among the promising technologies applied for a large number of applications such as medicine **[35]**, electronic **[36]**, solar cell **[37, 38]** and photocatalytic applications **[39, 40]**.

The thermal evaporation technique is based on two key parameters **[1]**:

- Thermally vaporized material
- Applying a potential difference to the substrate under medium or higher vacuum levels ranging from 10^{-5} to 10^{-9} mbar.

II.3.2.3.1 Types of thermal evaporation processes

Depending on the method of heating the source material to be deposited, thermal evaporation process is divided into two main techniques:

a) Thermal evaporation by resistive heating (Joule effect)

Resistance evaporation method involves the evaporation of source materials using electrical resistive heating filament, crucible or boat in which the material is placed **(figure II.9 (a))**, these heating elements typically constructed of refractory metals like W, Mo, or Ta. The usual tungsten or molybdenum crucible heated by the Joule effect can be deposited many kinds of materials, whose vapor pressure can be reasonable at a temperature of 1500-1600 ℃ or less **[41, 42]**. The prepared films in this study containing TiO_2, Fe, Ag materials were prepared using a resistive thermal evaporation deposition technique. Like any other coating deposition methods, this method may present some advantages and disadvantages, which are mentioned below in **table II.1**:

Table II.1 Presents the advantages and disadvantages of resistive thermal evaporation method.

Advantages	Disadvantages
• In comparison to other PVD, resistive thermal evaporation deposition offer high deposition rates at low cost **[43]**. • It is a simple and fast coating process provides high purity and good quality of films **[44]**, it can be used to fabricate variety of materials such as metals or non-metals, oxides, semiconductors, etc **[43]**. • The production of uniform multilayer material with easy thickness control and perfect controlled evaporation flow direction **[43, 45]**.	• Resistive thermal evaporation process cannot evaporate materials that require a high melting point **[42]**. • It has higher levels of possible contamination, which limits the quality of the vacuum in the deposition chamber **[43]**. • Material stoichiometry in compounds/alloys deposition is difficult **[44]**.

b) Electron beam evaporation

In electron beam evaporation, a target source is heated using an electron beam emitted from a hot filament and directed through an electric and magnetic fields with an energy ranging from 1 to 10 keV **(figure II.9 (b))**, which accelerates the emitted electrons towards the target material to create vaporized materials that deposit on substrates under high vacuum **[1, 29]**. The most commonly used sources of evaporation by electron bombardment include: a tungsten filament heated to high temperature (from 2500 ℃ to 2800 ℃). This method produces high purity films with good directionality. Furthermore, it is excellent process to deposit coating materials that have high melting points **[43]**.

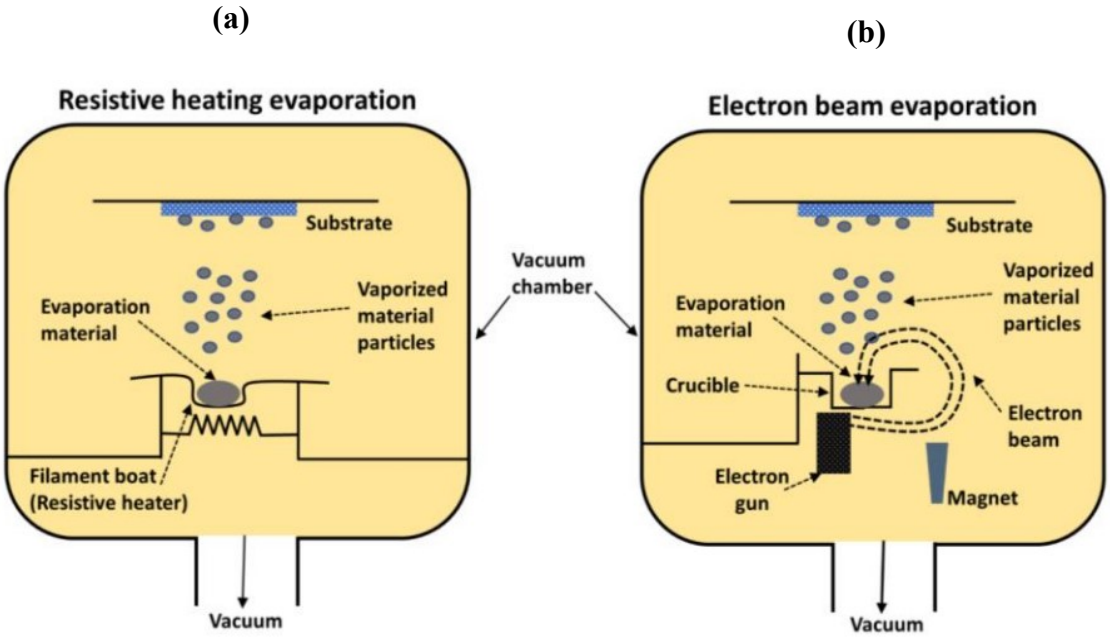

Figure II.9 Schematic representation of: (a) resistive heating, and (b) electron beam evaporation techniques **[46]**.

II.4 Thin film growth

The process of the formation and growth of thin films during the deposition consists of a number of successive stages. This process is strongly related to the deposition rate, substrate temperature, pressure, substrate structure and impurities. These parameters also have a vital impact on many properties of the resulting film such as film density, surface morphology, roughness, grain size, etc **[47, 48]**. The process of formation and growth of thin films can be described in the following sequence **[47, 49, 50]**:

1) In the initial stage, the materials (atoms, molecules, and cluster) to be deposited on the substrate are adsorbed on the substrate surface.

2) The adsorbed species in this step diffuse on the surface until they interact with other species, forming as they are called the nuclei.
3) After the nucleation stage, the nuclei grown in size, forming as they are called the islands.
4) The next stage in the process of film formation and growth is the coalescence stage, in which the formed islands combine together in the aim to form larger islands, decreasing the substrate surface area.
5) In the final stage, further deposition results the formation of a completely continuous film.

II.4.1 Modes of thin film growth

The growth of a thin film on the substrate surface by deposition processes can be classified into three basic growth forms **[51, 28]**:

- Frank-Van der Merwe (FVDM) mode or layer-by-layer growth is occurring as two-dimensional (2D) growth.
- Volmer-Weber (VW) mode or island is characterized by 3D growth that grows in all directions.
- Stranski-Krastanov (SK) mode or layer plus island growth is a mixed 2D/3D growth.

The different growth modes **(figure II.10)** are influenced by many factors, the most crucial of which are the thermodynamics and can be described in terms of the characteristic free surface energy **[51]**.

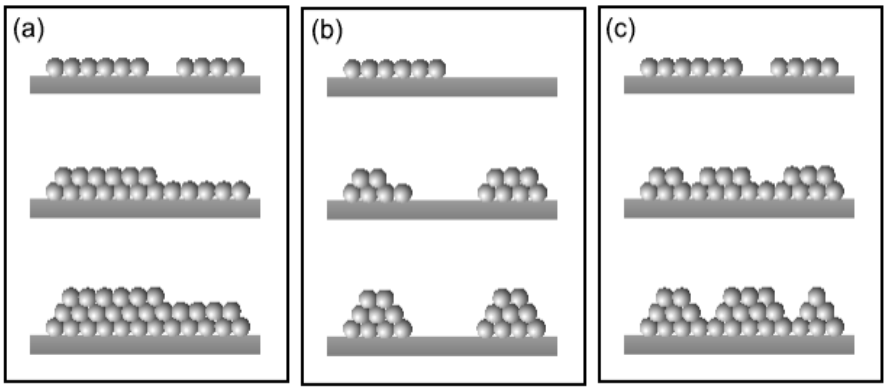

Figure II.10 The different growth modes: (a) Frank-van der Merve;(b) Vollmer-Weber; (c) Stranski-Krastanov **[51]**.

II.5 Antibacterial coatings

Antibacterial or antimicrobial coatings are a potent strategy for inhibiting microbial growth on material surfaces. These coatings offer protection against harmful microorganisms including bacteria, viruses, and fungi that cause infections. Recently, antimicrobial coatings have become an extremely prevalent subject due to their essential role in providing safe life from bacterial contamination, resulting in their wide use in clinical settings, home, industry and hospitals **[52, 53]**. Antibacterial coating systems are created using a variety of thin film coating techniques such as thermal evaporation, sol-gel, magnetron sputtering, chemical vapor deposition (CVD), etc. These coatings contain powerful antimicrobial agents that have the ability to kill or prevent microbes from adhering **[54]**.

II.5.1 Bacterial Attachment

Bacterial attachment is a process of colonizing a surface by bacteria and forming a biofilm due to the physicochemical interactions between microbial cell surface structures and the material surface (substrate) **[55]**. There are two unique stages of bacterial attachment or adhesion to a surface. the first stage of bacterial attachment when bacteria cell get into touch with material surfaces a reversible adhesion occurs, It operates by van der Walls and electrostatic forces, the second stage includes intermolecular interactions between components on the bacterial cell structures and the substrate surface, which produce irreversible bacterial attachment, resulting in biofilm formation **[55-57]**. Bacteria cell surface structure (cell wall components) is an important factor influencing the ways in which organisms adhere to surfaces. Bacteria cell wall surfaces contain carboxyl, amino, and phosphate groups, which give them a net negative charge **[58]**. Most bacteria cell walls can be divided into one of two main categories **(figure II.11)**. Gram-negative bacteria have a thin peptidoglycan cell wall and an outer membrane containing lipopolysaccharides that surrounds the cell. It includes numerous common organisms such as *Escherichia coli*, *Salmonella Morganella, and Pseudomonas*. While Gram-positive bacteria typically have a single membrane covered by a thick peptidoglycan such as *Lactobacillus, Bacillus, Listeria, and Staphylococcus* **[59, 60]**. Furthermore, the substrate surface characteristics, involving surface charge density, wettability, roughness, surface topography and stiffness are also essential parameters affecting bacterial attachment to surfaces and biofilm development. On the other hand, many approaches have been created to inhibit biofilm formation and bacteria growth using an antibacterial surface design based

on the incorporating of antibacterial agents into a coating, which solves the issue of bacterial contamination **[58]**.

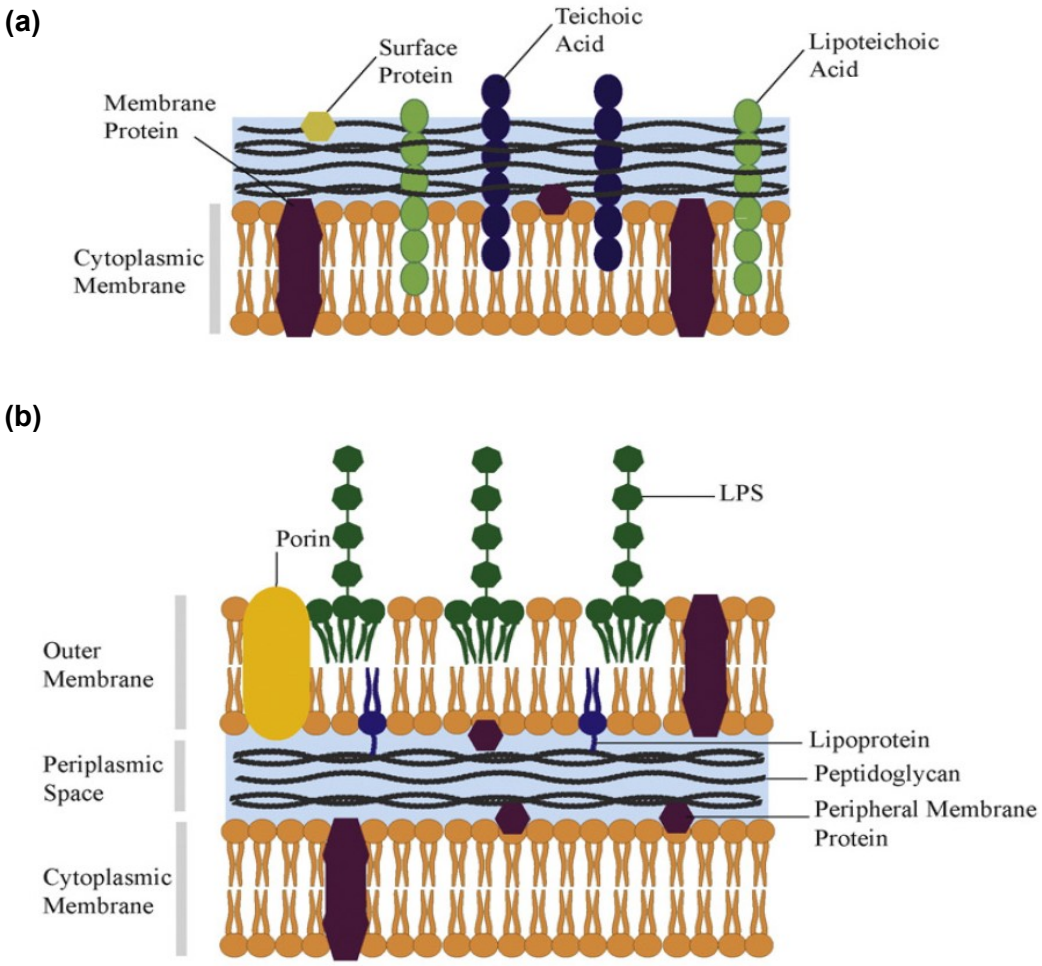

Figure II.11 Schematic diagram comparing (a) Gram-positive and (b) Gram-negative bacteria cell membranes **[61]**.

II.5.2 Antibacterial coating classifications

In order to avoid the spread of bacteria and the development of biofilm, antibacterial coatings are effective strategies and promising candidates against several harmful microorganisms **[62, 63]**. Antibacterial or antimicrobial coatings are classified based on the antibacterial agents or materials included in the coating **(figure II.12)**. They are divided into organic antibacterial coatings such as chlorhexidine, triclosan, polyaniline and polyethylenimine or inorganic antibacterial coatings, which include metals (Fe, Ag, Cu and gold Au) and metal oxides (TiO_2, ZnO and MgO) in their

micro or nano forms, which have been demonstrated to be favorable antibacterial coating agents in different fields, including medicine, food storage, and water treatment **[63, 64]**.

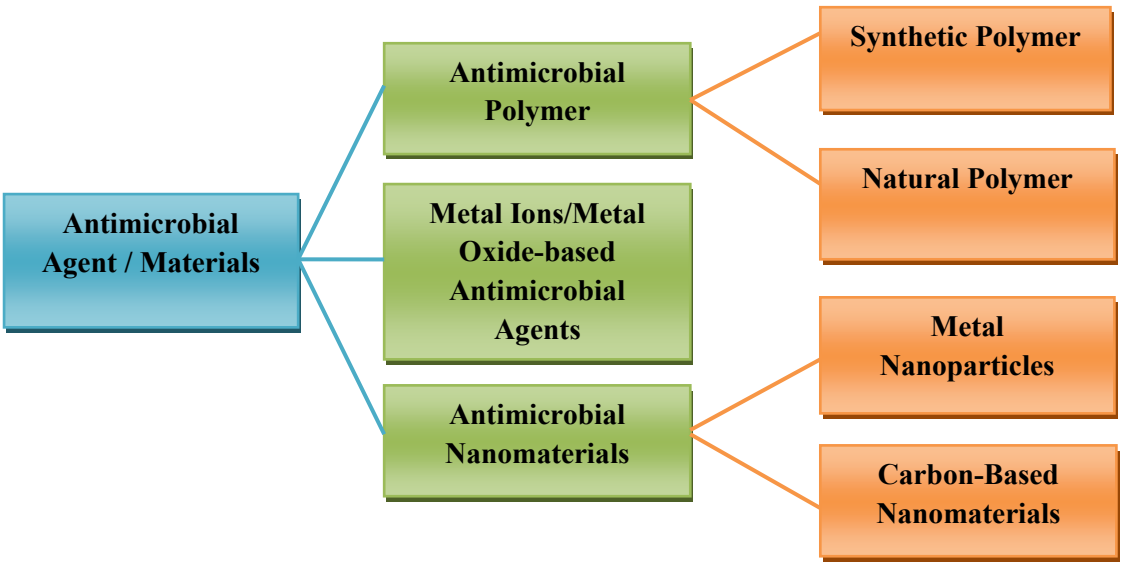

Figure II.12 Classification of different antimicrobial agents /materials for development of antimicrobial surface coating **[63]**.

In this study, the inorganic antibacterial coating agents used, as well as their mechanism of toxicity to bacteria are listed in this section.

II.5.2.1 Titanium dioxide antibacterial coating agent

When a TiO_2 coated surface exposed to UV radiation (wavelength <385nm), its antibacterial activity is activated, leading to the formation of various reactive oxygen species (ROS) such as hydroxyl radicals and hydrogen peroxide **(figure II.13)**, which kills bacteria that attach to a surface **[65]**. The antibacterial ability of TiO_2 semiconductor under UVA light was first proposed by Matsunaga et al **[66]**, Since then, numerous studies have been confirmed that TiO_2 photocatalyst is a powerful agent for killing a variety of microorganisms including Gram-negative and Gram-positive bacteria and fungi **[67- 71]**.

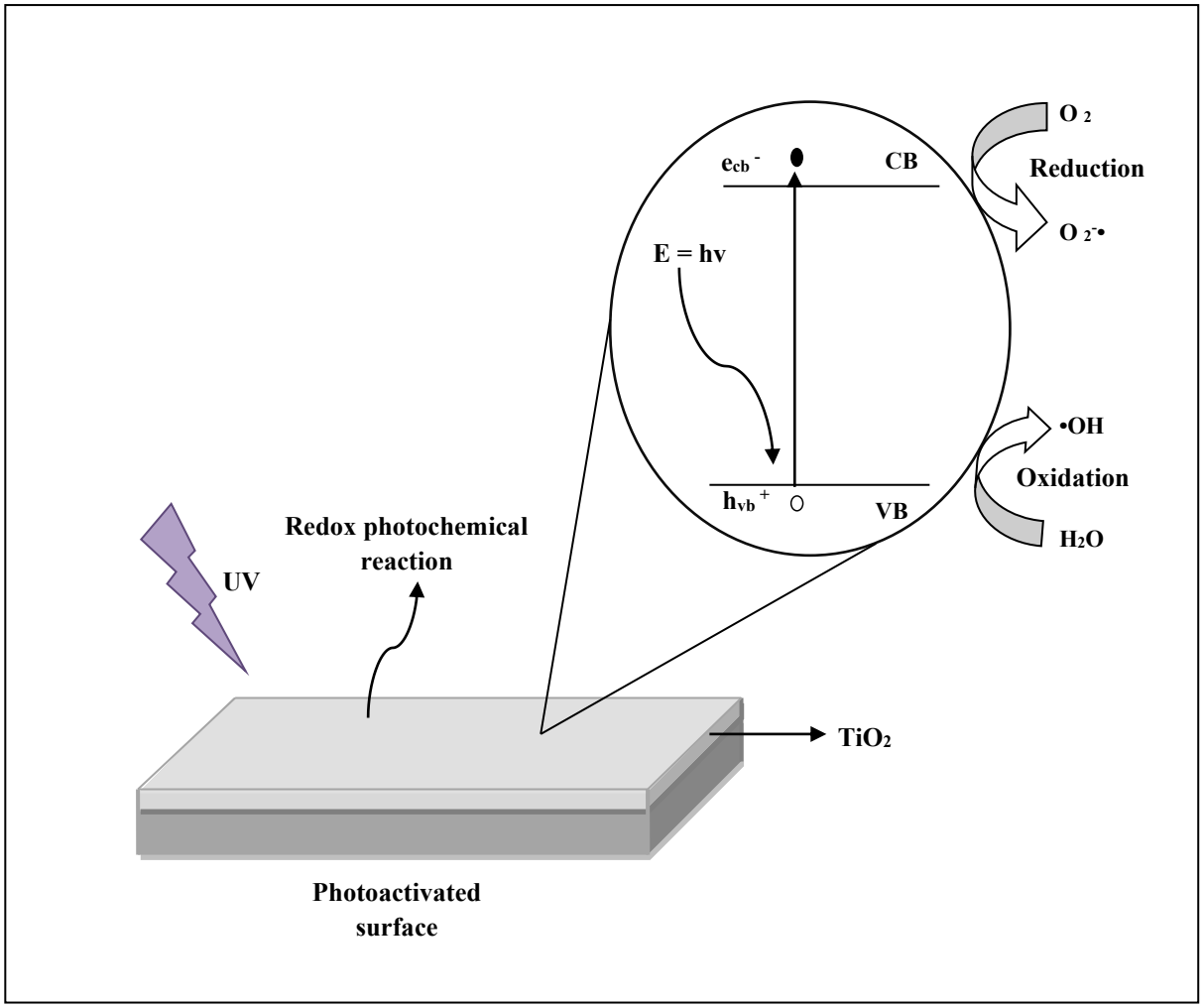

Figure II.13 Schematic representation of a photoactivated surface and the mechanism of photocatalysis of TiO_2 **[71]**.

On the other hand, studies have found that the presence of metal antibacterial agents, such as Cu **[72]**, Pt **[73]**, Fe **[74]**, and Ag **[75]**, improves the killing actions of photocatalyst TiO_2. **Table II.2** presents different studies on pure and modified TiO_2 coated films tested against various microorganisms and their antibacterial applications **[67, 3]**.

Table II.2 Summary on studies of the antibacterial properties of pure and modified TiO_2 coatings synthesized by different methods and their applications.

Coating Composition	**Coating Technique**	**Bacteria/ Microbial Strains**	**Applications**	**Ref.**
Fe-TiO_2 thin film	Sol–gel spin-coating	*Escherichia coli*	Disinfectant treatment of water and air	**[76]**
TiO_2 thin film	Sol-gel dip-coating	*Streptococcus mutans and Porphyromonas gingivali*	Orthodontic application	**[77]**
Fe- or Ag-doped TiO_2– MWCNT nanocomposite thin films	Sol–gel drop coating	*Escherichia coli*	Environmental protection applications	**[78]**
TiO_2 coating	Physical vapor deposition	*Streptococcus mutans*	Orthodontic Wires	**[79]**
Thin film TiO_2	Dip coating	*Escherichia coli K-12 Escherichia coli (ESBL E. coli) (CAH 57), methicillin resistant S. aureus (NCTC 10788), P. aeruginosa (NCTC 10662) and C. difficile (NCTC 11204)*	Surfaces and medical devices	**[80]**
Anatase TiO_2 thin films	Sol–gel and reverse micelle	*Escherichia coli DH5, JM109 and XL1 Blue MRF*	/	**[81]**
Anatase TiO_2 (film) -covered disk	Plasma source ion implantation (PSII)	*Actinobacillus actinomycetemcomitans and Fusobacterium nucleatum*	Dental implants	**[82]**
TiO_2-Coated filters	/	*Escherichiacoli (E. coli),Bacillussubtilis(B. subtilis)endospores,yeastcellsofCandidafamata (C. famata) var. flareri, and spores of Penicillium citrinum (P. citrinum)*	Indoor air quality applications	**[83]**
TiO_2 thin film	Magnetron sputtering	*Escherichia coli 078*	/	**[84]**
TiO_2 coated surface	Sol-gel dip-coating	*Porphyromonas gingivalis*	Orthodontic wires	**[77]**

Ag/TiO_2 nanocomposite thin film	Dip-coating	*Pseudomonas aeruginosa , Staphylococcus aureus , Escherichia coli*	Catheters (medical devices)	**[85]**
TiO_2 coated film	Dip-coating	*Aspergillus niger AS3315*	Coated wood surface	**[86]**
Ag-TiO_2 thin films	Anodic oxidation	*Escherichia coli (strain DH5)*	Water disinfection	**[87]**
Thin surface films of TiO_2, CuO and TiO_2/CuO dual layers	Atmospheric chemical vapour deposition	*Escherichia coli ATCC 10536 and bacteriophage T4*	Applications in the food and healthcare industries	**[88]**
TiO_2 coated soda lime glass	Spray pyrolysis	*Pseudomonas aeruginosa*	/	**[89]**

❖ **Toxicity of photoactivated TiO_2 against bacteria**

TiO_2 antibacterial action is typically related to reactive oxygen species (ROS) with high oxidative potentials **(figure II.14)**. Bacteria cells are damaged by ROS through a variety of mechanisms **[90]**. Numerous research efforts propose that photoactivated TiO_2 toxicity causes damage of the cell wall of bacteria **[91, 92, 65]**. Kiwi and Nadtochenko **[93]** demonstrated that the three major cell wall constituents LPS (lipopolysaccharides), PE (phosphatidyl-ethanolcholine), and PGN (peptidoglycan) of *E. coli* were all peroxidized by TiO_2 surfaces; leading to the death of the bacteria **[65]**. The basic mechanisms suggested by several researchers are as follows **[67, 71, 90, 94]**:

- Disruption of the bacterial cell wall and cytoplasmic membrane due to the potential ROS ($HO^{\bullet}$, $O_2^{\bullet -}$) attack, which is followed by the leakage of cellular components, e.g. cations, and protein, resulting in bacteria cell damage.
- Once the cell wall and cytoplasmic membrane become permeable ROS can penetrate the cell and inactivate internal cell components such as DNA, coenzyme-A... etc leading to bacteria death.

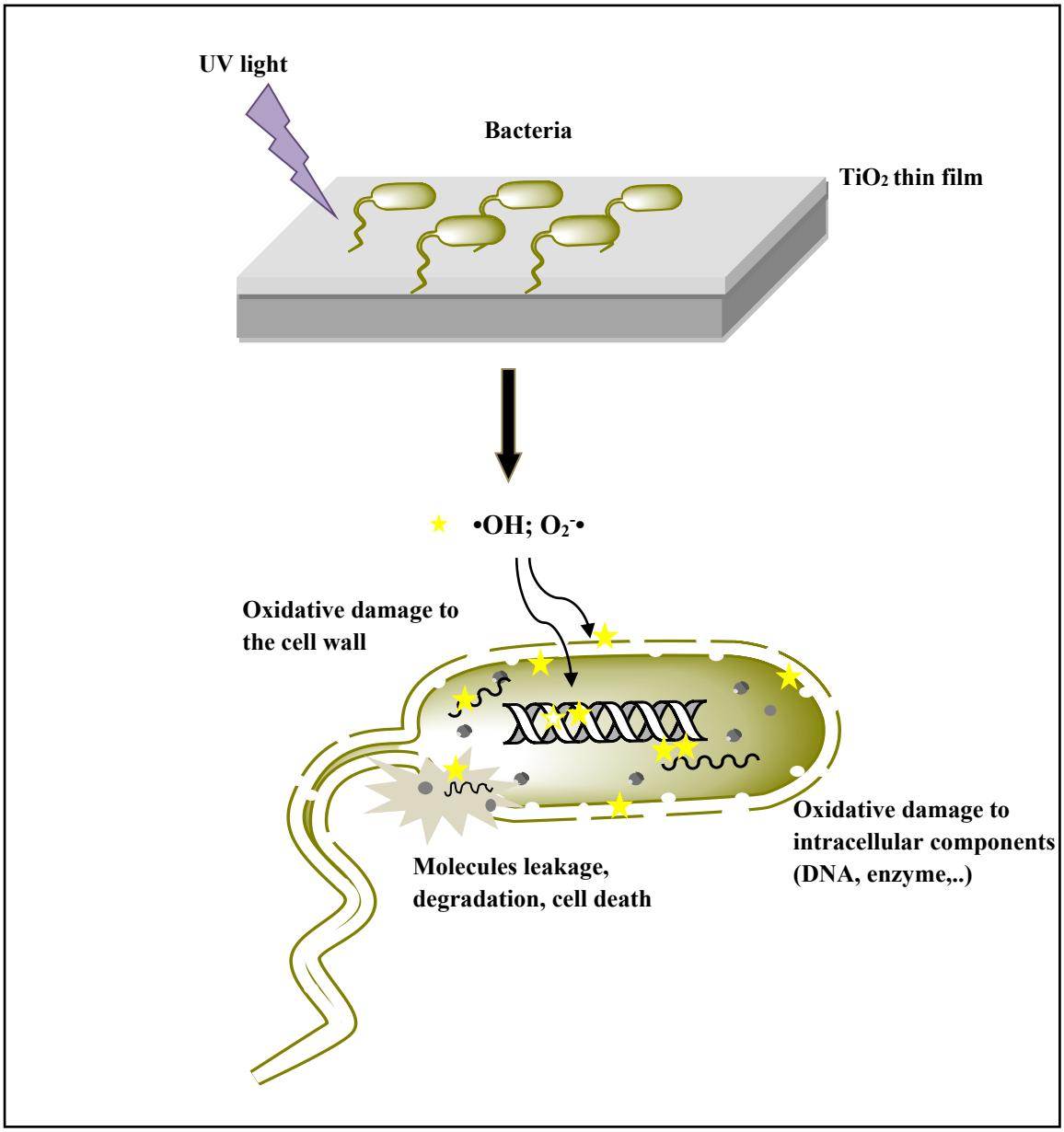

Figure II.14 Mechanism of photocatalytic inactivation of bacteria cell by TiO_2 coated surface **[71]**.

II.5.2.2 Silver coated surface

Silver in its micro or nano forms has been well known for its antibacterial properties for a long time, it is regarded as an antibacterial agent due to its great thermal stability and toxicity effect against a wide range of bacteria, viruses, and fungi **[95, 96]**. Silver coated surfaces are an excellent disinfection systems offer high antibacterial activity, inhibiting biofilm development and inactivating microorganisms, which make them suitable for use

in medical applications as coatings in bone prostheses and surgical devices, as well as disinfection coatings in air/water filters and on touch surfaces **[97]**.

❖ **Mechanisms of silver toxicity**

The antibacterial action of silver is attributed to the silver ion Ag^+ released **[98]**. By reacting with water, bodily fluids, or tissue exudates, silver compounds, metallic silver (particles, and nanoparticles) can be ionized to the active species Ag^+ **[98, 99]**. Jung et al. reported that silver ions have the ability to kill both *Escherichia coli* and *Staphylococcus aureus* pathogenic bacteria **[100]**. The three possible mechanisms of silver toxicity are: a) Ag^+ can attach to bacteria cell by the interaction with thiol groups and protein residues on cell membranes, it has been found that the interaction of silver with thiol groups in enzymes and proteins plays a vital role in the destruction of bacteria **[65, 99]**. b) When Ag^+ penetrates into the bacteria cell, it prevents cell division and disrupt the cell membrane. Moreover, silver ions can produce ROS, which may attack and damage many cellular components **[65, 101]**. C) The intracellular absorption of Ag^+ affects enzyme systems, causing in dysfunctional respiratory processes and also RNA and DNA replication, which results in the death of bacteria **[65, 99]**.

II.5.2.3 Iron and its toxicity

In numerous biological processes, including DNA synthesis and energy metabolism, iron is a necessary element for bacterial existence **[102]**. However, excessive amounts of iron can be fatal to bacterial cells. Under physiological conditions, iron predominantly exists in two reversible redox states **[103]**, the reduced Fe^{2+} and the oxidized Fe^{3+}. Fe^{2+} reacts with H_2O_2 to form ROS such as hydroxyl radicals ($HO^{\bullet}$)through the Fenton reaction **[104]** or by photo-Fenton process when the reaction occurs under light irradiation **[105, 106]**, Fagali et al. **[107]** demonstrated that microorganism cells interacting with Fe particles produced intracellular ROS. The ROS generated are highly oxidizing agents that can damage bacteria cells. Iron and iron oxide can be used as an antibacterial coating to prevent bacteria colonization on material surfaces, especially in healthcare settings including indoor or outdoor spaces, hence reducing pathogens contamination **[106, 108]**. Iron toxicity action is related to $HO^{\bullet}$ radicals, which can kill bacteria by causing oxidation of lipids in the cell membrane and damage protein and DNA, leading to cell death **[103]**.

II.6 Conclusion

We have seen in this chapter that antibacterial coatings are easy to apply using a variety of thin film deposition processes, in particular, the thermal evaporation technique used to make our samples. Furthermore, we will go into more detail about antibacterial coatings consisting of antibacterial agents or materials including TiO_2, Ag and Fe and their mechanism of action, which are regarded to be effective antibacterial systems for killing or inhibiting bacteria colonization, thus reducing numerous environmental and health problems.

References

[1] A. Jilani, M. S. Abdel-wahab, and A. H. Hammad, "Advance Deposition Techniques for Thin Film and Coating," in *Modern Technologies for Creating the Thin-film Systems and Coatings*, N. N. Nikitenkov, Ed., InTech, 2017. doi: 10.5772/65702.

[2] F. Papa, "Foreword," in *Modern Ion Plating Technology*, Elsevier, 2023, pp. xxv–xxvi. doi: 10.1016/C2019-0-03578-9

[3] J. Bącela, M. B. Łabowska, J. Detyna, A. Zięty, and I. Michalak, "Functional Coatings for Orthodontic Archwires—A Review," *Materials*, vol. 13, no. 15, p. 3257, Jul. 2020, doi: 10.3390/ma13153257.

[4] S. Obregón and V. Rodríguez-González, "Photocatalytic TiO2 thin films and coatings prepared by sol–gel processing: a brief review," *J Sol-Gel Sci Technol*, vol. 102, no. 1, pp. 125–141, Apr. 2022, doi: 10.1007/s10971-021-05628-5.

[5] M. O. Abou-Helal and W. T. Seeber, "Preparation of TiO2 thin films by spray pyrolysis to be used as a photocatalyst," *Applied Surface Science*, vol. 195, no. 1–4, pp. 53–62, Jul. 2002, doi: 10.1016/S0169-4332(02)00533-0.

[6] W. Selmi, N. Hosni, J. Ben Naceur, H. Maghraoui-Meherzi, and R. Chtourou, "Titanium Dioxide Thin Films for Environmental Applications," in *Titanium Dioxide - Advances and Applications*, H. Muhammad Ali, Ed., IntechOpen, 2022. doi: 10.5772/intechopen.99726.

[7] A. Arunachalam, S. Dhanapandian, C. Manoharan, and G. Sivakumar, "Physical properties of Zn doped TiO2 thin films with spray pyrolysis technique and its effects in antibacterial activity," *Spectrochimica Acta Part A: Molecular and Biomolecular Spectroscopy*, vol. 138, pp. 105–112, Mar. 2015, doi: 10.1016/j.saa.2014.11.016.

[8] M. B. Tahir, M. Rafique, M. S. Rafique, T. Nawaz, M. Rizwan, and M. Tanveer, "Photocatalytic nanomaterials for degradation of organic pollutants and heavy metals," in *Nanotechnology and Photocatalysis for Environmental Applications*, Elsevier, 2020, pp. 119–138. doi: 10.1016/B978-0-12-821192-2.00008-5.

[9] H. A. Hadi, "Fabrication and electrical properties of FTO Nano-particles/Nanocrystal porous silicon heterojunction under gamma radiation effect," *Mater. Sci.: An Indian J*, vol. 12, no. 3, pp. 100–106, 2015.

[10] P. Fornasiero and M. Cargnello, Eds., *Morphological, compositional, and shape control of materials for catalysis*. in Studies in surface science and catalysis, no. volume 177. Amsterdam Oxford Cambridge: Elsevier, 2017.

[11] M. I. Khan, K. A. Bhatti, R. Qindeel, L. G. Bousiakou, N. Alonizan, and Fazal-e-Aleem, "Investigations of the structural, morphological and electrical properties of multilayer ZnO/TiO 2 thin films, deposited by sol–gel technique," *Results in Physics*, vol. 6, pp. 156–160, 2016, doi: 10.1016/j.rinp.2016.01.015.

[12] G. Bahuguna, N. Kumar Mishra, P. Chaudhary, A. Kumar, and R. Singh, "Thin Film Coating through Sol-Gel Technique," *Res. J. Chem. Sci*, vol. 6, no. 7, Jul. 2016.

[13] L. Znaidi, "Sol–gel-deposited ZnO thin films: A review," *Materials Science and Engineering: B*, vol. 174, no. 1–3, pp. 18–30, Oct. 2010, doi: 10.1016/j.mseb.2010.07.001.

[14] D. Liu, Z. Chen, A. Cao, H. Zhang, and Y. Li, "2D Colloidal assembly," in *Encyclopedia of Nanomaterials*, vol. 3, Elsevier, 2023, pp. 198–213. doi: 10.1016/B978-0-12-822425-0.00078-6.

[15] C.-C. Chang, J.-Y. Chen, T.-L. Hsu, C.-K. Lin, and C.-C. Chan, "Photocatalytic properties of porous TiO2/Ag thin films," *Thin Solid Films*, vol. 516, no. 8, pp. 1743–1747, Feb. 2008, doi: 10.1016/j.tsf.2007.05.033.

[16] G. Amokrane, C. Falentin-Daudré, S. Ramtani, and V. Migonney, "A Simple Method to Functionalize PCL Surface by Grafting Bioactive Polymers Using UV Irradiation," *IRBM*, vol. 39, no. 4, pp. 268–278, Aug. 2018, doi: 10.1016/j.irbm.2018.07.002.

[17] K. Ubonchonlakate, L. Sikong, and F. Saito, "Photocatalytic disinfection of P.aeruginosa bacterial Ag-doped TiO2 film," *Procedia Engineering*, vol. 32, pp. 656–662, 2012, doi: 10.1016/j.proeng.2012.01.1323.

[18] M. Joshi and B. S. Butola, "Application technologies for coating, lamination and finishing of technical textiles," in *Advances in the Dyeing and Finishing of Technical Textiles*, Elsevier, 2013, pp. 355–411. doi: 10.1533/9780857097613.2.355.

[19] A. Nande, N. T. Kalyani, A. Tiwari, and S. J. Dhoble, "Exploring the world of functional materials," in *Functional Materials from Carbon, Inorganic, and Organic Sources*, Elsevier, 2023, pp. 1–19. doi: 10.1016/B978-0-323-85788-8.00014-8.

[20] A. Behera, P. Mallick, and S. S. Mohapatra, "Nanocoatings for anticorrosion," in *Corrosion Protection at the Nanoscale*, Elsevier, 2020, pp. 227–243. doi: 10.1016/B978-0-12-819359-4.00013-1.

[21] H. Sun *et al.*, "Photocatalytic TiO2 films prepared by chemical vapor deposition at atmosphere pressure," *Journal of Non-Crystalline Solids*, vol. 354, no. 12–13, pp. 1440–1443, Feb. 2008, doi: 10.1016/j.jnoncrysol.2007.01.108.

[22] H. Katsui and T. Goto, "Chemical Vapor Deposition," in *Multi-dimensional Additive Manufacturing*, S. Kirihara and K. Nakata, Eds., Singapore: Springer Singapore, 2021, pp. 75–95. doi: 10.1007/978-981-15-7910-3_6.

[23] K. V. Madhuri, "Thermal protection coatings of metal oxide powders," in *Metal Oxide Powder Technologies*, Elsevier, 2020, pp. 209–231. doi: 10.1016/B978-0-12-817505-7.00010-5.

[24] I. V. Tudose *et al.*, "Chemical and physical methods for multifunctional nanostructured interface fabrication," in *Functional Nanostructured Interfaces for Environmental and Biomedical Applications*, Elsevier, 2019, pp. 15–26. doi: 10.1016/B978-0-12-814401-5.00002-5.

[25] D. Gospodonova, I. Ivanova, and T. Vladkova, "Fabrication and Characterization of Antimicrobial Magnetron Cosputtered TiO2/Ag/Cu Composite Coatings," *Coatings*, vol. 11, no. 4, p. 473, Apr. 2021, doi: 10.3390/coatings11040473.

[26] F. Antoni and F. Stock, "Laser engineering of carbon materials for optoelectronic applications," in *Laser Annealing Processes in Semiconductor Technology*, Elsevier, 2021, pp. 293–321. doi: 10.1016/B978-0-12-820255-5.00005-2.

[27] L. Zhao, M. Han, and J. Lian, "Photocatalytic activity of TiO2 films with mixed anatase and rutile structures prepared by pulsed laser deposition," *Thin Solid Films*, vol. 516, no. 10, pp. 3394–3398, Mar. 2008, doi: 10.1016/j.tsf.2007.10.102.

[28] S. N. Ogugua, O. M. Ntwaeaborwa, and H. C. Swart, "Latest Development on Pulsed Laser Deposited Thin Films for Advanced Luminescence Applications," *Coatings*, vol. 10, no. 11, p. 1078, Nov. 2020, doi: 10.3390/coatings10111078.

[29] A. Bashir, T. I. Awan, A. Tehseen, M. B. Tahir, and M. Ijaz, "Interfaces and surfaces," in *Chemistry of Nanomaterials*, Elsevier, 2020, pp. 51–87. doi: 10.1016/B978-0-12-818908-5.00003-2.

[30] F. Lévy, "Film Growth and Epitaxy: Methods," in *Reference Module in Materials Science and Materials Engineering*, Elsevier, 2016, p. B9780128035818010122. doi: 10.1016/B978-0-12-803581-8.01012-2.

[31] SAM Sputter Targets Stanford Advanced Materials. Available: http://www.sputtering-targets.net/blog/history-of-thermal-evaporation-for-thin-film-coating

[32] B. Abdallah, M. Kakhia, W. Zetoun, and N. Alkafri, "PbS doped ZnO nanowires films synthesis by thermal evaporation method: Morphological, structural and optical

properties," *Microelectronics Journal*, vol. 111, p. 105045, May 2021, doi: 10.1016/j.mejo.2021.105045.

[33] K. Abidin *et al.*, "Optimization of Ag catalyst growth by vacuum thermal evaporation," *Fullerenes, Nanotubes and Carbon Nanostructures*, vol. 29, no. 9, pp. 695–702, Sep. 2021, doi: 10.1080/1536383X.2021.1881775.

[34] A. K. Vishwakarma, N. K. Yadav, A. K. Sharma, P. Yadav, S. K. Yadav, and L. Yadava, "Morphological and electronic properties of titanium dioxide thin film," *Materials Today: Proceedings*, vol. 42, pp. 1642–1646, 2021, doi: 10.1016/j.matpr.2020.07.474.

[35] S. Durdu *et al.*, "Characterization and in vitro properties of anti-bacterial Ag-based bioceramic coatings formed on zirconium by micro arc oxidation and thermal evaporation," *Surface and Coatings Technology*, vol. 331, pp. 107–115, Dec. 2017, doi: 10.1016/j.surfcoat.2017.10.023.

[36] Y. Lei *et al.*, "Thermal Evaporation of Large-Area SnS_2 Thin Films with a UV-to-NIR Photoelectric Response for Flexible Photodetector Applications," *ACS Appl. Mater. Interfaces*, vol. 12, no. 22, pp. 24940–24950, Jun. 2020, doi: 10.1021/acsami.0c01781.

[37] H. Song *et al.*, "Rapid thermal evaporation of Bi2S3 layer for thin film photovoltaics," *Solar Energy Materials and Solar Cells*, vol. 146, pp. 1–7, Mar. 2016, doi: 10.1016/j.solmat.2015.11.019.

[38] E. Peksu and H. Karaagac, "Characterization of Cu2ZnSnS4 thin films deposited by one-step thermal evaporation for a third generation solar cell," *Journal of Alloys and Compounds*, vol. 862, p. 158503, May 2021, doi: 10.1016/j.jallcom.2020.158503.

[39] E. L. Cuéllar, A. Martínez-de La Cruz, K. H. L. Rodríguez, and U. O. Méndez, "Preparation of γ-Bi2MoO6 thin films by thermal evaporation deposition and characterization for photocatalytic applications," *Catalysis Today*, vol. 166, no. 1, pp. 140–145, May 2011, doi: 10.1016/j.cattod.2010.05.005.

[40] A. Arfaoui, S. Touihri, A. Mhamdi, A. Labidi, and T. Manoubi, "Structural, morphological, gas sensing and photocatalytic characterization of MoO3 and WO3 thin films prepared by the thermal vacuum evaporation technique," *Applied Surface Science*, vol. 357, pp. 1089–1096, Dec. 2015, doi: 10.1016/j.apsusc.2015.09.124.

[41] P. H. Li and P. K. Chu, "Thin film deposition technologies and processing of biomaterials," in *Thin Film Coatings for Biomaterials and Biomedical Applications*, Elsevier, 2016, pp. 3–28. doi: 10.1016/B978-1-78242-453-6.00001-8.

[42] K. Wasa, M. Kitabatake, and H. Adachi, “Thin Film Processes,” in *Thin Film Materials Technology*, Elsevier, 2004, pp. 17–69. doi: 10.1016/B978-081551483-1.50003-4.

[43] M. Hughes, “what is thin film deposition by thermal evaporation ?,” 2013. Available: https://www.semicore.com/news/71-thin-film-deposition-thermal-evaporation

[44] D. Suthar, S. Chuhadiya, R. Sharma, Himanshu, and M. S. Dhaka, “An overview on the role of ZnTe as an efficient interface in CdTe thin film solar cells: a review,” *Mater. Adv.*, vol. 3, no. 22, pp. 8081–8107, 2022, doi: 10.1039/D2MA00817C.

[45] J. Shinar, R. Shinar, and Rj. Groarke, “An Overview of Organic Light-Emitting Diodes and their Applications,” in *Reference Module in Materials Science and Materials Engineering*, Elsevier, 2016, p. B9780128035818092547. doi: 10.1016/B978-0-12-803581-8.09254-7.

[46] S. Jena and N. K. Sahoo, “Evolutionary Design, Deposition and Characterization Techniques for Interference Optical Thin-Film Multilayer Coatings and Devices,” in *Recent Advances in Thin Films*, S. Kumar and D. K. Aswal, Eds., in Materials Horizons: From Nature to Nanomaterials. , Singapore: Springer Singapore, 2020, pp. 281–343. doi: 10.1007/978-981-15-6116-0_10.

[47] J. Zhu, X. Zhu, H. Liu, and J. Xing, “Formation and Growth of Thin Films,” in *Thin Film Physics and Devices*, WORLD SCIENTIFIC, 2021, pp. 297–360. doi: 10.1142/9789811223990_0005.

[48] M. Beigmohamadi, “Growth, structure and morphology of organic thin films,” thesis, Tehran/Iran, 2007.

[49] M. Ghougali, “Elaboration and characterization of nanostructuring NiO thin films for gas sensing applications,” thesis, University of Mohamed Khider,Biskra, Biskra, 2019.

[50] H. Liu, “Growth Kinetics of Thin Film Epitaxy,” in *21st Century Surface Science - a Handbook*, P. Pham, P. Goel, S. Kumar, and K. Yadav, Eds., IntechOpen, 2020. doi: 10.5772/intechopen.91224.

[51] H. L. Brown, “The Properties and Performance of Moisture/Oxygen Barrier Layers Deposited by Remote Plasma Sputtering .,” thesis, University of Surrey, 2015.

[52] M. Casini, “Advanced construction materials,” in *Construction 4.0*, Elsevier, 2022, pp. 337–404. doi: 10.1016/B978-0-12-821797-9.00005-2.

[53] "Antimicrobial surface." Available: https://en.wikipedia.org/wiki/Antimicrobial_surface

[54] Z. Li and K. Aik Khor, "Preparation and Properties of Coatings and Thin Films on Metal Implants," in *Encyclopedia of Biomedical Engineering*, Elsevier, 2019, pp. 203–212. doi: 10.1016/B978-0-12-801238-3.11025-6.

[55] K. Page, "Photocatalytic Thin films Their Caracterisation and Antimicrobial Properties," thesis, University college London, 2009.

[56] A. S. Sant'Ana, F. F. P. Silva, D. F. Maffei, and B. D. G. M. Franco, "FRUITS AND VEGETABLES | Introduction," in *Encyclopedia of Food Microbiology* -, Elsevier, 2014, pp. 972–982. doi: 10.1016/B978-0-12-384730-0.00427-4.

[57] X. Zhang, L. Wang, and E. Levänen, "Superhydrophobic surfaces for the reduction of bacterial adhesion," *RSC Adv.*, vol. 3, no. 30, p. 12003, 2013, doi: 10.1039/c3ra40497h.

[58] S. Zheng *et al.*, "Implication of Surface Properties, Bacterial Motility, and Hydrodynamic Conditions on Bacterial Surface Sensing and Their Initial Adhesion," *Front. Bioeng. Biotechnol.*, vol. 9, p. 643722, Feb. 2021, doi: 10.3389/fbioe.2021.643722.

[59] T. J. Silhavy, D. Kahne, and S. Walker, "The Bacterial Cell Envelope," *Cold Spring Harbor Perspectives in Biology*, vol. 2, no. 5, p. a000414, May 2010, doi: 10.1101/cshperspect.a000414.

[60] "Gram stain." Available: https://en.wikipedia.org/wiki/Gram_stain

[61] R. M. Epand, C. Walker, R. F. Epand, and N. A. Magarvey, "Molecular mechanisms of membrane targeting antibiotics," *Biochimica et Biophysica Acta (BBA) - Biomembranes*, vol. 1858, no. 5, pp. 980–987, May 2016, doi: 10.1016/j.bbamem.2015.10.018.

[62] S. M. Imani, L. Ladouceur, T. Marshall, R. Maclachlan, L. Soleymani, and T. F. Didar, "Antimicrobial Nanomaterials and Coatings: Current Mechanisms and Future Perspectives to Control the Spread of Viruses Including SARS-CoV-2," *ACS Nano*, vol. 14, no. 10, pp. 12341–12369, Oct. 2020, doi: 10.1021/acsnano.0c05937.

[63] N. Nasri *et al.*, "Past and Current Progress in the Development of Antiviral/Antimicrobial Polymer Coating towards COVID-19 Prevention: A Review," *Polymers*, vol. 13, no. 23, p. 4234, Dec. 2021, doi: 10.3390/polym13234234.

[64] S. Saidin, M. A. Jumat, N. A. A. Mohd Amin, and A. S. Saleh Al-Hammadi, "Organic and inorganic antibacterial approaches in combating bacterial infection for

biomedical application," *Materials Science and Engineering: C*, vol. 118, p. 111382, Jan. 2021, doi: 10.1016/j.msec.2020.111382.

[65] S. Omar Elfakhri, "Antibacterial Activity of Novel Self-Disinfecting Surface Coatings," thesis, University of Salford, 2014.

[66] T. Matsunaga, R. Tomoda, T. Nakajima, and H. Wake, "Photoelectrochemical sterilization of microbial cells by semiconductor powders," *FEMS Microbiology Letters*, vol. 29, no. 1–2, pp. 211–214, 1985.

[67] H. A. Foster, I. B. Ditta, S. Varghese, and A. Steele, "Photocatalytic disinfection using titanium dioxide: spectrum and mechanism of antimicrobial activity," *Appl Microbiol Biotechnol*, vol. 90, no. 6, pp. 1847–1868, Jun. 2011, doi: 10.1007/s00253-011-3213-7.

[68] T. P. T. Cushnie *et al.*, "Photobactericidal effects of TiO2 thin films at low temperatures—A preliminary study," *Journal of Photochemistry and Photobiology A: Chemistry*, vol. 216, no. 2–3, pp. 290–294, Dec. 2010, doi: 10.1016/j.jphotochem.2010.06.027.

[69] J. A. Ibáñez, M. I. Litter, and R. A. Pizarro, "Photocatalytic bactericidal effect of TiO2 on Enterobacter cloacae," *Journal of Photochemistry and Photobiology A: Chemistry*, vol. 157, no. 1, pp. 81–85, Apr. 2003, doi: 10.1016/S1010-6030(03)00074-1.

[70] P. S. M. Dunlop, J. A. Byrne, N. Manga, and B. R. Eggins, "The photocatalytic removal of bacterial pollutants from drinking water," *Journal of Photochemistry and Photobiology A: Chemistry*, vol. 148, no. 1–3, pp. 355–363, May 2002, doi: 10.1016/S1010-6030(02)00063-1.

[71] N. Bono, F. Ponti, C. Punta, and G. Candiani, "Effect of UV Irradiation and TiO2-Photocatalysis on Airborne Bacteria and Viruses: An Overview," *Materials*, vol. 14, no. 5, p. 1075, Feb. 2021, doi: 10.3390/ma14051075.

[72] K. Sunada, T. Watanabe, and K. Hashimoto, "Bactericidal Activity of Copper-Deposited TiO $_2$ Thin Film under Weak UV Light Illumination," *Environ. Sci. Technol.*, vol. 37, no. 20, pp. 4785–4789, Oct. 2003, doi: 10.1021/es034106g.

[73] B. Pal, I. Singh, K. Angrish, R. Aminedi, and N. Das, "Rapid photokilling of gram-negative Escherichia coli bacteria by platinum dispersed titania nanocomposite films," *Materials Chemistry and Physics*, vol. 136, no. 1, pp. 21–27, Sep. 2012, doi: 10.1016/j.matchemphys.2012.06.001.

[74] S. M. H. AL-Jawad, A. A. Taha, and M. M. Salim, "Synthesis and characterization of pure and Fe doped TiO2 thin films for antimicrobial activity," *Optik*, vol. 142, pp. 42–53, Aug. 2017, doi: 10.1016/j.ijleo.2017.05.048.

[75] Y. Liu, X. Wang, F. Yang, and X. Yang, "Excellent antimicrobial properties of mesoporous anatase TiO2 and Ag/TiO2 composite films," *Microporous and Mesoporous Materials*, vol. 114, no. 1–3, pp. 431–439, Sep. 2008, doi: 10.1016/j.micromeso.2008.01.032.

[76] U. Arellano, M. Asomoza, and F. Ramírez, "Antimicrobial activity of Fe–TiO2 thin film photocatalysts," *Journal of Photochemistry and Photobiology A: Chemistry*, vol. 222, no. 1, pp. 159–165, Jul. 2011, doi: 10.1016/j.jphotochem.2011.05.016.

[77] M.-J. Chun *et al.*, "Surface modification of orthodontic wires with photocatalytic titanium oxide for its antiadherent and antibacterial properties," *Angle Orthod*, vol. 77, no. 3, pp. 483–488, May 2007, doi: 10.2319/0003-3219(2007)077[0483:SMOOWW]2.0.CO;2.

[78] Md. A. Hossain *et al.*, "Synthesis of Fe- or Ag-doped TiO2–MWCNT nanocomposite thin films and their visible-light-induced catalysis of dye degradation and antibacterial activity," *Res Chem Intermed*, vol. 44, no. 4, pp. 2667–2683, Apr. 2018, doi: 10.1007/s11164-018-3253-z.

[79] V. Mollabashi *et al.*, "Effects of TiO_2-Coated Stainless Steel Orthodontic Wires on Streptococcus mutans Bacteria: A Clinical Study," *IJN*, vol. Volume 15, pp. 8759–8766, Nov. 2020, doi: 10.2147/IJN.S258440.

[80] P. S. M. Dunlop, C. P. Sheeran, J. A. Byrne, M. A. S. McMahon, M. A. Boyle, and K. G. McGuigan, "Inactivation of clinically relevant pathogens by photocatalytic coatings," *Journal of Photochemistry and Photobiology A: Chemistry*, vol. 216, no. 2–3, pp. 303–310, Dec. 2010, doi: 10.1016/j.jphotochem.2010.07.004.

[81] J. C. Yu *et al.*, "Bactericidal and photocatalytic activities of TiO2 thin films prepared by sol–gel and reverse micelle methods," *Journal of Photochemistry and Photobiology A: Chemistry*, vol. 153, no. 1–3, pp. 211–219, Nov. 2002, doi: 10.1016/S1010-6030(02)00275-7.

[82] N. Suketa *et al.*, "An Antibacterial Surface on Dental Implants, Based on the Photocatalytic Bactericidal Effect," *Clin Implant Dent Rel Res*, vol. 7, no. 2, pp. 105–111, Apr. 2005, doi: 10.1111/j.1708-8208.2005.tb00053.x.

[83] C.-Y. Lin and C.-S. Li, "Effectiveness of Titanium Dioxide Photocatalyst Filters for Controlling Bioaerosols," *Aerosol Science and Technology*, vol. 37, no. 2, pp. 162–170, Feb. 2003, doi: 10.1080/02786820300951.

[84] Y.-L. Choi, S.-H. Kim, Y.-S. Song, and D. Y. Lee, "Photodecomposition and bactericidal effects of TiO_2 thin films prepared by a magnetron sputtering," *Journal of Materials Science*, vol. 39, no. 18, pp. 5695–5699, Sep. 2004, doi: 10.1023/B:JMSC.0000040078.09843.cb.

[85] Y. Yao, Y. Ohko, Y. Sekiguchi, A. Fujishima, and Y. Kubota, "Self-sterilization using silicone catheters coated with Ag and TiO_2 nanocomposite thin film," *J Biomed Mater Res*, vol. 85B, no. 2, pp. 453–460, May 2008, doi: 10.1002/jbm.b.30965.

[86] F. Chen, X. Yang, and Q. Wu, "Antifungal capability of TiO2 coated film on moist wood," *Building and Environment*, vol. 44, no. 5, pp. 1088–1093, May 2009, doi: 10.1016/j.buildenv.2008.07.018.

[87] D. Wu, H. You, D. Jin, and X. Li, "Enhanced inactivation of Escherichia coli with Ag-coated TiO2 thin film under UV-C irradiation," *Journal of Photochemistry and Photobiology A: Chemistry*, vol. 217, no. 1, pp. 177–183, Jan. 2011, doi: 10.1016/j.jphotochem.2010.10.006.

[88] I. B. Ditta *et al.*, "Photocatalytic antimicrobial activity of thin surface films of TiO2, CuO and TiO2/CuO dual layers on Escherichia coli and bacteriophage T4," *Appl Microbiol Biotechnol*, vol. 79, no. 1, pp. 127–133, May 2008, doi: 10.1007/s00253-008-1411-8.

[89] P. Amézaga-Madrid, G. Nevarez-Moorillon, E. Orrantia-Borunda, and M. Miki-Yoshida, "Photoinduced bactericidal activity against Pseudomonas aeruginosa by TiO2 based thin films," *FEMS Microbiology Letters*, vol. 211, no. 2, pp. 183–188, Jun. 2002, doi: 10.1016/S0378-1097(02)00686-9.

[90] C. López De Dicastillo, M. Guerrero Correa, F. B. Martínez, C. Streitt, and M. José Galotto, "Antimicrobial Effect of Titanium Dioxide Nanoparticles," in *Antimicrobial Resistance - A One Health Perspective*, M. Mareș, S. Hua Erin Lim, K.-S. Lai, and R.-T. Cristina, Eds., IntechOpen, 2021. doi: 10.5772/intechopen.90891.

[91] J. Kiwi, S. Rtimi, R. Sanjines, and C. Pulgarin, "TiO_2 and TiO_2 -Doped Films Able to Kill Bacteria by Contact: New Evidence for the Dynamics of Bacterial Inactivation in the Dark and under Light Irradiation," *International Journal of Photoenergy*, vol. 2014, pp. 1–17, 2014, doi: 10.1155/2014/785037.

[92] P.-C. Maness, S. Smolinski, D. M. Blake, Z. Huang, E. J. Wolfrum, and W. A. Jacoby, "Bactericidal Activity of Photocatalytic TiO $_2$ Reaction: toward an Understanding of Its Killing Mechanism," *Appl Environ Microbiol*, vol. 65, no. 9, pp. 4094–4098, Sep. 1999, doi: 10.1128/AEM.65.9.4094-4098.1999.

[93] J. Kiwi and V. Nadtochenko, "Evidence for the Mechanism of Photocatalytic Degradation of the Bacterial Wall Membrane at the TiO $_2$ Interface by ATR-FTIR and Laser Kinetic Spectroscopy," *Langmuir*, vol. 21, no. 10, pp. 4631–4641, May 2005, doi: 10.1021/la046983l.

[94] K. Sunada, T. Watanabe, and K. Hashimoto, "Studies on photokilling of bacteria on TiO2 thin film," *Journal of Photochemistry and Photobiology A: Chemistry*, vol. 156, no. 1–3, pp. 227–233, Mar. 2003, doi: 10.1016/S1010-6030(02)00434-3.

[95] A. Sadeghnejad, A. Aroujalian, A. Raisi, and S. Fazel, "Antibacterial nano silver coating on the surface of polyethylene films using corona discharge," *Surface and Coatings Technology*, vol. 245, pp. 1–8, Apr. 2014, doi: 10.1016/j.surfcoat.2014.02.023.

[96] N. Durán, M. Durán, M. B. de Jesus, A. B. Seabra, W. J. Fávaro, and G. Nakazato, "Silver nanoparticles: A new view on mechanistic aspects on antimicrobial activity," *Nanomedicine: Nanotechnology, Biology and Medicine*, vol. 12, no. 3, pp. 789–799, Apr. 2016, doi: 10.1016/j.nano.2015.11.016.

[97] S. Agnihotri, S. Mukherji, and S. Mukherji, "Immobilized silver nanoparticles enhance contact killing and show highest efficacy: elucidation of the mechanism of bactericidal action of silver," *Nanoscale*, vol. 5, no. 16, p. 7328, 2013, doi: 10.1039/c3nr00024a.

[98] R. Kumar and H. Münstedt, "Silver ion release from antimicrobial polyamide/silver composites," *Biomaterials*, vol. 26, no. 14, pp. 2081–2088, May 2005, doi: 10.1016/j.biomaterials.2004.05.030.

[99] A. B. G. Lansdown, "Silver in Health Care: Antimicrobial Effects and Safety in Use," in *Current Problems in Dermatology*, vol. 33, U.-C. Hipler and P. Elsner, Eds., Basel: KARGER, 2006, pp. 17–34. doi: 10.1159/000093928.

[100] W. K. Jung, H. C. Koo, K. W. Kim, S. Shin, S. H. Kim, and Y. H. Park, "Antibacterial Activity and Mechanism of Action of the Silver Ion in *Staphylococcus aureus* and *Escherichia coli*," *Appl Environ Microbiol*, vol. 74, no. 7, pp. 2171–2178, Apr. 2008, doi: 10.1128/AEM.02001-07.

[101] B. Sharma *et al.*, "Antimicrobial Agents Based on Metal Complexes: Present Situation and Future Prospects," *International Journal of Biomaterials*, vol. 2022, pp. 1–21, Dec. 2022, doi: 10.1155/2022/6819080.

[102] S. Dev and J. L. Babitt, "Overview of iron metabolism in health and disease," *Hemodialysis International*, vol. 21, pp. s6–s20, Apr. 2017, doi: 10.1111/hdi.12542.

[103] M. Godoy-Gallardo *et al.*, "Antibacterial approaches in tissue engineering using metal ions and nanoparticles: From mechanisms to applications," *Bioactive Materials*, vol. 6, no. 12, pp. 4470–4490, Dec. 2021, doi: 10.1016/j.bioactmat.2021.04.033.

[104] H. J. H. Fenton, "Oxidation of tartaric acid in presence of iron," *J. Chem. Soc., Trans.*, vol. 65, pp. 899–910, 1894, doi: 10.1039/CT8946500899.

[105] S. V. Gudkov, D. E. Burmistrov, D. A. Serov, M. B. Rebezov, A. A. Semenova, and A. B. Lisitsyn, "Do Iron Oxide Nanoparticles Have Significant Antibacterial Properties?," *Antibiotics*, vol. 10, no. 7, p. 884, Jul. 2021, doi: 10.3390/antibiotics10070884.

[106] E. Scarcello, A. Herpain, M. Tomatis, F. Turci, P. J. Jacques, and D. Lison, "Hydroxyl radicals and oxidative stress: the dark side of Fe corrosion," *Colloids and Surfaces B: Biointerfaces*, vol. 185, p. 110542, Jan. 2020, doi: 10.1016/j.colsurfb.2019.110542.

[107] N. S. Fagali, C. A. Grillo, S. Puntarulo, and M. A. Fernández Lorenzo De Mele, "Is there any difference in the biological impact of soluble and insoluble degradation products of iron-containing biomaterials?," *Colloids and Surfaces B: Biointerfaces*, vol. 160, pp. 238–246, Dec. 2017, doi: 10.1016/j.colsurfb.2017.09.032.

[108] L. V. Suárez Murillo, A. Schärer, S. Giannakis, S. Rtimi, and C. Pulgarín, "Iron-coated polymer films with high antibacterial activity under indoor and outdoor light, prepared by different facile pre-treatment and deposition methods," *Applied Catalysis B: Environmental*, vol. 243, pp. 161–174, Apr. 2019, doi: 10.1016/j.apcatb.2018.10.035.

ChapterIII

Materials and methods

III.1 Introduction

This chapter contains a detailed description of the used materials and the experimental procedures adopted to prepare TiO_2 composite thin films via thermal evaporation method. As well as, the *Escherichia coli* inactivation efficiency of the films was investigated. In order to better understand the relation between the different properties of the prepared films with their photocatalytic antibacterial activity, various characterization techniques were employed. These characterization methods, equipments, and their working principle are discussed in this section.

III.2 Materials and chemicals

For the experimental aspect, a variety of chemicals were used in this work. The essential reagents have been showed in **table III.1**

Table III.1 Chemicals used in this study.

Reagents	**Formula**	**Purity**	**Manufacturer**
Titanium dioxide	TiO_2	99.50%	Sigma Aldrich
Iron	Fe	99.00%	Biochem
Silver lump	Ag	99.99%	GoodFellow
Absolute ethanol	C_2H_6O	99.00%	Sigma Aldrich
Acetone	C_3H_6O	≥99.50%	Sigma Aldrich

III.3 Microorganism

Strain of *Escherichia coli* ATCC was obtained from medical analysis laboratory selected as a model for testing photocatalytic antimicrobial activity. *Escherichia coli (E.coli)* is prokaryotic cell **(figure III.1)** in the form of a rod (bacillus) Gram-negative bacterium that is the most favorable model organism for the study of many fundamental aspects of biochemistry and biology, because of their comparative simplicity, its ability to grow fast and using cheap media **[1, 2]**. *E. coli* strain can be revived by inoculation on blood agar, nutrient agar, or any nonselective media and incubated at 37 °C for 18 – 24 h. It can be found from water, soil, contaminated food material, and surfaces **[3]**. **Figure III.2** shows *Escherichia.coli* colonies on a petri dish agar plate used in our study.

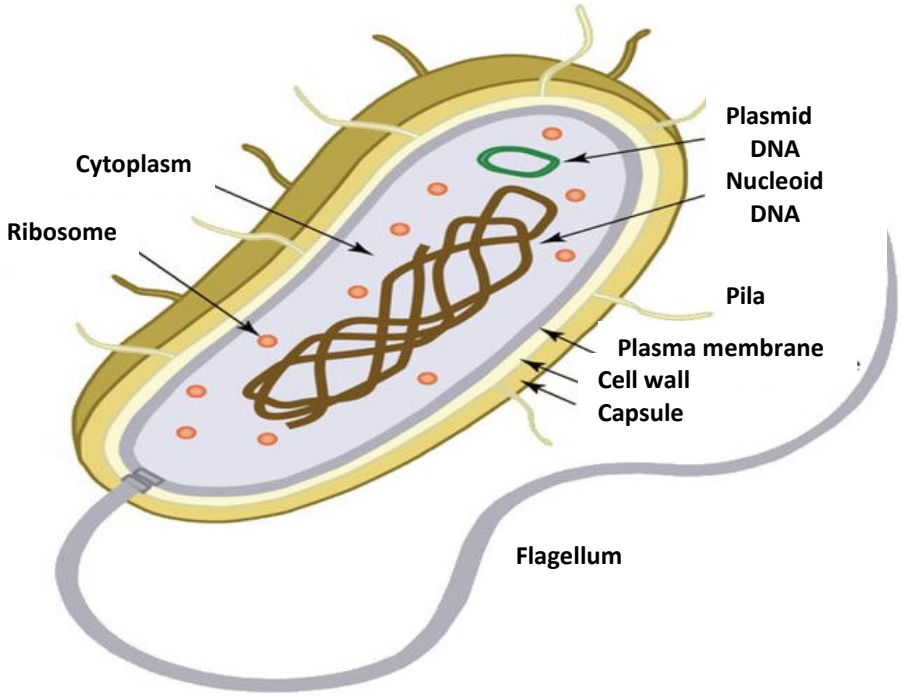

Figure III.1 Prokaryotic cell structure **[4]**.

Figure III.2 *Escherichia coli* colonies on nutrient agar.

III.4 Experimental procedures of TiO_2, TiO_2-Fe, and Ag-TiO_2-Fe composite thin films

III.4.1 Substrate preparation

In our study all the films were deposited onto glass substrates. Glass is an amorphous solid material; it is commonly used because of its several properties such as transparency, heat resistance, insulation and chemical resistance. The substrates (microscope slides) dimensions were 25 ×75 ×1.0 mm.

- Cleaning process

For certain thin film coatings and applications, substrate cleaning process is very important step to realize the fabrication of a high quality thin films without particle contamination, by removing hydrocarbons, metal contamination, organic contamination, ionic contamination, water molecules, and other particles or contaminants from a substrate surface before thin film deposition step. This process greatly improves adhesion to the substrate, leading to better performance and reliability for the coating. In this work the glass substrates were ultrasonically cleaned for 10 min in acetone and ethanol solution, then drying by compressed air.

III.4.2 Elaboration of TiO_2, TiO_2-Fe, and Ag-TiO_2-Fe films by thermal evaporation method

The thin film preparation and deposition process is carried out by the thermal evaporation unit, which is a homemade system developed in our institution (centre de développement des technologies avancées (CDTA)).

III.4.2.1 Description of the instrument and experimental technique

TiO_2, TiO_2-Fe, Ag-TiO_2-Fe composite thin films were elaborated using thermal evaporation process **[5]**. The evaporator system is equipped with a pumping unit; usually low pressures are used, about 10^{-6} or 10^{-5} mbar. It is consists of a vane pump for the primary vacuum of the order of 1. 10^{-2} mbar and oil diffusion pump for the secondary vacuum **(figure III.3)**. In the vacuum chamber, glass substrates are placed directly onto the substrate holder above the source (crucible) at a distance of 11 cm **[6]**, the deposition process was carried out by heating a tungsten crucible (boat) with electrical current containing only pure TiO_2 or a mixture of TiO_2-Fe powders or Ag-TiO_2-Fe with Fe fixed at 5.0 wt% and different Ag lump mass ratio (0, 5, 10, 15 and 20 wt%). The mixtures were

thermally evaporated to form a gaseous atmosphere, which condense to form our deposited thin films **[7]**. A schematic illustrating the thermal evaporation method is exhibited in **figure III.4**.

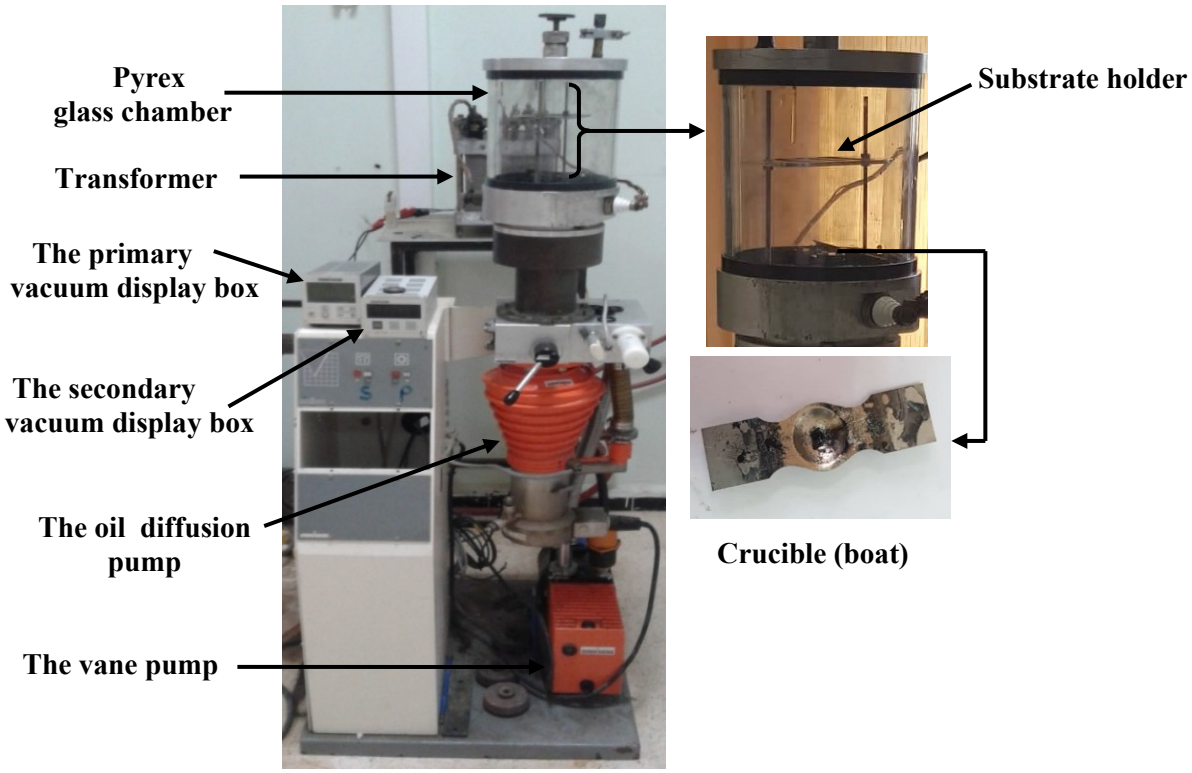

Figure III.3 Photograph of the experimental thermal evaporation under vacuum system.

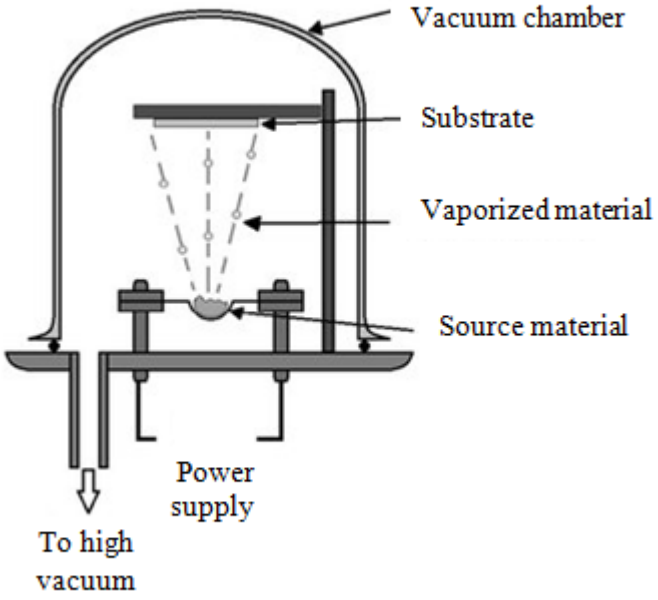

Figure III.4 Schematic diagram of vacuum thermal evaporation method **[8]**.

III.4.2.2 Principles deposition parameters of the prepared thin films

TiO_2, TiO_2-Fe and Ag-TiO_2-Fe thin films were elaborated at high temperature and very low pressure; deposition parameters affect the properties and the quality of the thin films. The deposition parameters of the prepared samples are presented in **table III.2**:

Table III.2 The deposition parameters of the prepared thin films.

Parameters / Samples	Primary pressure (mbar)	Secondary pressure (mbar)	Working pressure (mbar)	Time of deposit (s)
TiO_2	$1.7.10^{-2}$	$2.6.10^{-5}$	$8.5.10^{-5}$	45
TiO_2-Fe	$1.63.10^{-2}$	$1.7.10^{-5}$	6.10^{-5}	40
5Ag-TiO_2-Fe	$1.6.10^{-2}$	$1.6.10^{-5}$	8.10^{-5}	45
10Ag-TiO_2-Fe	$1.9.10^{-2}$	$2.9.10^{-5}$	$6.7.10^{-5}$	40
15Ag-TiO_2-Fe	$1.3.10^{-2}$	$1.2.10^{-5}$	5.10^{-5}	40
20Ag-TiO_2-Fe	$1.67.10^{-2}$	$2.7.10^{-5}$	$5.0.10^{-5}$	42

III.4.3 Heat treatment

After the deposition step, the heat treatment of prepared thin films has a vital role in the synthesis of nanoparticles, affecting morphology, crystallinity, porosity and phase transformation. The samples were annealed in air at 400 °C for 1h. The experiment flowcharts for pure TiO_2, TiO_2-Fe and Ag-TiO_2-Fe composite thin films are shown in **figure III.5**:

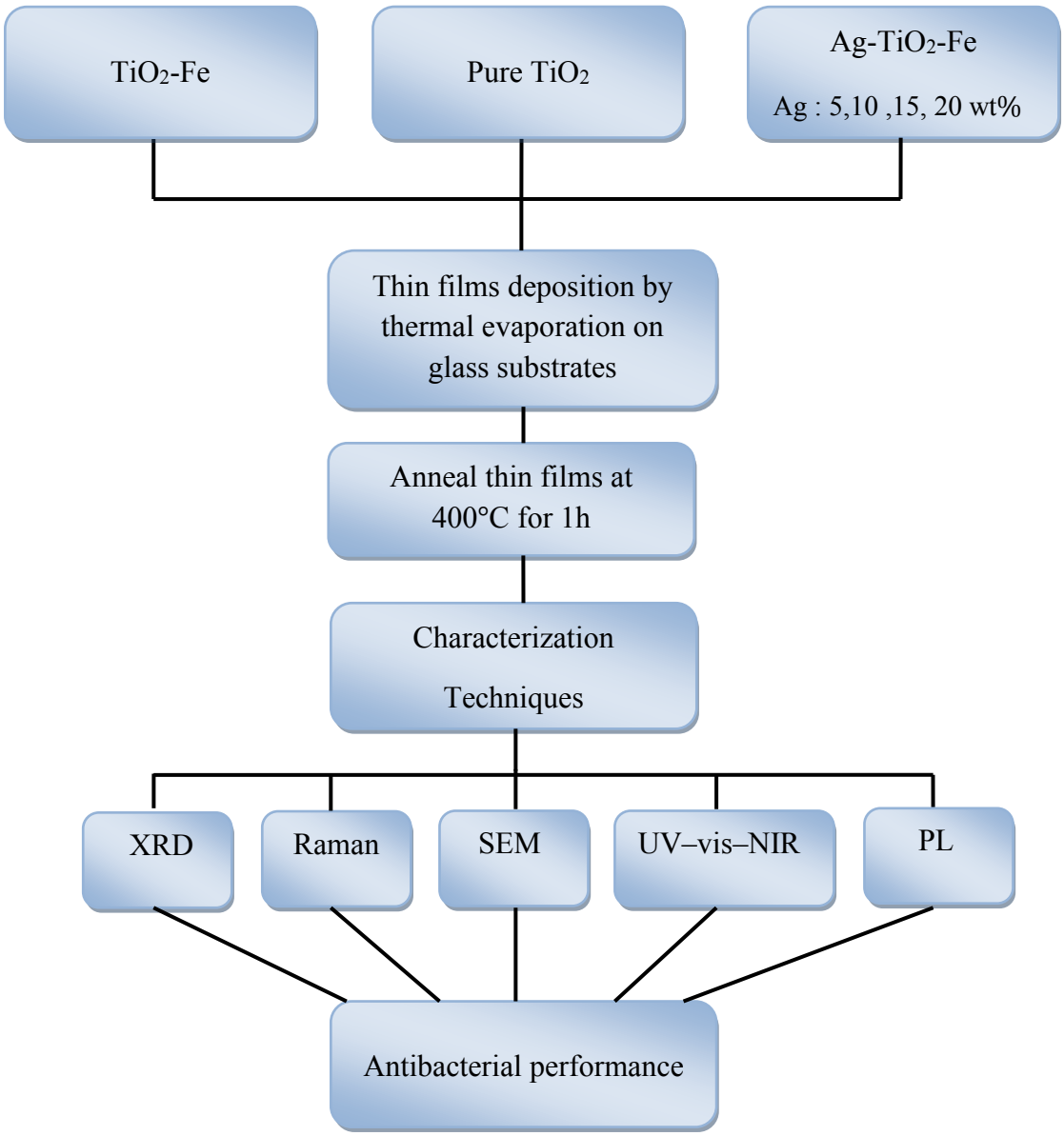

Figure III.5 The experiment flowcharts for pure TiO_2, TiO_2-Fe and Ag-TiO_2-Fe composite thin films.

III.5 Characterization techniques

Several characterisation techniques have been applied in this work to identify and understand different aspects of the films produced, in this section chemical, structural analysis and other analysis techniques used at various stages to characterize TiO_2, TiO_2-Fe and Ag-TiO_2-Fe composite films will be described.

III.5.1 X-ray Diffraction

X-ray diffraction (XRD) is one of the most powerful nondestructive technique used to identify the crystallographic structure of a material **[9]**. Moreover, the XRD can provide data on chemical composition, lattice parameters, impurities, geometry and defects, etc **[10]**. It is based on the constructive interference of monochromatic X-rays scattered at specific angles from each set of lattice planes in a sample **[11]**. Copper (Cu) or molybdenum (Mo) targets are bombarded with high energy electrons to produce X-rays. The released X-rays are then passed through a monochromator to produce K_α radiation from the respective metal. The intensity of the diffracted rays scattering at various angles of material are recorded by a detector and plotted to exhibit a diffraction pattern **[10, 12]**, which is associated with d-spacing values of the corresponding structure. In order to diffract constructively the X-rays should satisfy Bragg's law as follows (equation III.1) **[9, 13]**;

$$\lambda n = 2d \sin\theta \qquad \text{(eq.1)}$$

where λ is the wavelength of the incident X-rays, n is the order of diffraction, d is the interplaner spacing and θ is the angle of incidence. **Figure III.6** shows schema of the basic XRD principle.

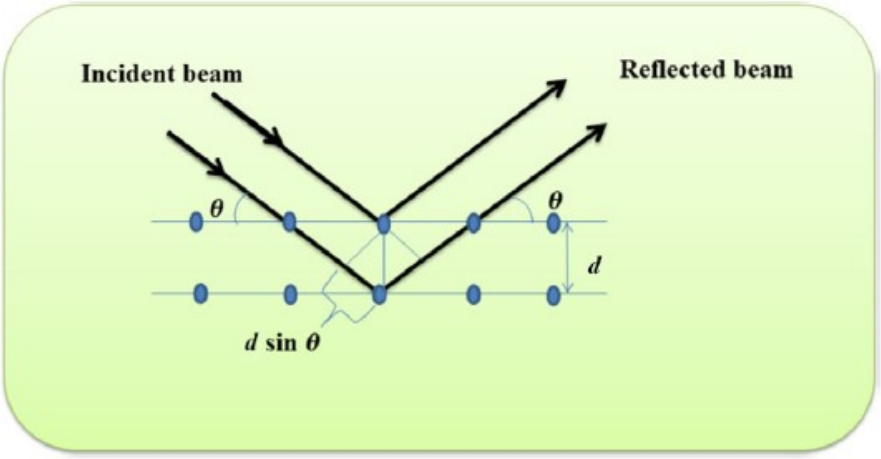

Figure III.6 Principle of X-ray diffraction **[13]**.

The structural analysis of the prepared TiO_2 composite films were determined using PANalytical X'Pert PRO MRD diffractometer with a monochromator using Cu K_α source ($K_\alpha 1$: 1.5406 Å) operated at 45 kV with 40 mA emission current. The scanning range was from 20° to 80°. The identification of phase was carried out by comparing the d-spacings obtained from the samples with the Joint Committee on Powder Diffraction Standards (JCPDS) standard database.

III.5.2 Raman Spectroscopy

Raman spectroscopy is an analytical technique used to identify molecules and study the vibrational, rotational and other modes of a molecular system. It based on the principle of inelastic scattering of monochromatic light from a laser source. The Raman scattering happens spontaneously when a molecule is excited from its stable state to a higher energy state by a photon with frequency ν_0 from the incident beam of light **[13, 14]**. It is also known as the Raman effect. Rayleigh, Stoke, and Antistoke are three different types of scattering. Rayleigh scattering is an elastic interaction between a photon and a molecule. In this case the excited molecule returns to its initial vibrational state and emits light at the same frequency ν_0 as an excitation source. The Stoke frequency is produced when a portion of the photon energy is transferred with frequency ν_m and the resulting frequency of scattered light is reduced to $\nu_0 - \nu_m$. Antistoke frequency is generated when a photon with frequency ν_0 is excited by a Raman active molecule with already excited vibrational state, the energy level rises to $\nu_0 + \nu_m$ **[15]**. **Figure III.7** illustrates simplified diagram of Raman spectrometer.

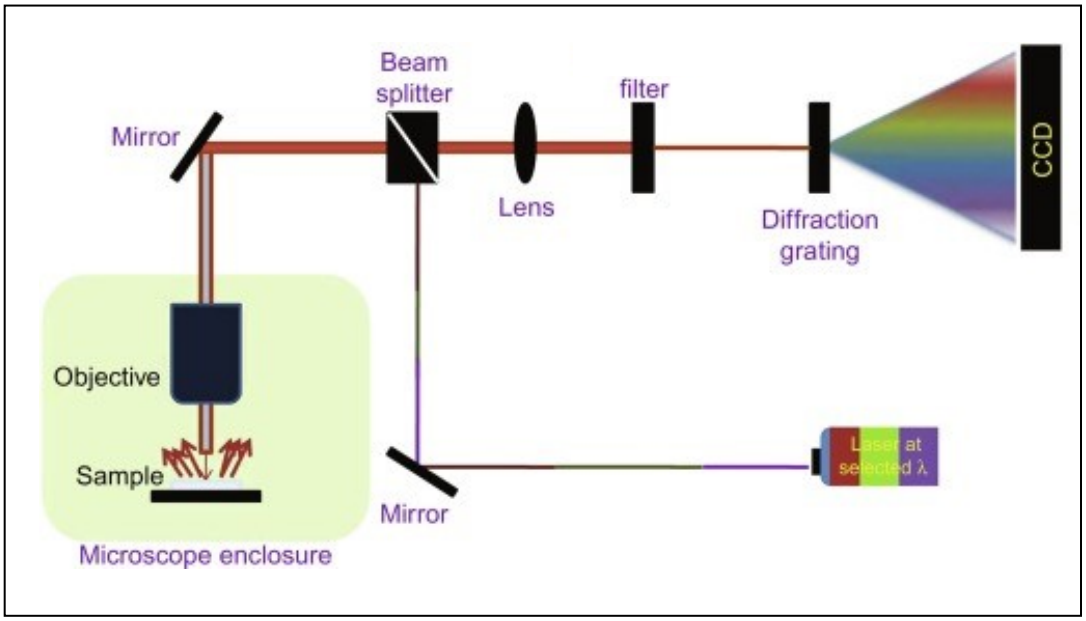

Figure III.7 Instrumentation of Raman spectrometer **[16]**.

Raman spectroscopy uses scattered light to know about molecular vibrations, which can gives information about structure, symmetry, electronic environment and bonding of the molecule furthermore, it provides the quantitative and qualitative analysis of the individual compounds **[17]**. Micro-Raman measurements of the prepared films were performed at room temperature in a confocal microscope Horiba Jobin-Yvon LabRAM HR800 confocal microscope. Raman spectra were recorded under excitation at 633 nm line of a He-Ne laser.

III.5.3 Scanning Electron Microscopy

Scanning Electron Microscopy (SEM) is a type of electron microscope and a helpful tool for investigating the topography and microstructure of many types of materials at greater depth. It is extremely popular because of its capacity to create three dimensional images. A highly focused electron beam produced from an electron gun interacts with a specimen, resulting in the emission of particles such as X-rays, primary electrons, secondary electrons and Auger electrons. The emitted particles are analyzed with the detector to yield information about the surface **[9, 13, 18]**. Images obtained by SEM can show details on size, shape, composition, distribution, material interface and cross section of films and bulk materials **[19]**. **Figure III.8** represents the components of scanning electron microscopy (SEM).

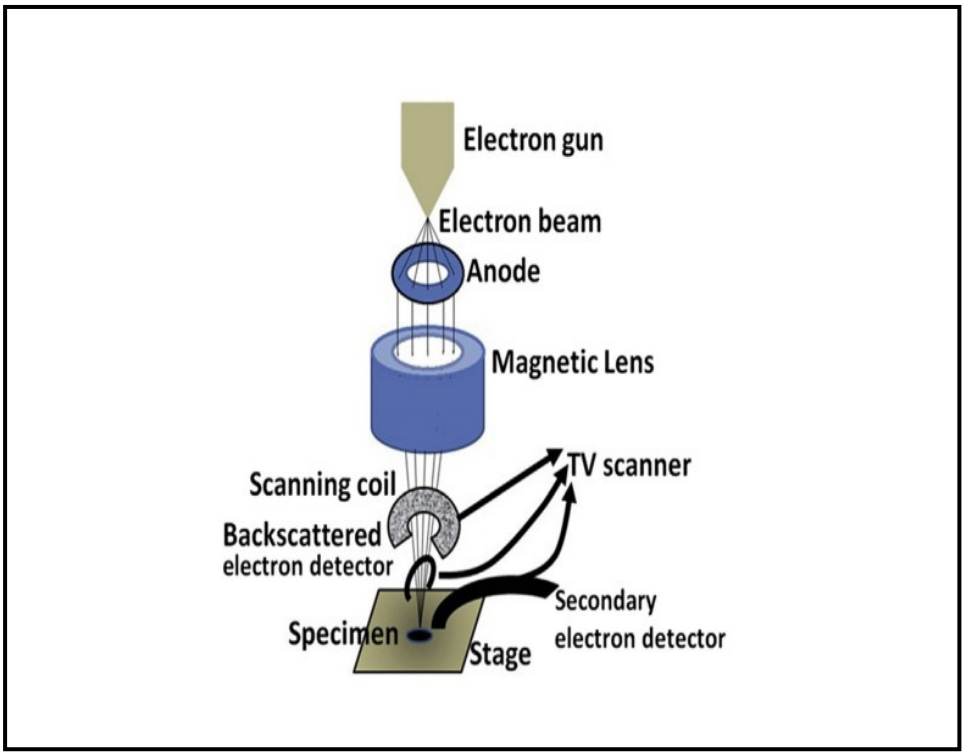

Figure III.8 Schematic representation of the scanning electron microscope **[20]**.

In addition, SEM is also equipped with energy dispersive X-ray (EDX) spectrometer; this technique provides an overall mapping of the sample by using the X-rays to determine the elemental compositions at small localized areas of the sample **[9, 13]**. The surface morphology of the prepared films was investigated with a FEI Inspect scanning electron microscope (SEM) operating at 15 kV.

III.5.4 UV-Vis-NIR spectroscopy

UV-Vis-NIR spectroscopy is an efficient technique for studying the optical properties of liquid solutions and solids materials in different forms (semiconductors, thin films, bulk materials and nanoparticles) **[9, 14]**. Ultraviolet–visible–near–infrared (UV–vis–NIR) spectroscopy analyzes a large wavelength range of (200–2500 nm), which is divided into the appropriate UV, Vis, and NIR regions of the electromagnetic spectrum. It is based on the absorption of light by the substance, which leads the excitation of the electrons from lower to higher energy levels **[21]**. When the light beam is passed through the sample, a part of the light may be absorbed, and the rest will be transmitted through the sample over a certain range of wavelength **[13]**. **Figure III.9** schematically shows the principle of a UV-visible spectrometer.

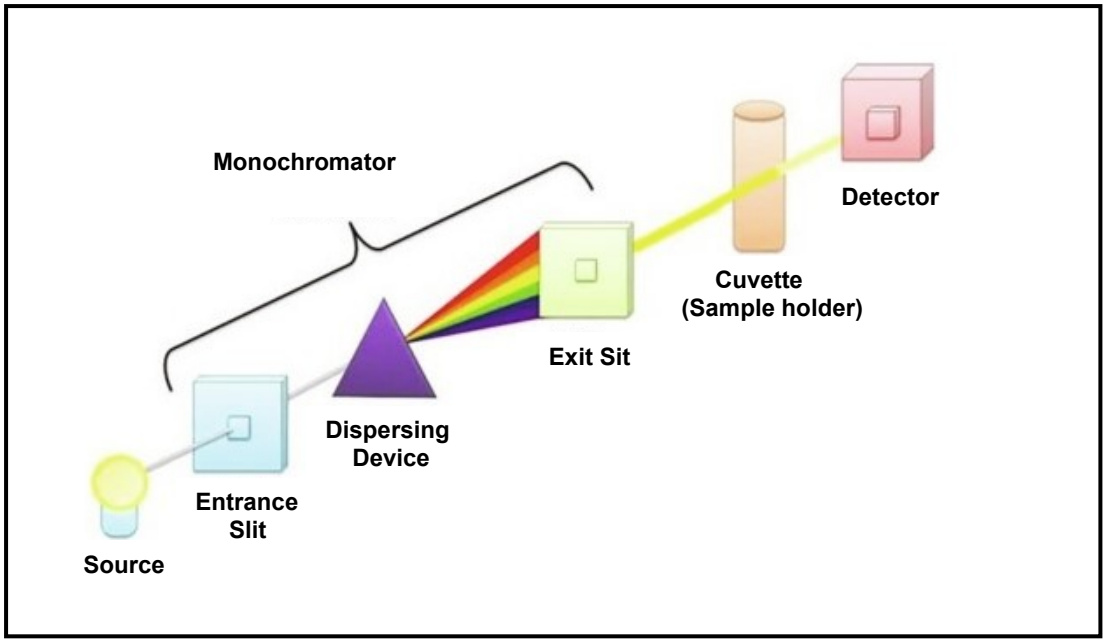

Figure III.9 Schematic diagram of UV-Vis spectrometer **[22]**.

The transmission (T) and the absorbance (A) of various materials is calculated by the using the following formulas **[23]**;

$$T = \frac{I}{I_0} \qquad \text{(eq.2)}$$

$$A = -\log T \qquad \text{(eq.3)}$$

where I is the intensity of transmitted light, I_0 is the intensity of incident light.

The transmittance and absorption spectra of different TiO_2-based composite films were determined by using a Shimadzu UV-1700 UV-VIS-NIR spectrophotometer in the wavelength range of 300–1100 nm.

III.5.5 Photoluminescence spectroscopy

Photoluminescence (PL) spectroscopy is an advantageous method due to its non-destructive nature and capacity to provide important data on both intrinsic and extrinsic transitions; it has been quite successful and preferred choice of the optical characterization techniques because of the simplicity of the method and no sample processing requirements **[24, 25]**. In Photoluminescence (PL) spectroscopy, laser beam is directed onto a sample, which inducing an electronic photoexcitation and as these states relax the optical emission is analyzed **[26] (figure III.10)**, this is in order to determine material properties including

electronic structure of the materials, energy transfer, impurities and also surface defects **[27]**.

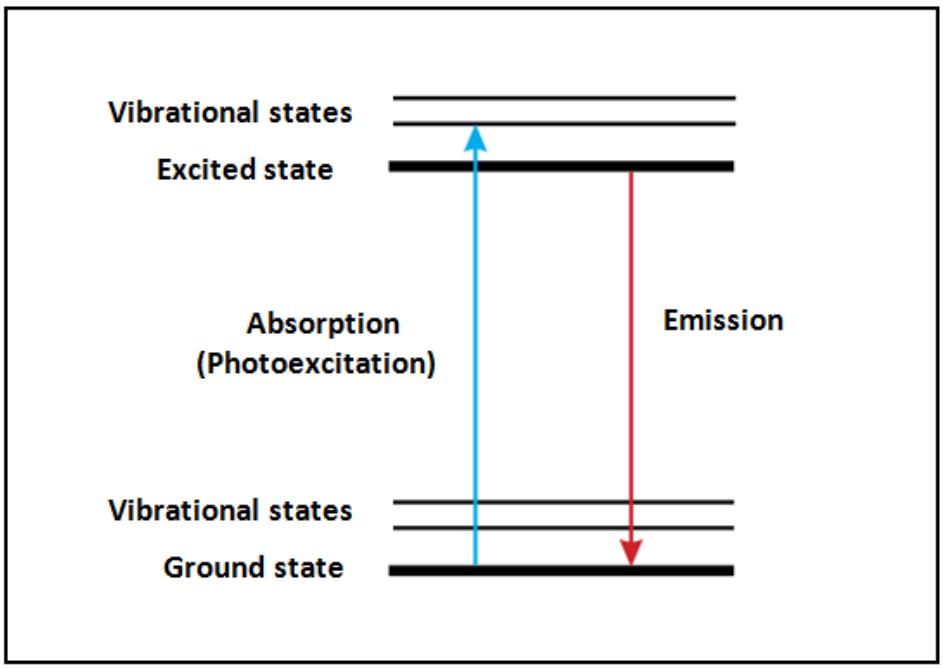

Figure III.10 Principle of the photoluminescence (PL) spectroscopy **[28]**.

Micro-Photoluminescence (μ-PL) measurements of the samples were performed at room temperature in a Horiba Jobin-Yvon LabRAM HR800 confocal microscope. The UV excitation sources employed include a He-Cd laser operating at λ_{ex}= 325 nm.

III.5.6 Antibacterial activity test

The antibacterial activity of pure TiO_2, TiO_2-Fe and Ag-TiO_2-Fe composite thin films with different Ag content was investigated using the so-called antibacterial drop-test. The test was carried out against *Escherichia coli (E. coli)* as a model for the Gram-negative bacteria in the dark and under UV light.

III.5.6.1 Bacterial growth

The bacterial stock was stored in preservation agar tube at (2 – 4 °C) for short-term or long-term storage of bacterial isolates in the deep freezer (-70 to -80 °C). In order to always keep the availability of strain, a subculturing procedure is carried out **[29, 30]**. This process is done by following these steps:

Under sterile conditions, small volume of *E.coli* is taken from the stock culture and streaked onto nutrient agar plates using a sterile inoculation loop. Then the streak plate is

incubated at 37 °C for 24 h. After given time for growth, separated (or isolated) colonies are formed **(figure III.11)**, the next step, an isolated colony is subcultured to fresh nutrient agar medium and so on to prolong life of cells **[29]**.

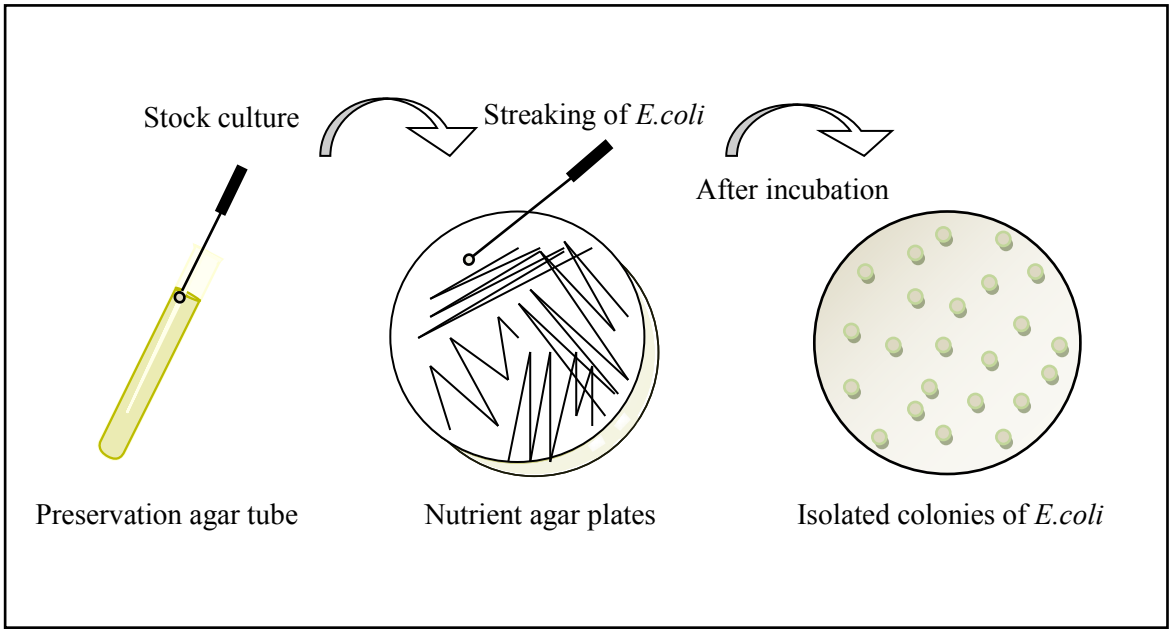

Figure III.11 Subculturing method of *E.coli.*

III.5.6.2 Antibacterial activity test of the prepared coating films (in the dark)

In this part of the procedure, all glassware and samples were autoclaved for 15 min at 120 °C to sterilize them. The thin films (size of 15 mm × 10 mm) were placed in a sterilized petri dish. Then, 100 µL of bacteria suspension (10^5 CFU/mL) was dropped onto the surface of the control sample and the coated thin films, the plates were then incubated at 37 °C for 1 h in the dark. Following that, 5 mL of sterile physiological saline were used for washing bacteria from the sample surfaces. Subsequently, 50 µL of every diluted solution were spread onto nutrient agar plates. After being incubated for 24 h at 37 °C, the number of viable bacteria colonies on the agar plates was counted. The reported values are averages of three similar independent experiments **[7]**.The bacteria killing percentage "*BK"* was calculated by using (equation III.4) as follow:

$$BK = \frac{A - B}{A} \times 100\% \qquad \text{(eq.4)}$$

where, A and B are the number of bacteria colonies grown in the culture medium corresponding to the control sample and coated films, respectively.

III.5.6.3 Antibacterial activity test of the prepared coating films (under UV light)

Under UV light, the antibacterial activity of the samples was determined according to the same procedure steps described above, and examined under similar conditions as in the dark. However, the samples were continuously irradiated with a UV light lamp (8 W, 365 nm, Philips) for 1 h at 37 °C incubation. The bacteria viable count was determined as in (equation III.4). **Figure III.12** demonstrates the test method for antibacterial evaluation.

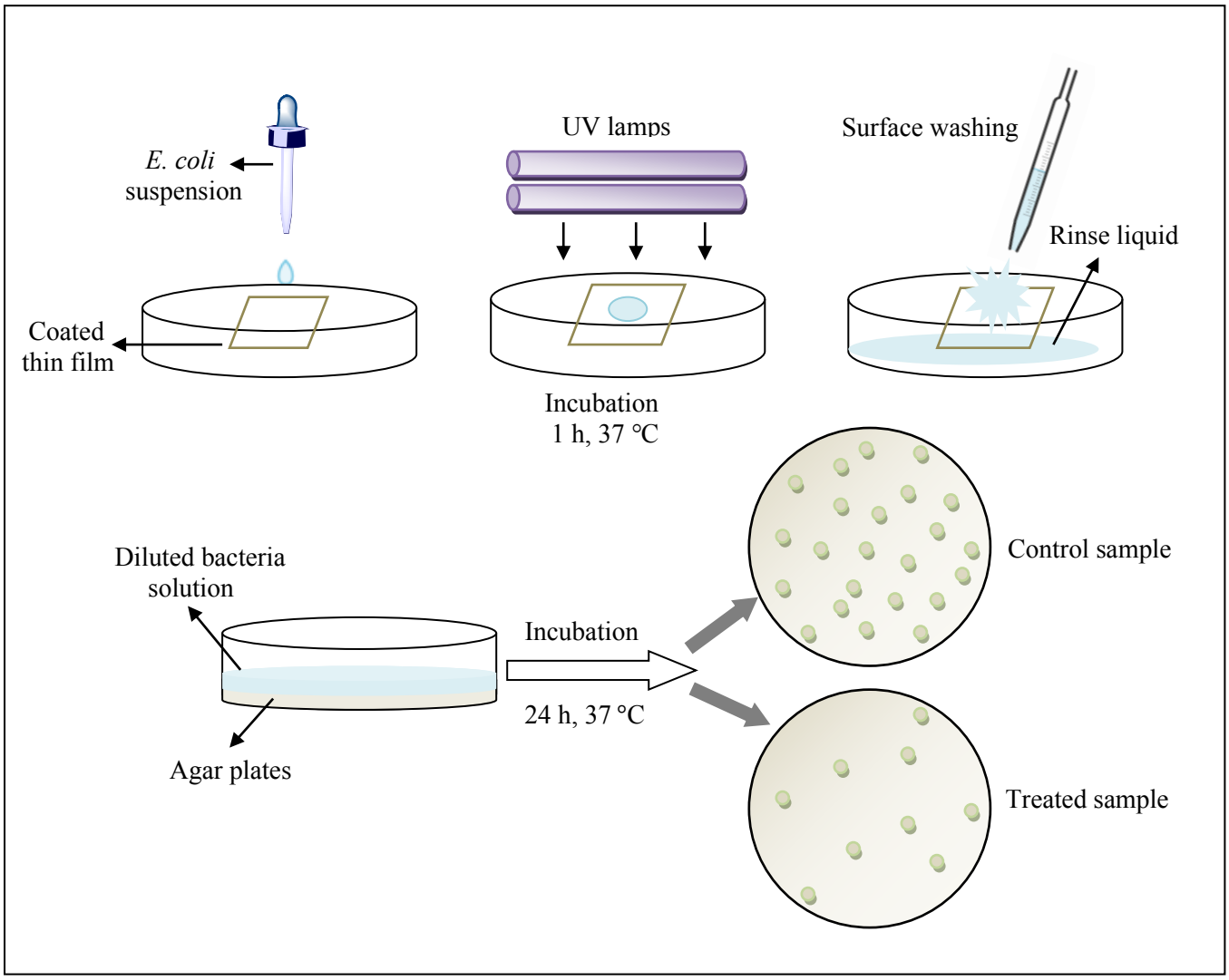

Figure III.12 Illustration of the antibacterial test.

III.6 Conclusion

In this chapter, we have attempted to highlight the various materials utilized in this study and the experimental procedures followed for fabricating the TiO_2 composite thin films. In addition to describing the characterization techniques applied to analyze the different properties of the films. Finally, we have given the experimental details of the antibacterial test of prepared films against *Escherichia coli*.

References

[1] "Escherichia coli (E. coli) as a Model Organism or Host Cell." Apr. 30, 2013. Available: Study.com. April 30, 2013. https://study.com/academy/lesson/escherichia-coli-e-coli-as-a-model-organism-or-host-cell.htm

[2] G. M. Cooper, *The cell: a molecular approach*, 2. ed. Washington, DC: ASM Press [u.a.], 2000.

[3] A. M. Lupindu, "Isolation and Characterization of *Escherichia coli* from Animals, Humans, and Environment," in Escherichia coli - *Recent Advances on Physiology, Pathogenesis and Biotechnological Applications*, A. Samie, Ed., InTech, 2017. doi: 10.5772/67390.

[4] M. Basavaraju and B. S. Gunashree, "*Escherichia coli*: An Overview of Main Characteristics," in *Escherichia coli - Old and New Insights*, M. Starčič Erjavec, Ed., IntechOpen, 2023. doi: 10.5772/intechopen.105508.

[5] F. Lekoui, M. Ouchabane, H. Akkari, S. Hassani, and D. Dergham, "Effect of annealing temperature on the properties of Ag doped ZnO thin films," *Mater. Res. Express*, vol. 5, no. 10, p. 106406, Aug. 2018, doi: 10.1088/2053-1591/aadafa.

[6] F. Lekoui, "Elaboration et Caractérisation d'un système en couches minces fonctionnelles Zn-Ag-Mg-O," thése, Université 20 Août 1955 – Skikda, Skikda, 2019.

[7] D. Grine, H. Akkari, P. Fernández, T. Mekhalif, S. Hassani, and F. Lekoui, "Synthesis, Characterization, and Antibacterial Activity of Ag–TiO2–Fe Composite Thin Films," *Phys. Status Solidi A*, vol. 219, no. 11, p. 2200036, Apr. 2022, doi: 10.1002/pssa.202200036.

[8] A. A. Najim, M. A. H. Muhi, K. R. Gbashi, and A. T. Salih, "Synthesis of Efficient and Effective γ-MnO2/α-Bi2O3/a-Si Solar Cell by Vacuum Thermal Evaporation Technique," *Plasmonics*, vol. 13, no. 3, pp. 891–895, Jun. 2018, doi: 10.1007/s11468-017-0585-2.

[9] Y. Faheem Joya, "Titanium Dioxide Films Prepared by Sol-Gel/Laser-Induced Technique for Inactivation of Bacteria," The University of Manchester, Manchester, 2011.

[10] H. Mahipati Yadav, "Antibacterial studies with metal-doped TiO2 nanoparticles," D. Y. Patil University, Kolhapur, India, 2014.

[11] A. A. Bunaciu, E. G. Udriştioiu, and H. Y. Aboul-Enein, "X-ray diffraction: instrumentation and applications," *Crit Rev Anal Chem*, vol. 45, no. 4, pp. 99–289, Apr. 2015, doi: 10.1080/10408347.2014.949616.

[12] P. B. Raja, K. R. Munusamy, V. Perumal, and M. N. M. Ibrahim, "Characterization of nanomaterial used in nanobioremediation," in *Nano-Bioremediation: Fundamentals and Applications*, Elsevier, 2022, pp. 57–83. doi: 10.1016/B978-0-12-823962-9.00037-4.

[13] D. Titus, E. James Jebaseelan Samuel, and S. M. Roopan, "Nanoparticle characterization techniques," in *Green Synthesis, Characterization and Applications of Nanoparticles*, Elsevier, 2019, pp. 303–319. doi: 10.1016/B978-0-08-102579-6.00012-5.

[14] D. Grine, "Elaboration of TiO2/Ag thin layers for the detection of a biomolecule," Master Thesis, August 20, 1955 University of Skikda, Skikda, 2016.

[15] H. H. Kim, "Endoscopic Raman Spectroscopy for Molecular Fingerprinting of Gastric Cancer: Principle to Implementation," *BioMed Research International*, vol. 2015, pp. 1–9, 2015, doi: 10.1155/2015/670121.

[16] P. Minakshi *et al.*, "Single-Cell Metabolomics: Technology and Applications," in *Single-Cell Omics*, Elsevier, 2019, pp. 319–353. doi: 10.1016/B978-0-12-814919-5.00015-4.

[17] R. S. Das and Y. K. Agrawal, "Raman spectroscopy: Recent advancements, techniques and applications," *Vibrational Spectroscopy*, vol. 57, no. 2, pp. 163–176, Nov. 2011, doi: 10.1016/j.vibspec.2011.08.003.

[18] S. Ebnesajjad, "Surface and Material Characterization Techniques," in *Surface Treatment of Materials for Adhesive Bonding*, Elsevier, 2014, pp. 39–75. doi: 10.1016/B978-0-323-26435-8.00004-6.

[19] J. I. Goldstein, D. E. Newbury, J. R. Michael, N. W. M. Ritchie, J. H. J. Scott, and D. C. Joy, *Scanning Electron Microscopy and X-Ray Microanalysis*. New York, NY: Springer New York, 2018. doi: 10.1007/978-1-4939-6676-9.

[20] A. K. Singh, "Experimental Methodologies for the Characterization of Nanoparticles," in *Engineered Nanoparticles*, Elsevier, 2016, pp. 125–170. doi: 10.1016/B978-0-12-801406-6.00004-2.

[21] S. Pentassuglia, V. Agostino, and T. Tommasi, "EAB—Electroactive Biofilm: A Biotechnological Resource," in *Encyclopedia of Interfacial Chemistry*, Elsevier, 2018, pp. 110–123. doi: 10.1016/B978-0-12-409547-2.13461-4.

[22] O. S. Oluwafemi, E. H. M. Sakho, S. Parani, and T. C. Lebepe, "Characterization techniques for ternary I–III–VI quantum dots," in *Ternary Quantum Dots*, Elsevier, 2021, pp. 117–135. doi: 10.1016/B978-0-12-818303-8.00007-1.

[23] F. Ramadhani, A. Supriyanto, M. K. B. Ahmad, N. E.-H. Diyanahesa, and D. G. Saputri, "Optical properties of dye DN-F01 as sensitizer," *J. Phys.: Theor. Appl.*, vol. 3, no. 1, p. 36, Mar. 2019, doi: 10.20961/jphystheor-appl.v3i1.38146.

[24] G. D. Gilliland, "Photoluminescence spectroscopy of crystalline semiconductors," *Materials Science and Engineering: R: Reports*, vol. 18, no. 3–6, pp. 99–399, Mar. 1997, doi: 10.1016/S0927-796X(97)80003-4.

[25] J. T. Torvik, "Dopants in GaN," in *III-Nitride Semiconductors: Electrical, Structural and Defects Properties*, Elsevier, 2000, pp. 17–49. doi: 10.1016/B978-044450630-6/50003-9.

[26] F. Adams and C. Barbante, "Spectroscopic Imaging," in *Comprehensive Analytical Chemistry*, vol. 69, Elsevier, 2015, pp. 339–384. doi: 10.1016/B978-0-444-63439-9.00009-8.

[27] A. Erbe *et al.*, "How to Probe Structure, Kinetics, and Dynamics at Complex Interfaces In Situ and Operando by Optical Spectroscopy," in *Encyclopedia of Interfacial Chemistry*, Elsevier, 2018, pp. 199–219. doi: 10.1016/B978-0-12-409547-2.14061-2.

[28] A. Gao, P. J. Rizo, L. Scaccabarozzi, C. J. Lee, V. Banine, and F. Bijkerk, "Photoluminescence-based detection of particle contamination on extreme ultraviolet reticles," *Review of Scientific Instruments*, vol. 86, no. 6, p. 063109, Jun. 2015, doi: 10.1063/1.4922883.

[29] A. Jain, R. Jain, and S. Jain, "Sub-culturing of Bacteria, Fungi and Actinomycetes," in *Basic Techniques in Biochemistry, Microbiology and Molecular Biology*, in Springer Protocols Handbooks. , New York, NY: Springer US, 2020, pp. 101–103. doi: 10.1007/978-1-4939-9861-6_29.

[30] Sunarno *et al.*, "Long-term Storage of Bacterial Isolates by Using Tryptic Soy Broth with 15% Glycerol in The Deep Freezer (-70 to -80 °C)," *IOP Conf. Ser.: Earth Environ. Sci.*, vol. 913, no. 1, p. 012070, Nov. 2021, doi: 10.1088/1755-1315/913/1/012070.

ChapterIV

Results and discussion

IV.1 Introduction

In this chapter the results on the characterization of pure TiO_2, TiO_2-Fe and Ag-TiO_2-Fe thin films with varied silver contents prepared by thermal evaporation technique are discussed. The effect of silver content and the presence of iron on structural, morphological, chemical, optical and antibacterial properties on unmodified TiO_2 thin films are studied. Furthermore, the antibacterial efficiency of the prepared films against *E.coli* bacteria in dark and under UV light is investigated.

IV.2 Analysis and characterization of composite thin films

IV.2.1 XRD characterization

The XRD patterns of TiO_2, TiO_2-Fe, and Ag-TiO_2-Fe composite films with varied Ag contents annealed at 400 °C for 1 h are illustrated in **figure IV.1**. The Pure TiO_2 and TiO_2-Fe films show no diffraction peaks, hence they are in amorphous form. The films started to crystallize into the anatase phase when Ag was added to TiO_2-Fe films. As a result, it was observed that the intensity of the diffraction peaks rises with increasing Ag content. This increase is especially remarkable for Ag content at 15%, which signifies an improvement in the crystallinity of the films **[1]**. A series of diffraction peaks are detected for Ag-TiO_2-Fe composite films at 25.3°, 37.0°, 38.0°, 38.5°, 48.0°, 54.0°, 55.0°, 62.0°, 62.7°, 68.0°, 70.1°, and 75.1° corresponding to the (101),(103), (004), (112), (200), (102), (211), (213), (204), (116), (220), and (215) crystallographic planes of TiO_2 anatase phase (JCPDS no. 21-1272), with no additional TiO_2 phases. The other peaks located at 38.1°, 44.2°, 64.5°, and 77.5° are assigned to the (111), (200), (220), and (311) crystal planes associated with the face-centered cubic (fcc) structure of metallic silver (JCPDS card no. 04-0783). The diffraction peaks corresponding to (004) of TiO_2 and (111) of Ag is very close to one another. Thus, it is difficult to differentiate the Ag signals from the TiO_2 signals.

There are no diffraction peaks associated with iron or iron oxides, which could be explained by the low quantity of Fe present in the titanium oxide matrix **[2]**. The crystallite size of TiO_2 in Ag-TiO_2-Fe composite thin films with different Ag content (5, 10, 15, 20 wt%) was calculated using Scherrer's formula (equation IV.1) **[3]** from TiO_2 (101) main peak, the results are shown in **table IV.1**

$$D = \frac{0.9\lambda}{\beta \cos \theta} \qquad \text{(eq.1)}$$

where:

β (rad): the full width at half maximum (FWHM) of the (101) diffraction peak;

θ (rad): the Bragg's diffraction angle;

λ: wavelength of the copper radiation (1.54060Å).

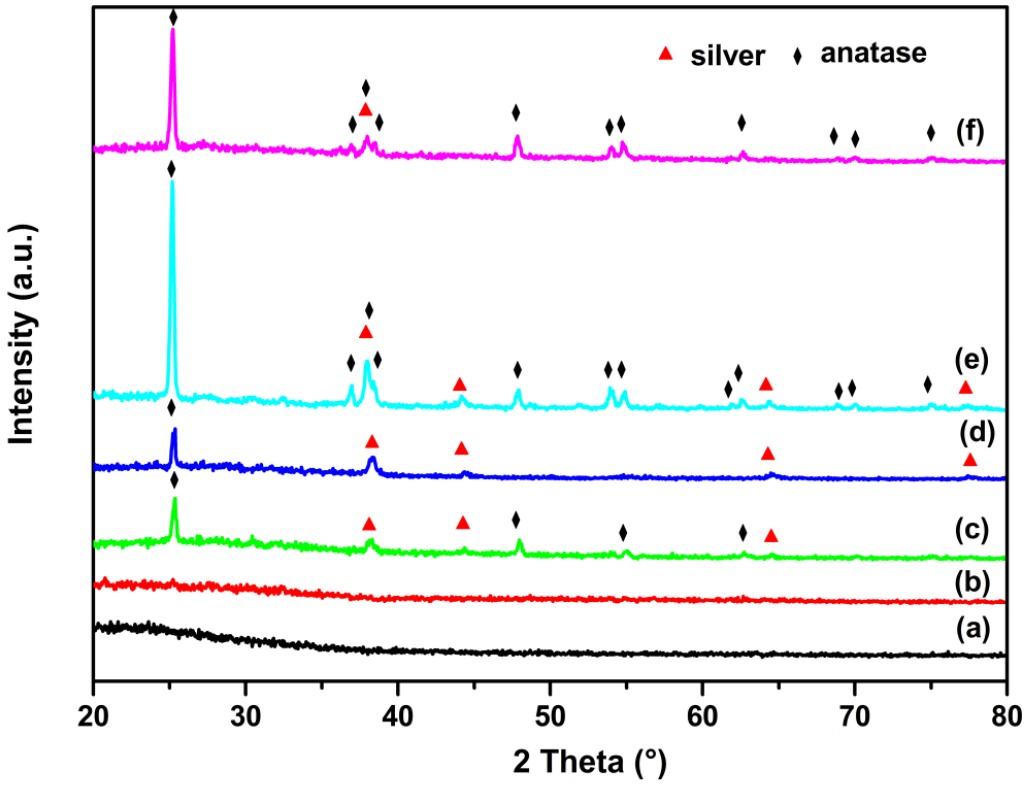

Figure IV.1 XRD patterns of (a) pure TiO_2, (b) TiO_2-Fe and (c-f) Ag-TiO_2-Fe composite thin films at different Ag contents (5-20 wt%).

Table IV.1 XRD data of Ag-TiO_2-Fe composite thin films.

Sample	$\beta(rad)$	$\lambda(nm)$	$\theta(rad)$	$d_{(101)}(Å)$	Crystallite size *D(nm)*
5%Ag-TiO_2-Fe	0.004305	0.15406	0.22194375	3.508568417	33.1014794
10%Ag-TiO_2-Fe	0.004305	0.15406	0.221449375	3.5162729277	33.0978110
15%Ag-TiO_2-Fe	0.004305	0.15406	0.221356625	3.5177222424	33.0971237
20%Ag-TiO_2-Fe	0.004305	0.15406	0.221571	3.514374266	33.0987126

Table IV.1 shows that there is no significant change in TiO_2 crystallite size with increasing silver content in all Ag-TiO_2-Fe composite thin films, and these results are in agreement with the literature **[4, 5]**. The crystallite size of TiO_2 is estimated to be around 33 nm **[2]**.

IV.2.2 Raman Analysis

Figure IV.2 presents the Raman spectra of pure and modified TiO_2 thin films annealed at 400 °C. The Raman spectra of pure TiO_2 and TiO_2-Fe thin films clearly show the amorphous characteristic; this coincides completely with the obtained XRD results. It can be seen that the Ag-TiO_2-Fe composite films exhibit a main characteristic peak slightly above 151 cm^{-1} is attributed to the $E_g(1)$ mode of anatase. Whereas at 15 and 20 wt% of silver content two weak bands appeared at 640 cm^{-1}, which corresponds to the $E_g(3)$ Raman active modes of anatase phase **[6]**, and the other one at 328 cm^{-1} can be ascribed to the Ag–O stretching vibration **[7, 8]** as a result of the oxidation of a few Ag nanoparticles on irregularities such as pits or bumps formed on the surface of the composite thin films, on which the Ag atoms could preferentially locate **[2]**. No characteristic bands of iron species were observed due to the low level of Fe present in the samples. With increasing silver content (from 5 to 20 wt%), the main peak $E_g(1)$ in Ag-TiO_2-Fe composite thin films shifts towards higher wavenumber (from 151 to 158 cm^{-1}) compared to typical TiO_2 bonding modes **[9]**. This shift in Raman peaks can be attributed to nonstoichiometry defects in structure and surface interaction between metal and TiO_2 **[10, 11]**. In addition,

the increase in silver content enhanced the $E_g(1)$ Raman intensities of Ag-TiO_2-Fe samples significantly at 15 wt% Ag. The observed rise in Raman intensity can also be related to the surface-enhanced Raman spectra (SERS) characteristic of Ag. Similar results have been reported by Xu et al **[12]**.

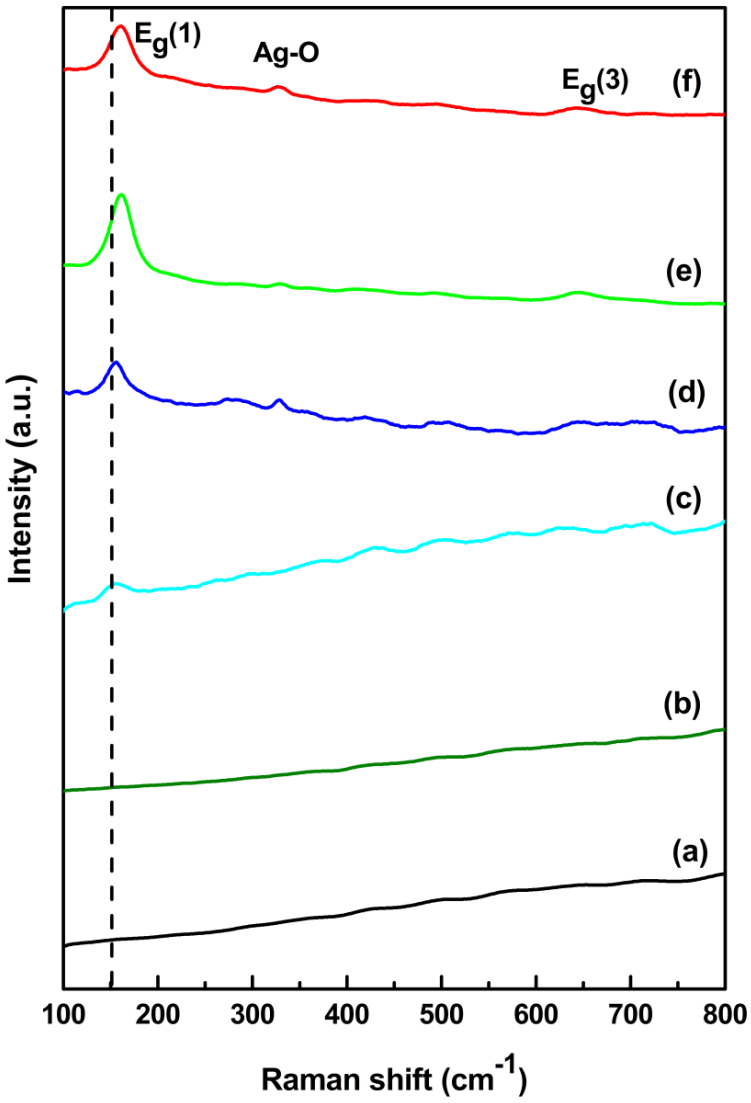

Figure IV.2 Raman spectra of (a) pure TiO_2, (b) TiO_2-Fe and (c-f) Ag-TiO_2-Fe composite thin films at different Ag contents (5-20 wt%).

IV.2.3 Morphology of the samples

Figure IV.3 shows the SEM morphology of pure TiO_2, TiO_2-Fe, and Ag-TiO_2-Fe composite thin films with different Ag content after annealing at 400 °C for 1 h. It could be seen that the pure TiO_2 film shows a uniform bubble distribution **(figure IV.3 (a))**. The surface morphology of the deposited TiO_2 film became smoother after the addition of Fe, which resulted in the disappearance of the bubbles **(figure IV.3 (b))**. However, silver content has a considerable impact on the surface morphology of the composite thin films. At 5 wt% Ag the composite film exhibited a random distribution of particles containing bright spots of different sizes of metallic silver (confirmed by the EDX analysis) dispersed upon the flat surface of TiO_2 **(figure IV.3 (c))**. With increasing silver content to 10 wt% the film displayed a flat surface morphology with voids **(figure IV.3 (d))**, For higher silver content (15, 20 wt%), Ag nanoparticles (bright spots) are uniformly distributed on the whole surface **(inset of figure IV.3 (e))** with varied sizes ranging from 70 to 400 nm and the film structure becomes smoother and more homogeneous **(figure IV.3 (f)) [2]**.

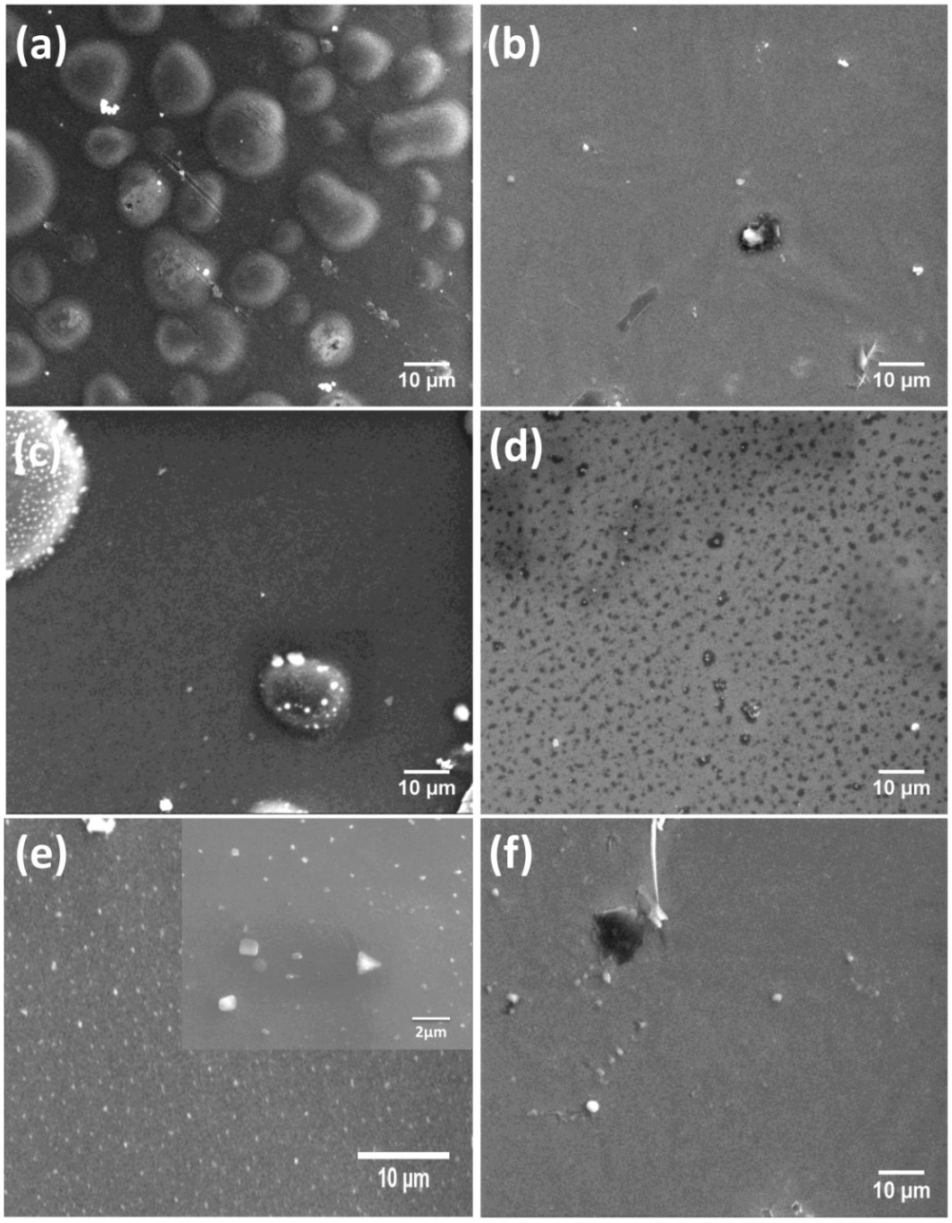

Figure IV.3 SEM images of (a) pure TiO_2, (b) TiO_2-Fe and (c-f) Ag-TiO_2-Fe composite thin films at different Ag contents (5-20 wt%).

IV.2.4 EDX analysis of the prepared samples

EDX analysis of the pure TiO_2, TiO_2-Fe and Ag-TiO_2-Fe composite films was carried out to determine the chemical composition of the prepared films, the qualitative results acquired are given in **figure IV.4 (a, b)** and **figure IV.5 (c-f)**. The EDX spectrum of the pure TiO_2 and TiO_2-Fe films **(figure IV.4 (a, b))** displayed energy peaks from Ti, O, and Fe which generated by the films. Additional energy peaks including Si, Ca, Al, Mg, Na, etc. were also detected, which correspond to the glass substrates on which the films are

grown. Similar results are reported by Moslah et al **[13, 14]**. The EDX analysis of Ag-TiO_2-Fe composite films with varied silver content (5-20 wt%) is presented in **figure IV.5 (c-f)**. All spectra exhibited characteristic silver peaks around 3 keV, this confirmed the presence of silver particles on the TiO_2-Fe surface, and the bright spots found distributed on the TiO_2-Fe surface at 15Ag wt% as indicated in the previous SEM images (**figure IV.3(e)**) were identified as silver nanoparticles according to the elemental mapping (**figure IV.6)**. Whereas the produced Si, Ca, Mg, Al, Na energy peaks were associated with the glass substrate **[13, 14]**.

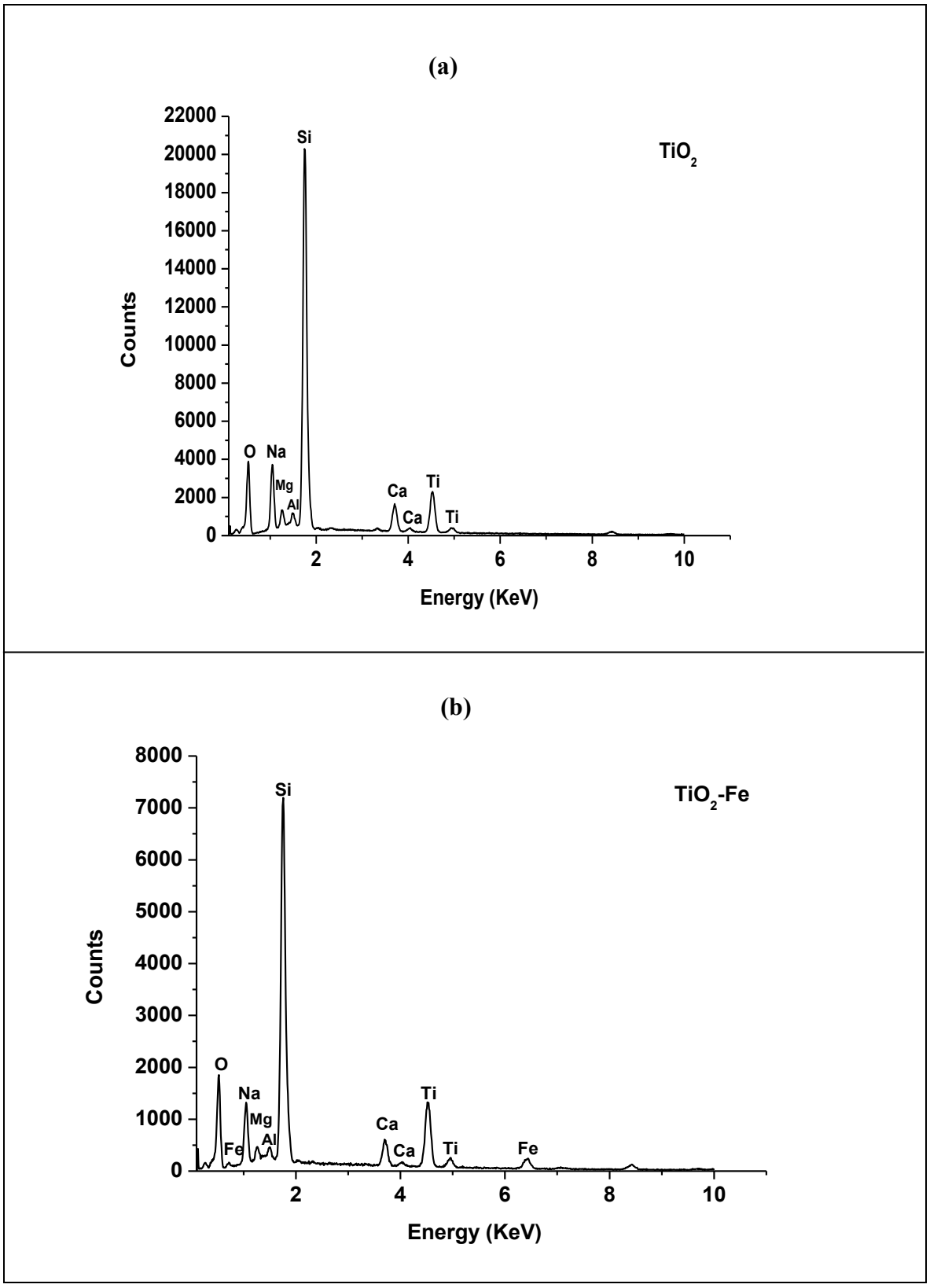

Figure IV.4 EDX spectra of (a) pure TiO_2, (b) TiO_2-Fe thin film.

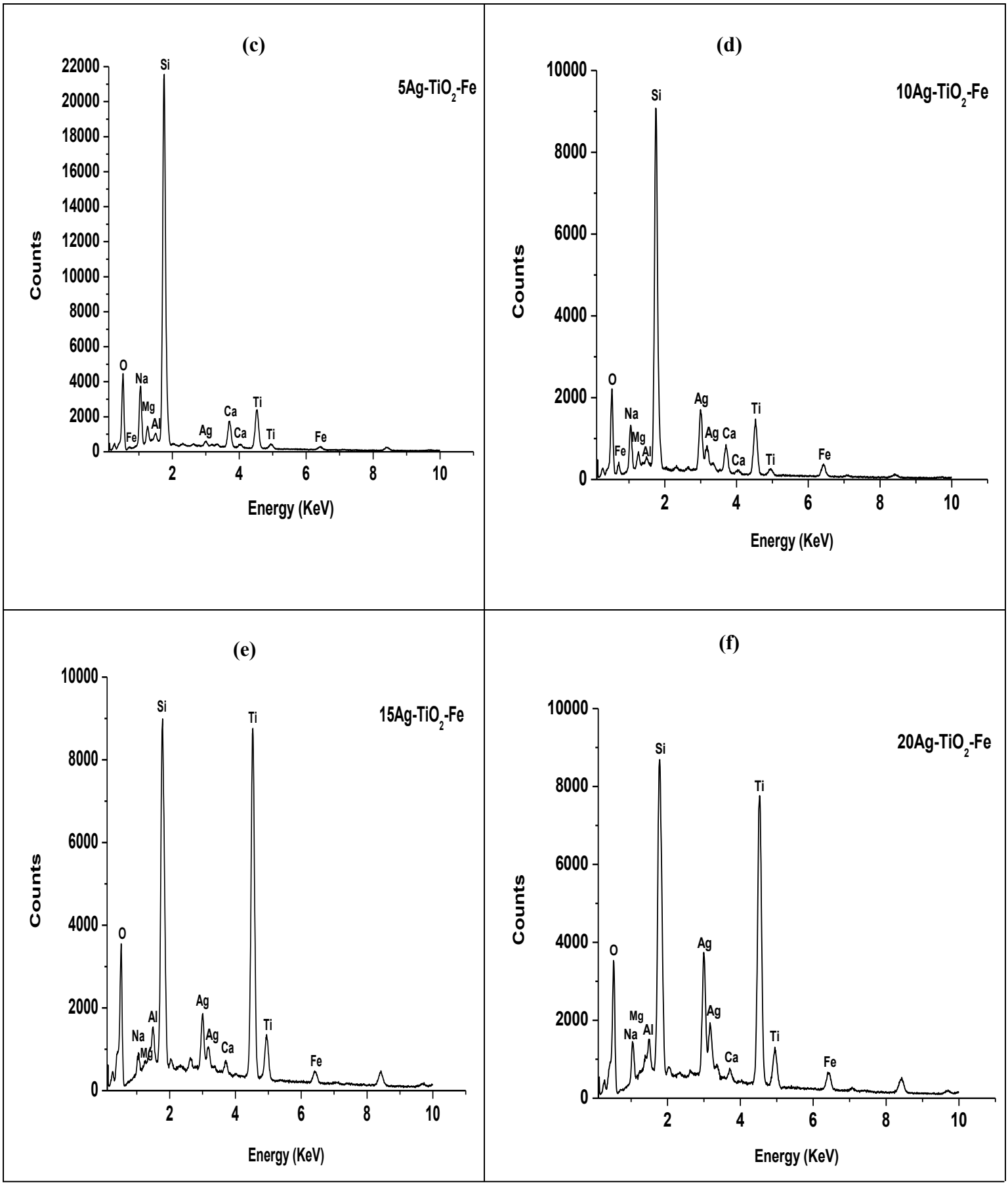

Figure IV.5 EDX spectra of Ag-TiO_2-Fe composite thin films at different Ag contents.

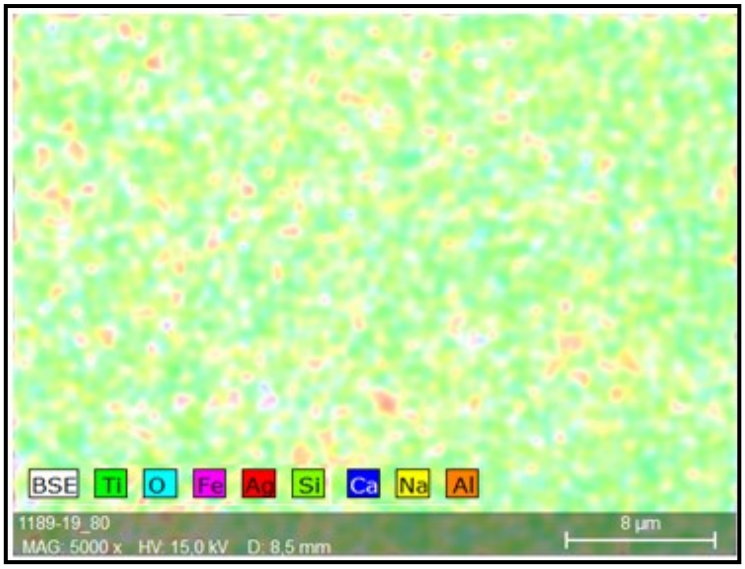

Figure IV.6 Elemental mapping of 15%Ag-TiO_2-Fe composite thin film.

IV.2.5 UV–vis–NIR spectroscopy analysis

IV.2.5.1 Optical transmittance of the prepared films

Figure IV.7 depicts the optical transmittance spectra of TiO_2, TiO_2-Fe, and Ag-TiO_2-Fe composite films with different Ag contents measured in the region of (300-1100 nm) by using UV-VIS-NIR spectrometer at room temperature. It is evident that, among the samples, the pure TiO_2 film exhibits the highest level of transparency, approximately 83.02%, within the visible region. However, the presence of iron (Fe) results in a noticeable reduction in transmittance, which decreases to around 76.84%, particularly in the infrared region. Interestingly, after introducing silver into the TiO_2-Fe composite thin films, the transmittance further decreases in a rapid manner in the visible region with increasing silver content. The observed oscillation in the transmittance spectra is due to the interference that occurs between the interfaces of the air-film and film-substrate **[15]**.

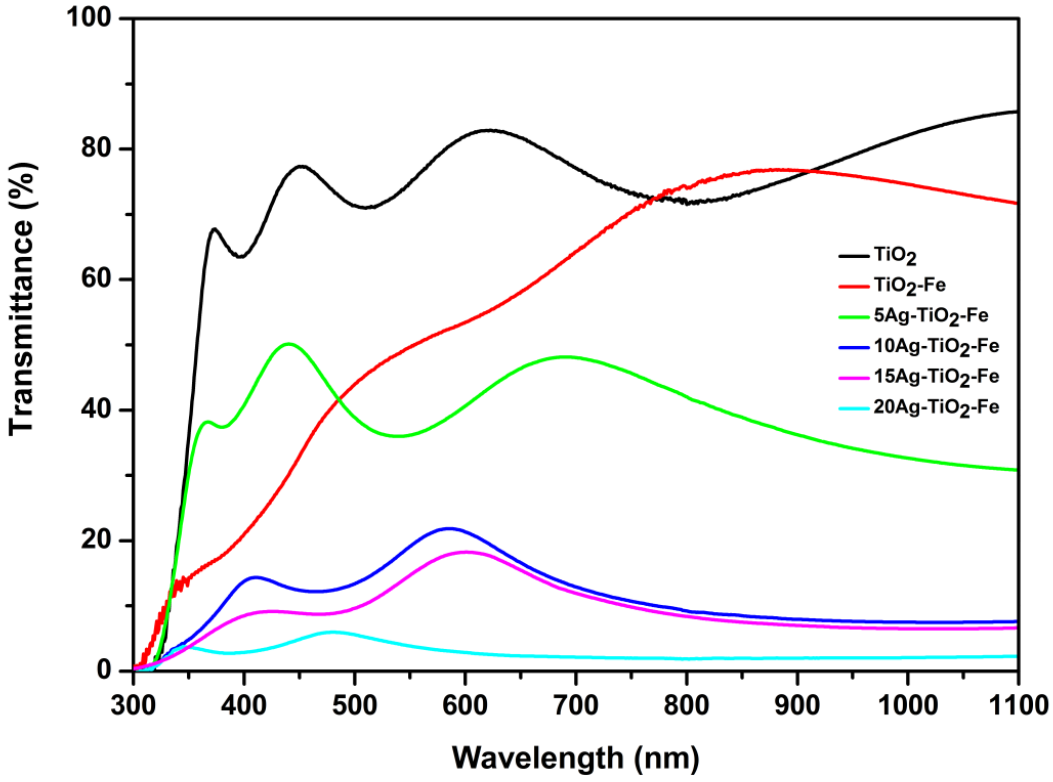

Figure IV.7 Transmission spectra of pure TiO_2, TiO_2-Fe and Ag-TiO_2-Fe composite thin films at different Ag contents.

IV.2.5.2 Absorbance of the prepared films

The optical absorbance spectra obtained from the TiO_2, TiO_2-Fe and Ag-TiO_2-Fe films are plotted in **figure IV.8**. Notably, the introduction of Fe and Ag into the TiO_2 matrix enhances absorption in the visible region and the absorption edge of the TiO_2-Fe and Ag-TiO_2-Fe composite thin films exhibited a redshift, which becomes more pronounced as the Ag content increases. Furthermore, large absorption bands at 467, 474, and 389 nm are observed in the 10%, 15%, and 20% Ag-TiO_2-Fe composite films, respectively. These broad absorption bands are associated with the surface plasmon absorption (SPA) of Ag nanoparticles **[16, 17]**, it is worth noting that the location of SPA band of silver nanoparticles can be affected by a variety of parameters, including their size, shape, and surface charge chemistry **[16]**.

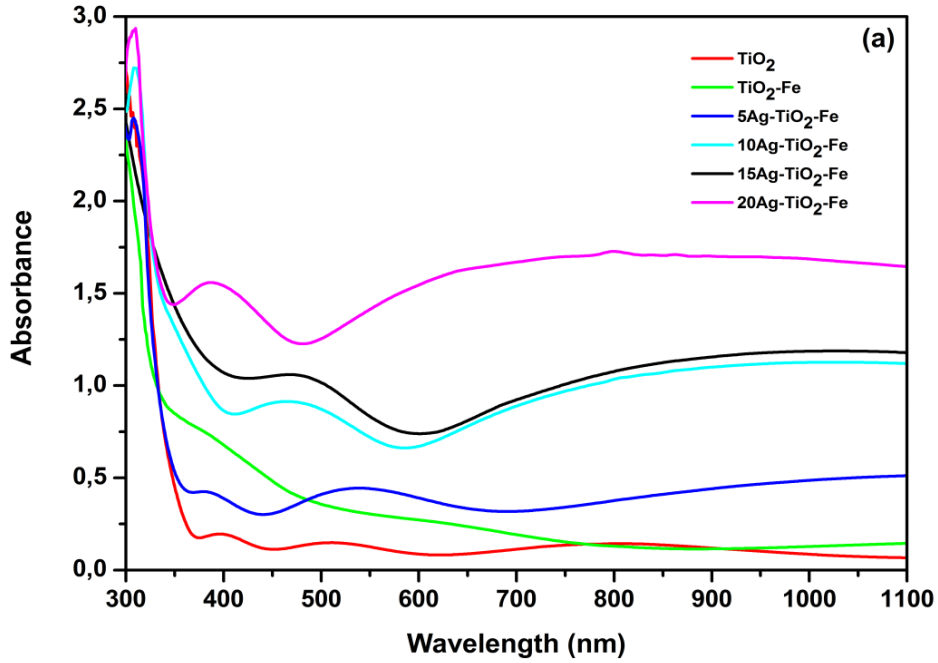

Figure IV.8 UV–vis–NIR absorption spectra of pure TiO_2, TiO_2-Fe and Ag-TiO_2-Fe composite thin films at different Ag contents.

The optical band gap (E_g) of the prepared films calculated by the Tauc method (equation IV.2)) **[18]**;

$$\alpha h\nu = A(h\nu - Eg)^{1/2} \qquad \text{(eq.2)}$$

where $h\nu$ is the photon energy, α is the absorption coefficient, A is the proportionality constant, and Eg is the optical band gap.

The optical indirect band gaps (E_g) are given in **table IV.2** and the graphs of $(\alpha h\nu)^{1/2}$ versus $h\nu$ of samples are presented in **figure IV.9**. It is obvious that the E_g values of the modified films decrease with the addition of Fe and Ag compared to pure TiO_2. While the E_g values of the composite films further decrease at higher silver levels (10, 15, and 20 wt%). Other investigations have documented the decrease in optical band gap with the incorporation of Fe or Ag metals **[19, 10, 20]**. The reduction in band gap is caused by intrinsic and extrinsic defects created into the band gap of anatase TiO_2, where the absorption edge shifted toward longer wavelengths, this leads to an improvement in the photocatalytic activity **[2]**.

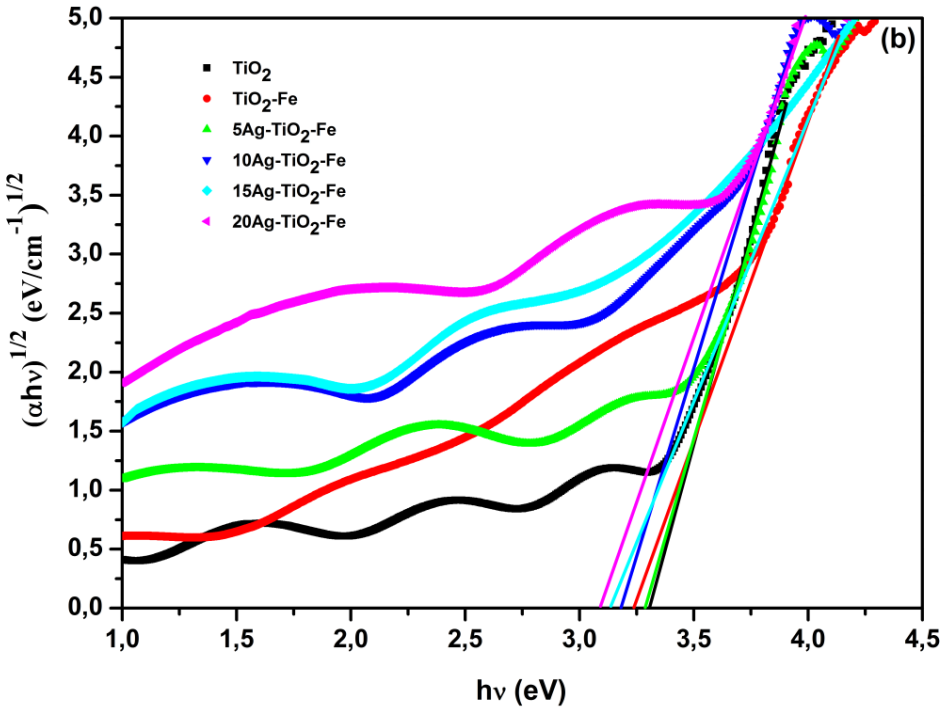

Figure IV.9 Plots of $(\alpha h\nu)^{1/2}$ versus $h\nu$ to determine band gap of each samples.

Table IV.2 Band gap energy of all samples.

Samples	**Band gap (eV)**
TiO_2	3.31
TiO_2-Fe	3.24
5Ag-TiO_2-Fe	3.29
10Ag-TiO_2-Fe	3.18
15Ag-TiO_2-Fe	3.13
20Ag-TiO_2-Fe	3.09

IV.2.6 Photoluminescence analysis

Photoluminescence (PL) emission analysis has been frequently employed in order to comprehend the separation and recombination of the electron-hole pairs, which represent the fundamental processes in the domain of photocatalysis **[21]**. **Figure IV.10** illustrates the PL emission spectra of the prepared films excited at a wavelength of 325 nm at room temperature. The PL spectra of all the prepared films possess emission peaks

between 404 and 410 nm, which may be attributed to free exciton recombination **[22, 23]** . There is also a visible emission peak centered at 516-707 nm, which is generally related to defects in structure and oxygen vacancy levels **[23]**. Furthermore, pure TiO_2 had the highest PL intensity compared with the other samples; however, adding Fe and Ag to the TiO_2 film resulted in a decrease in PL intensity. It is observed that with increasing silver content, the PL peaks of Ag-TiO_2-Fe composite thin films shift towards longer wavelengths and their intensities further decrease. A decrease in the PL intensity signifies a lower recombination rate of electron-hole pairs and thus, higher separation efficiency **[24]**. Ag can act as a trap, capturing photogenerated electrons from the TiO_2 conduction band, preventing electron–hole pairs recombination. As a result, electron–hole separation is promoted, as well as more photogenerated charge carriers actively engage in photokiling **[21, 24, 25]**, thereby elevating the photocatalytic efficiency and antibacterial properties **[2]**.

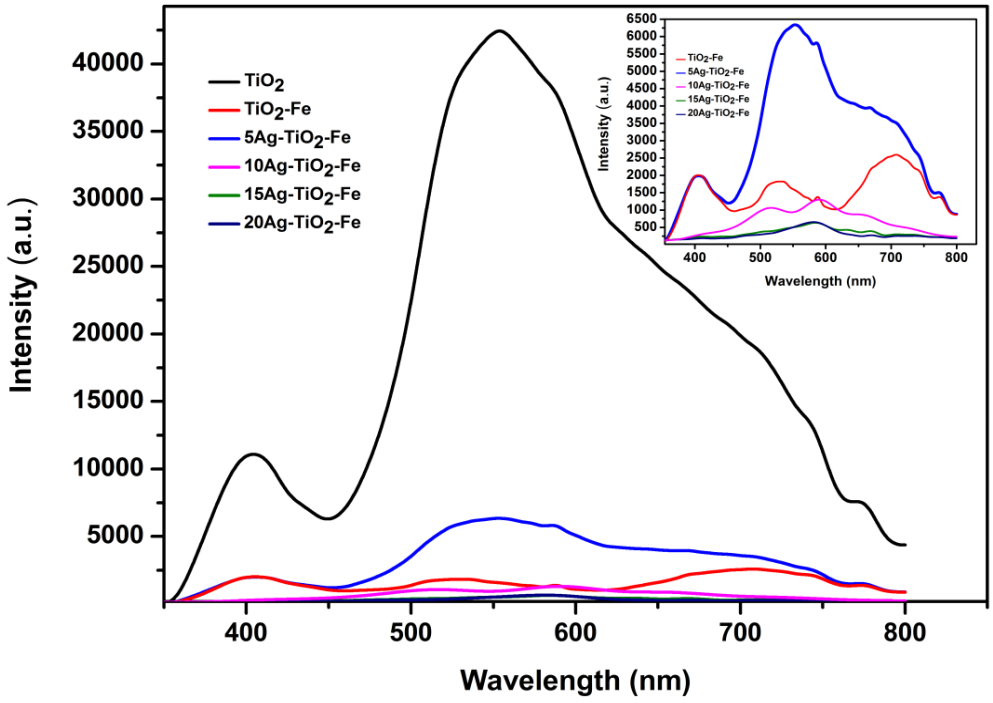

Figure IV.10 Photoluminescence (PL) spectra of pure TiO_2, TiO_2-Fe and Ag-TiO_2-Fe composite thin films at different Ag contents.

IV.3 Antibacterial activity testing of composite thin film against *E. coli* bacteria in the dark and under UV irradiation

The antibacterial efficiency of the prepared thin films against *Escherichia coli* was investigated. The bacteria killing percentage for all the samples in the dark and under UV irradiation after 1 h of interaction are summarized in **figure IV.11**. In the dark experiment, the TiO_2 thin film exhibited no antibacterial effect on *E. coli*. It was found that TiO_2-Fe film did not show a significant bacterial reduction (20%), while Ag-TiO_2-Fe composite films revealed higher antibacterial activity. The results showed complete bacteria inhibition (100%) when 20% Ag-TiO_2-Fe was used, and bacteria killing percentage of 94%, 87% and 55% were observed at 15, 10 and 5 wt% Ag, respectively. This indicates that the presence of silver was responsible for the antibacterial effect of the composite films in dark. It is worth noting that the antibacterial properties of silver have been extensively documented **[26-28]**. There was no obvious bacterial reduction in the control sample in the dark.

Under UV irradiation, the control sample showed no reduction in bacteria, indicating that light irradiation had no adverse effect on bacteria without a catalyst. Pure TiO_2 thin film possessed only 25% of bacterial reduction; this poor antibacterial activity may have been ascribed to the film amorphous nature. It is clearly seen that the reduction of *E. coli* was raised in case of the TiO_2-Fe film (~50%) when exposed to UV light. This related to the presence of iron. On the other hand, the antibacterial activity of the Ag-TiO_2-Fe composite thin films significantly improved under UV irradiation, these composite coatings exhibit excellent photo-killing activity of *E.coli* up to 81% bacterial reduction was found for 5 wt% Ag, and 100% for each of 10, 15, and 20 wt% Ag-TiO_2-Fe composite films, this attributed to the synergistic combination of titanium dioxide (TiO_2) with silver (Ag) and iron (Fe) which present a powerful trio that emerges an excellent antibacterial effects; the TiO_2 anatase phase is known for its exceptional photocatalytic properties, this crystalline structure exhibits high reactivity under UV light by producing ROS such as superoxide radicals and hydroxyl radicals which destroy organisms **[29]**. When combined with silver nanoparticles, known for their broad-spectrum antimicrobial activity, while iron acts as a co-catalyst, promoting electron transfer, which leads to boosted photocatalytic antibacterial efficiency of TiO_2 **[2]**.

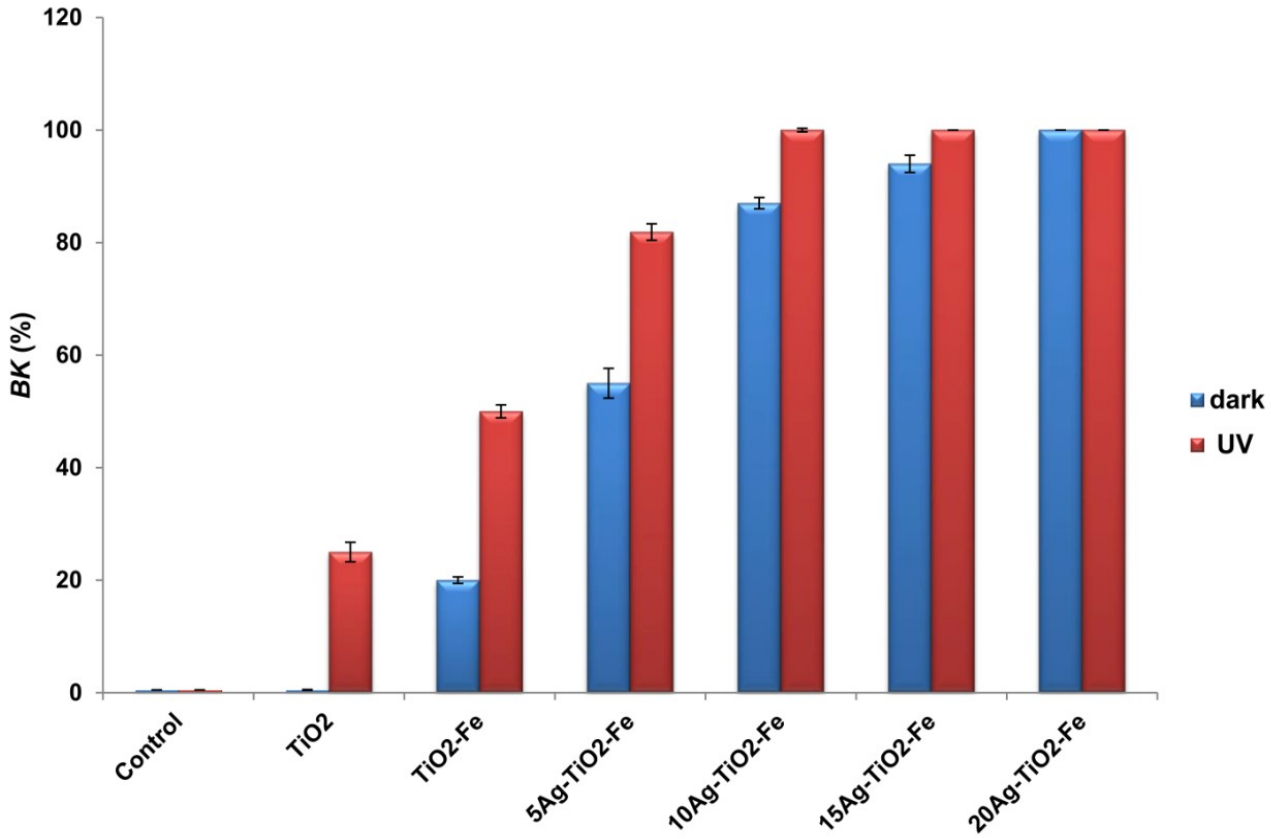

Figure IV.11 Bacteria killing percentage of pure TiO_2, TiO_2-Fe and Ag-TiO_2-Fe composite thin films at different Ag contents in dark and under UV irradiation.

The spread plate technique for the drop test of the prepared films A (in the dark) and B (under UV irradiation) used to count the viable number of *E. coli* colonies is presented in **figure IV.12** and **figure IV.13** shows the bacteria survival percentage in dark (a) and under UV light (b). The results demonstrated a significant decrease in viable number of bacteria colonies with an increase in silver content on the Ag-TiO_2-Fe composite films compared to pure TiO_2 and TiO_2-Fe films in the dark. It was observed that the antibacterial activity of all samples was improved under UV irradiation, with no colonies surviving on the surface of 10, 15, and 20 wt% Ag-TiO_2-Fe composite films within 1 h under UV light **[2]**.

A

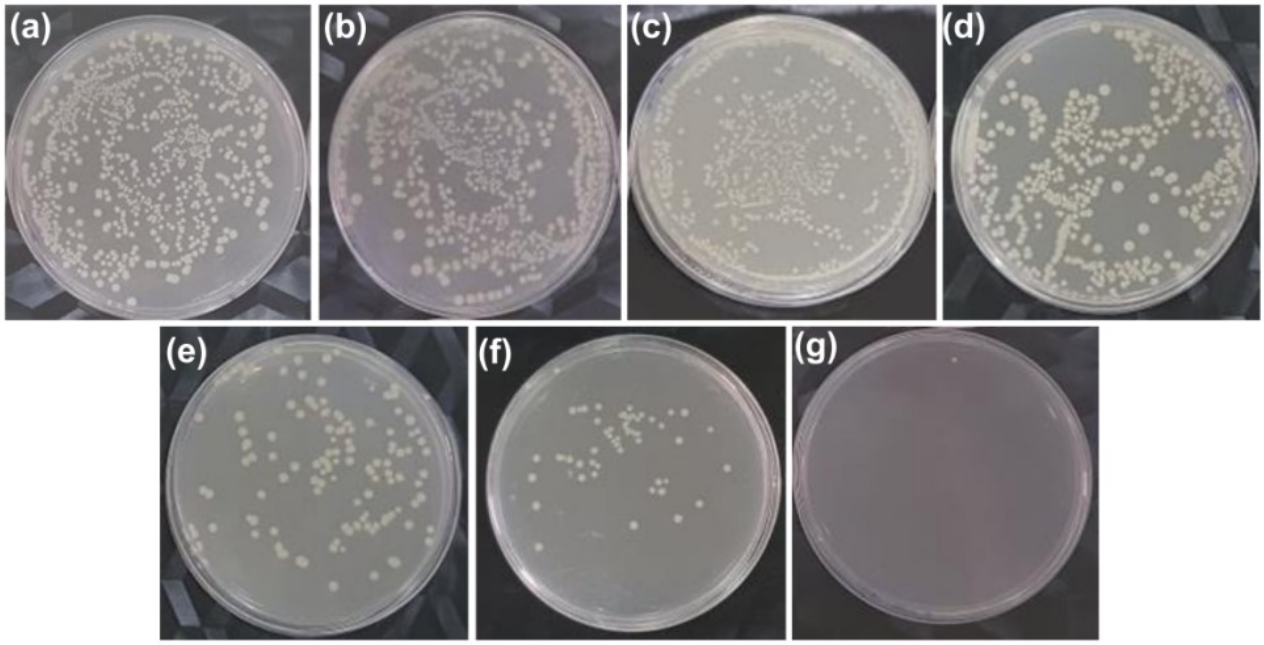

B

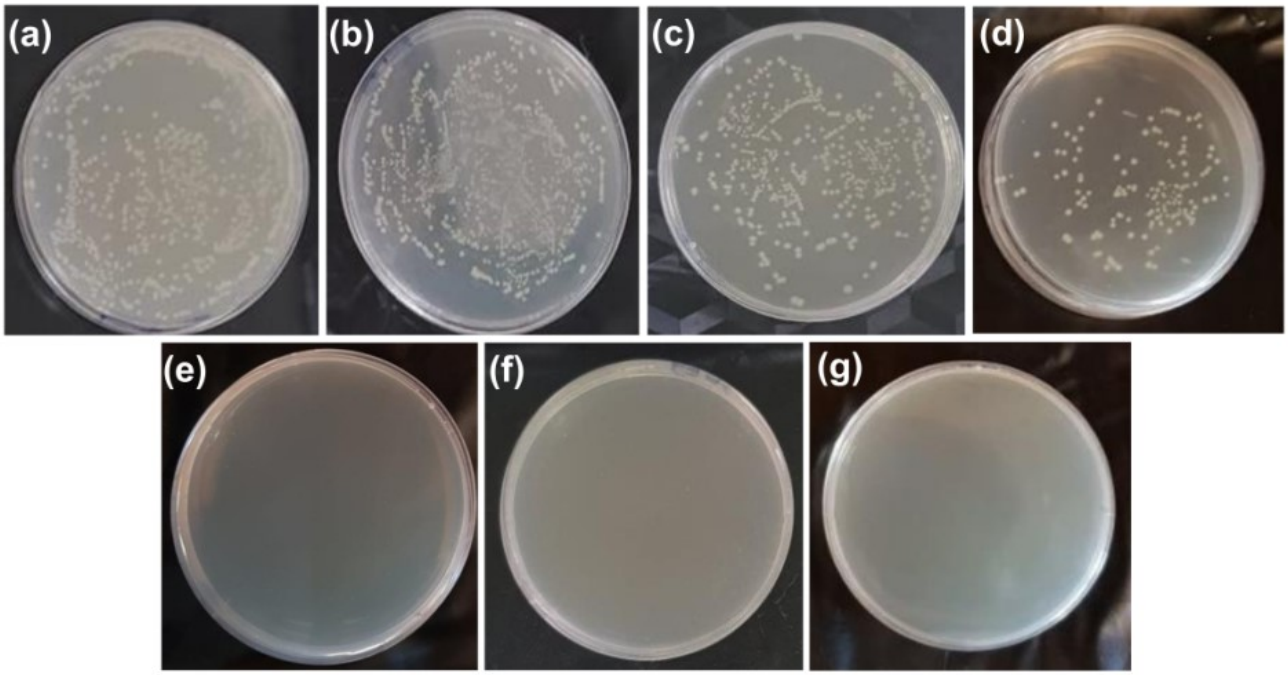

Figure IV.12 Photographs of agar plates containing viable *E.coli* colonies after 1h at 37 ℃: A) in the dark, B) under UV irradiation for (a) Control, (b) Pure TiO_2, (c) TiO_2-Fe and (d-g) Ag-TiO_2-Fe composite thin films at different Ag contents (5-20 wt%).

.

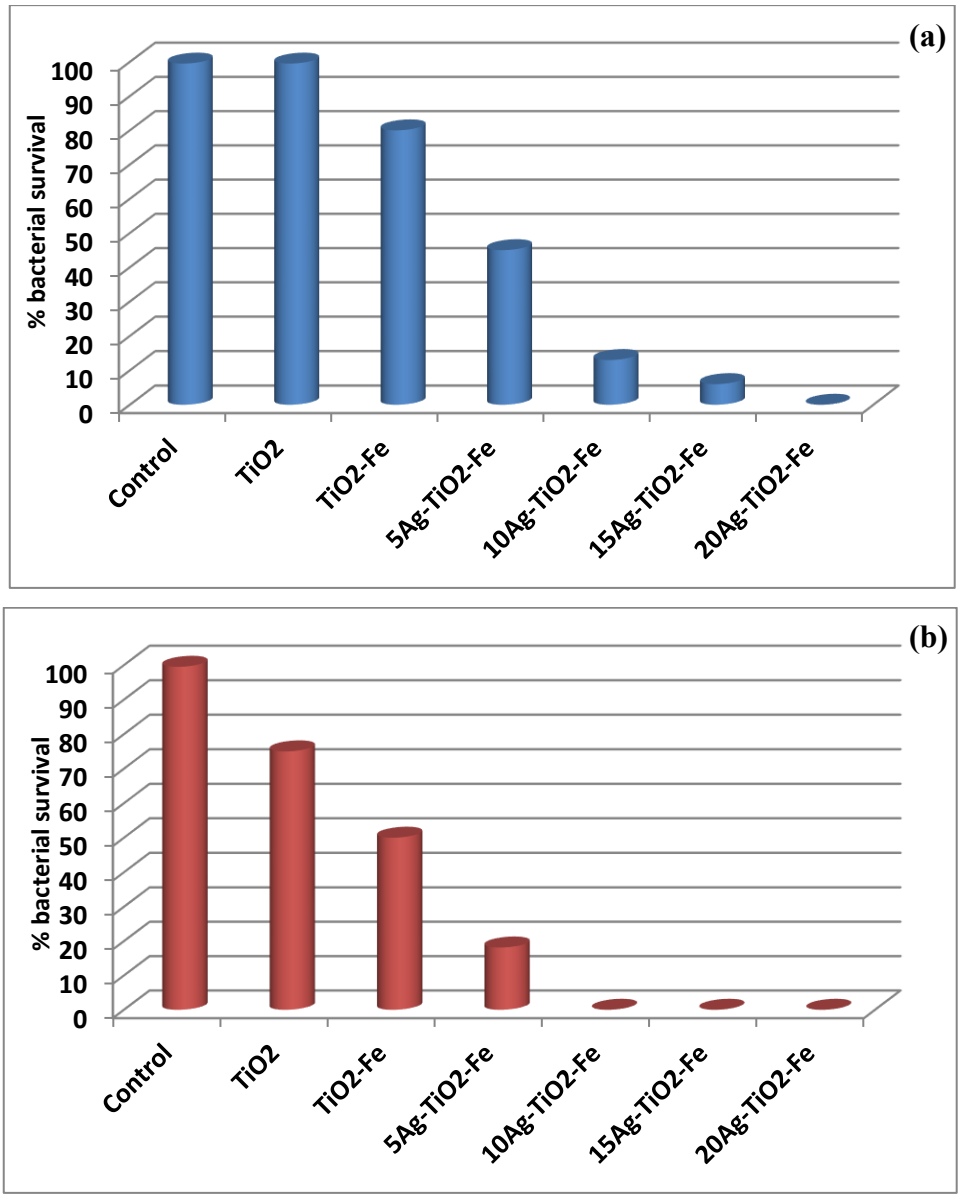

Figure IV.13 Bacteria survival percentage of pure and modified TiO_2 films: a) in the dark and b) under UV irradiation.

IV.3.1 Proposed antibacterial killing mechanism of the Ag-TiO_2-Fe composite films

Synergistic effect on the photokilling activity of *E.coli* was found for the Ag-TiO_2-Fe composite films under UV irradiation, the photokilling activity of anatase TiO_2 photocatalyst involves the generation of reactive oxygen species under UV light, which initiates from conduction band electrons or valence band holes provided by TiO_2 via photo-excitation. The formation of reactive oxygen species (ROS) at films surfaces such as superoxide anion ($O_2^{\bullet -}$) and hydroxyl radicals ($HO^{\bullet}$) have high oxidative stress and possess strong antibacterial properties. This generated ROS interact with the bacterial cell membrane, causing damage to lipids, proteins, and DNA. This oxidative stress leads to the

disruption of cellular functions and, ultimately, bacterial cell death **[29]**. The addition of metals (Fe and Ag) in the TiO_2 matrix had the dual effect of promoting the generation of more (ROS) under UV irradiation by inhibiting the electron–hole pairs recombination, resulting in improved antibacterial efficiency of composite films **[30, 31]**. Whereas iron can produce free radicals through photo-Fenton reaction reactions, causing oxidative damage to bacteria cell **[32, 33]**. On the other hand, silver is known to have antibacterial effects in itself **[26]**. In our case, it is supposed that Ag functioned as both a dopant and an antibacterial agent in the TiO_2 matrix, in the dark; the silver nanoparticles play the main role as antibacterial agent in Ag-TiO_2-Fe composite thin film to kill *E. coli* bacteria **[2]**. The antibacterial activity of silver is still unknown. Previous research has demonstrated that both Ag nanoparticles and released Ag^+ exhibit antibacterial effects through several mechanisms **[34, 35]**.

The antibacterial mechanism of silver involves multiple actions, including membrane disruption, interference with DNA processes, generation of reactive oxygen species, inactivation of enzymes, and alteration of cellular proteins. These combined effects cause the death of bacteria **[28, 36, 26]**. **Figure IV.14** depicts a proposed mechanism of antibacterial performance of Ag-TiO_2-Fe composite thin films in the dark and under UV light.

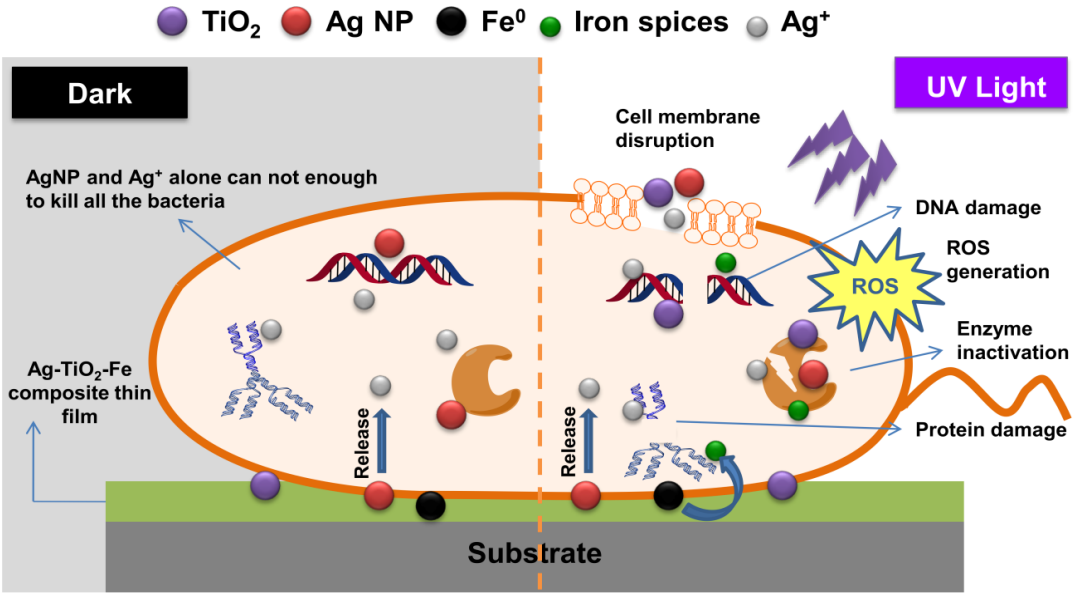

Figure IV.14 Schematic diagram of the antibacterial killing mechanism of the Ag-TiO_2-Fe composite thin film in the dark and under UV light.

IV.4 Conclusion

In summary, antibacterial Ag-TiO_2-Fe composite thin films with varied silver content were successfully synthesized by thermal evaporation technique. The effect of the incorporation of iron and silver on several properties of TiO_2 and on its antibacterial performance was studied. The results revealed that Ag-TiO_2-Fe composite films exhibited great photo-killing activity against the *E. coli* strains under UV (365 nm) light, these composite films displayed complete bacteria inhibition (100%) when 10, 15 and 20% Ag-TiO_2-Fe was used. Moreover, it was observed that Ag significantly improves the antibacterial efficiency in the dark. Various parameters including band gap energy, crystallinity, phase purity, particle size, absorption of light, formation of electron–hole pairs, and generation of ROS were responsible for better antibacterial activity of the Ag-TiO_2-Fe coatings compared to pure TiO_2 film.

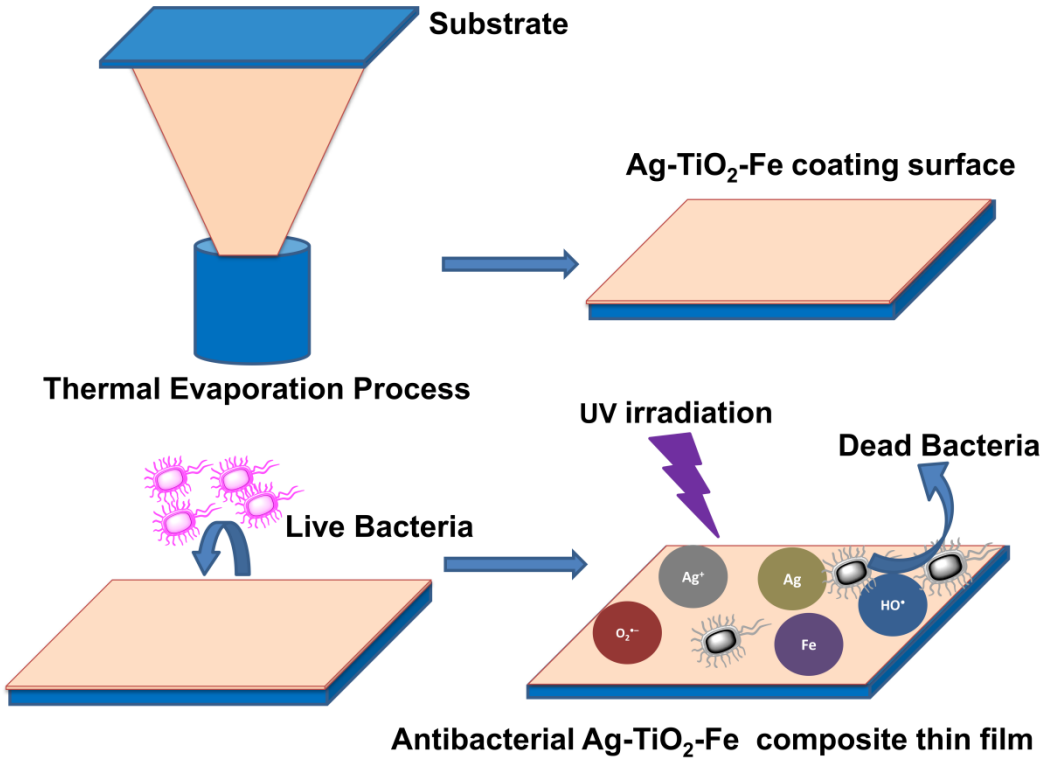

References

[1] B. A. Akgun, C. Durucan, and N. P. Mellott, "Effect of silver incorporation on crystallization and microstructural properties of sol–gel derived titania thin films on glass," *J. Sol-Gel Sci. Technol.*, vol. 58, no. 1, pp. 277–289, Apr. 2011, doi: 10.1007/s10971-010-2388-1.

[2] D. Grine, H. Akkari, P. Fernández, T. Mekhalif, S. Hassani, and F. Lekoui, "Synthesis, Characterization, and Antibacterial Activity of Ag–TiO2–Fe Composite Thin Films," *Phys. Status Solidi Appl. Mater. Sci.*, vol. 219, no. 11, p. 2200036, Apr. 2022, doi: 10.1002/pssa.202200036.

[3] M. A. Majeed Khan, S. Kumar, M. Naziruddin Khan, M. Ahamed, and A. S. Al Dwayyan, "Microstructure and blueshift in optical band gap of nanocrystalline AlxZn1−xO thin films," *J. Lumin.*, vol. 155, pp. 275–281, Nov. 2014, doi: 10.1016/j.jlumin.2014.06.007.

[4] B. Yu, K. M. Leung, Q. Guo, W. M. Lau, and J. Yang, "Synthesis of Ag–TiO2 composite nano thin film for antimicrobial application," *Nanotechnology*, vol. 22, no. 11, p. 115603, Mar. 2011, doi: 10.1088/0957-4484/22/11/115603.

[5] S. Demirci, T. Dikici, M. Yurddaskal, S. Gultekin, M. Toparli, and E. Celik, "Synthesis and characterization of Ag doped TiO2 heterojunction films and their photocatalytic performances," *Appl. Surf. Sci.*, vol. 390, pp. 591–601, Dec. 2016, doi: 10.1016/j.apsusc.2016.08.145.

[6] T. Ohsaka, F. Izumi, and Y. Fujiki, "Raman spectrum of anatase, TiO2," *J. Raman Spectrosc.*, vol. 7, no. 6, pp. 321–324, Dec. 1978, doi: 10.1002/jrs.1250070606.

[7] N. Iwasaki, Y. Sasaki, and Y. Nishina, "Ag electrode reaction in NaOH solution studied by in-situ Raman spectroscopy," *Surf. Sci.*, vol. 198, no. 3, pp. 524–540, Jan. 1988, doi: 10.1016/0039-6028(88)90382-2.

[8] X.-D. Wang and R. G. Greenler, "Direct structure determination of oxygen adsorbed on silver by reflection-absorption infrared spectroscopy with isotopic substitution," *Phys. Rev. B*, vol. 43, no. 8, pp. 6808–6811, Mar. 1991, doi: 10.1103/PhysRevB.43.6808.

[9] J. M. Walls, J. S. Sagu, and K. G. Upul Wijayantha, "Microwave synthesised Pd–TiO $_2$ for photocatalytic ammonia production," *RSC Adv.*, vol. 9, no. 11, pp. 6387–6394, 2019, doi: 10.1039/C8RA09762C.

[10] T. Sun, E. Liu, X. Liang, X. Hu, and J. Fan, "Enhanced hydrogen evolution from water splitting using Fe-Ni codoped and Ag deposited anatase TiO2 synthesized by solvothermal method," *Appl. Surf. Sci.*, vol. 347, pp. 696–705, Aug. 2015, doi: 10.1016/j.apsusc.2015.04.162.

[11] K. Baba *et al.*, "Significance of a Noble Metal Nanolayer on the UV and Visible Light Photocatalytic Activity of Anatase TiO_2 Thin Films Grown from a Scalable PECVD/PVD Approach," *ACS Appl. Mater. Interfaces*, vol. 9, no. 47, pp. 41200–41209, Nov. 2017, doi: 10.1021/acsami.7b10904.

[12] J. Xu *et al.*, "Enhanced photocatalysis by coupling of anatase TiO2 film to triangular Ag nanoparticle island," *Nanoscale Res. Lett.*, vol. 7, no. 1, p. 239, 2012, doi: 10.1186/1556-276X-7-239.

[13] C. Moslah, M. Kandyla, G. A. Mousdis, G. Petropoulou, and M. Ksibi, "Photocatalytic Properties of Titanium Dioxide Thin Films Doped with Noble Metals (Ag, Au, Pd, and Pt)," *Phys. Status Solidi A*, vol. 215, no. 17, p. 1800023, Sep. 2018, doi: 10.1002/pssa.201800023.

[14] Y. Faheem Joya, "Titanium Dioxide Films Prepared by Sol-Gel/Laser-Induced Technique for Inactivation of Bacteria," The University of Manchester, Manchester, 2011.

[15] D. Komaraiah, E. Radha, J. Sivakumar, M. V. Ramana Reddy, and R. Sayanna, "Structural, optical properties and photocatalytic activity of Fe3+ doped TiO2 thin films deposited by sol-gel spin coating," *Surf. Interfaces*, vol. 17, p. 100368, Dec. 2019, doi: 10.1016/j.surfin.2019.100368.

[16] J. Yu, J. Xiong, B. Cheng, and S. Liu, "Fabrication and characterization of Ag–TiO2 multiphase nanocomposite thin films with enhanced photocatalytic activity," *Appl. Catal. B Environ.*, vol. 60, no. 3–4, pp. 211–221, Oct. 2005, doi: 10.1016/j.apcatb.2005.03.009.

[17] J. Xu, Z. Wang, W. Li, X. Zhang, D. He, and X. Xiao, "Ag Nanoparticles Located on Three-Dimensional Pine Tree-Like Hierarchical TiO2 Nanotube Array Films as High-Efficiency Plasmonic Photocatalysts," *Nanoscale Res. Lett.*, vol. 12, no. 1, p. 54, Dec. 2017, doi: 10.1186/s11671-017-1834-1.

[18] J. Tauc, *Amorphous and Liquid Semiconductors*. Springer Science & Business Media, 2012.

[19] U. Arellano, M. Asomoza, and F. Ramírez, "Antimicrobial activity of Fe–TiO2 thin film photocatalysts," *J. Photochem. Photobiol. Chem.*, vol. 222, no. 1, pp. 159–165, Jul. 2011, doi: 10.1016/j.jphotochem.2011.05.016.

[20] S. Khan *et al.*, "Structural and optical properties of macroporous Ag@TiO2 thin films prepared by a facile one-step sol–gel method," *J. Sol-Gel Sci. Technol.*, vol. 93, no. 2, pp. 273–280, Feb. 2020, doi: 10.1007/s10971-019-05199-6.

[21] O. Akhavan and E. Ghaderi, "Self-accumulated Ag nanoparticles on mesoporous TiO2 thin film with high bactericidal activities," *Surf. Coat. Technol.*, vol. 204, no. 21–22, pp. 3676–3683, Aug. 2010, doi: 10.1016/j.surfcoat.2010.04.048.

[22] Y. X. Zhang, G. H. Li, Y. X. Jin, Y. Zhang, J. Zhang, and L. D. Zhang, "Hydrothermal synthesis and photoluminescence of TiO2 nanowires," *Chem. Phys. Lett.*, vol. 365, no. 3–4, pp. 300–304, Oct. 2002, doi: 10.1016/S0009-2614(02)01499-9.

[23] J. Dhanalakshmi, S. Iyyapushpam, S. T. Nishanthi, M. Malligavathy, and D. Pathinettam Padiyan, "Investigation of oxygen vacancies in Ce coupled TiO_2 nanocomposites by Raman and PL spectra," *Adv. Nat. Sci. Nanosci. Nanotechnol.*, vol. 8, no. 1, p. 015015, Mar. 2017, doi: 10.1088/2043-6254/aa5984.

[24] H. Mahipati Yadav, "Antibacterial studies with metal-doped TiO2 nanoparticles," D. Y. Patil University, Kolhapur, India, 2014.

[25] S. P. Lim, A. Pandikumar, H. N. Lim, R. Ramaraj, and N. M. Huang, "Boosting Photovoltaic Performance of Dye-Sensitized Solar Cells Using Silver Nanoparticle-Decorated N,S-Co-Doped-TiO2 Photoanode," *Sci. Rep.*, vol. 5, no. 1, p. 11922, Dec. 2015, doi: 10.1038/srep11922.

[26] B. Le Ouay and F. Stellacci, "Antibacterial activity of silver nanoparticles: A surface science insight," *Nano Today*, vol. 10, no. 3, pp. 339–354, Jun. 2015, doi: 10.1016/j.nantod.2015.04.002.

[27] S. D. Ponja, S. K. Sehmi, E. Allan, A. J. MacRobert, I. P. Parkin, and C. J. Carmalt, "Enhanced Bactericidal Activity of Silver Thin Films Deposited via Aerosol-Assisted Chemical Vapor Deposition," *ACS Appl. Mater. Interfaces*, vol. 7, no. 51, pp. 28616–28623, Dec. 2015, doi: 10.1021/acsami.5b10171.

[28] N. Durán, M. Durán, M. B. de Jesus, A. B. Seabra, W. J. Fávaro, and G. Nakazato, "Silver nanoparticles: A new view on mechanistic aspects on antimicrobial activity," *Nanomedicine Nanotechnol. Biol. Med.*, vol. 12, no. 3, pp. 789–799, Apr. 2016, doi: 10.1016/j.nano.2015.11.016.

[29] U. Joost *et al.*, "Photocatalytic antibacterial activity of nano-TiO2 (anatase)-based thin films: Effects on Escherichia coli cells and fatty acids," *J. Photochem. Photobiol. B*, vol. 142, pp. 178–185, Jan. 2015, doi: 10.1016/j.jphotobiol.2014.12.010.

[30] Y. Liu, X. Wang, F. Yang, and X. Yang, "Excellent antimicrobial properties of mesoporous anatase TiO2 and Ag/TiO2 composite films," *Microporous Mesoporous Mater.*, vol. 114, no. 1–3, pp. 431–439, Sep. 2008, doi: 10.1016/j.micromeso.2008.01.032.

[31] Md. A. Hossain *et al.*, "Synthesis of Fe- or Ag-doped TiO2–MWCNT nanocomposite thin films and their visible-light-induced catalysis of dye degradation and antibacterial activity," *Res. Chem. Intermed.*, vol. 44, no. 4, pp. 2667–2683, Apr. 2018, doi: 10.1007/s11164-018-3253-z.

[32] C. Lee, J. Y. Kim, W. I. Lee, K. L. Nelson, J. Yoon, and D. L. Sedlak, "Bactericidal Effect of Zero-Valent Iron Nanoparticles on Escherichia coli," *Environ. Sci. Technol.*, vol. 42, no. 13, pp. 4927–4933, Jul. 2008, doi: 10.1021/es800408u.

[33] Q. Chen, J. Li, Y. Wu, F. Shen, and M. Yao, "Biological responses of Gram-positive and Gram-negative bacteria to nZVI (Fe0), Fe2+ and Fe3+," *RSC Adv.*, vol. 3, no. 33, p. 13835, 2013, doi: 10.1039/c3ra40570b.

[34] M.-S. Wong, C.-W. Chen, C.-C. Hsieh, S.-C. Hung, D.-S. Sun, and H.-H. Chang, "Antibacterial property of Ag nanoparticle-impregnated N-doped titania films under visible light," *Sci. Rep.*, vol. 5, no. 1, p. 11978, Dec. 2015, doi: 10.1038/srep11978.

[35] I. Sondi and B. Salopek-Sondi, "Silver nanoparticles as antimicrobial agent: a case study on E. coli as a model for Gram-negative bacteria," *J. Colloid Interface Sci.*, vol. 275, no. 1, pp. 177–182, Jul. 2004, doi: 10.1016/j.jcis.2004.02.012.

[36] Y. Qing *et al.*, "Potential antibacterial mechanism of silver nanoparticles and the optimization of orthopedic implants by advanced modification technologies," *Int. J. Nanomedicine*, vol. Volume 13, pp. 3311–3327, Jun. 2018, doi: 10.2147/IJN.S165125.

Conclusion

Conclusion

This research conducted provides a comprehensive study on the synthesis, characterization and evaluation of antibacterial activity against *Escherichia coli* bacteria in both dark and under UV light of new kind of composite thin films based on Ag-TiO_2-Fe system.

The modification of TiO_2 by metal doping has a significant impact on the photocatalyst and its performance as antibacterial material. Photocatalytic antibacterial activity is affected by many factors including method of preparation, band gap energy, particle size, absorption of light, surface area, formation of electron-hole pairs, generation of ROS, crystallinity, phase purity, etc

In this study, pure TiO_2, TiO_2-Fe, and Ag-TiO_2-Fe composite thin films have been successfully synthesized by thermal evaporation method and subsequent annealing in air at 400℃ for 1h, The influence of Fe and Ag dopants as well as the variation in the silver content (5-20 wt%) on the properties and antibacterial performance of the composite films has been investigated. The films produced during this study were characterized using various techniques.

Structural data revealed that adding Ag to the TiO_2-Fe matrix resulted in the formation of anatase crystalline phase. It is noted that the presence of silver also enhance the Raman intensities of $E_g(1)$ mode of anatase in Ag-TiO_2-Fe composite films, which attributed to the surface-enhanced Raman spectra (SERS) characteristic of Ag. Morphological characterization confirmed the presence of silver in the metallic form (bright spots) in the composite films, where Ag particles with different sizes ranging from 70 to 400 nm are uniformly distributed on the surface.

Optical analysis showed that the pure TiO_2 film had the highest transmittance (~ 83.02%) in the visible region compared to the other samples. The obvious shift of the absorption edge toward the red region is due to the incorporation of Fe and Ag into the TiO_2 lattice, which resulted in the reduction of the energy band gap of the TiO_2-Fe and Ag-TiO_2-Fe composite films. Photoluminescence (PL) analysis showed that when silver content increases, the PL peaks of Ag-TiO_2-Fe composite thin films shift to longer wavelengths and their intensities further decrease, which indicates a decrease in the recombination rate of electron–hole pairs, and consequently an improvement in separation

efficiency, which leads to the production of more ROS and the increase in photocatalytic efficiency as well as antibacterial properties.

The antibacterial activity of the films was tested against *E. coli* bacteria in the dark and under UV light. Ag-TiO_2-Fe composite films showed an increase in the antibacterial activity with increasing Ag content in the dark. The experimental results reveal antibacterial efficiency of 55%, 87%, 94%, and 100% for the 5, 10, 15, and 20 wt% Ag-TiO_2-Fe composite films, respectively. The Ag plays a major role in influencing the antibacterial efficiency in dark. Under UV irradiation, synergistic effect on the photokilling activity of *E.coli* was observed for the Ag-TiO_2-Fe composite films, which exhibited higher photokilling activity than pure TiO_2 and TiO_2-Fe. Ag-TiO_2-Fe composite films demonstrated an excellent photokilling activity of *E.coli* up to 81% bacterial reduction was observed for 5 wt% Ag, and 100% for each of 10, 15, and 20 wt% Ag-TiO_2-Fe composite films.

Based on all of these results, we conclude that Ag-TiO_2-Fe films hold great promise as an effective antibacterial coating suitable for a range of applications, including medical devices, environmental surface disinfection, and water treatment field.

Further investigations will be performed in parallel with the results of this research in the future. These are summarized as follows;

- Explore the hydrophilic/hydrophobic properties of the Ag-TiO_2-Fe coatings by measuring the contact angle of water droplet on the surface. In addition to study the durability and hardness of composite films.
- Investigate the effect of the percentage of Fe and Ag added to titanium dioxide with the aim of reducing the amount of both metals to lower samples costs.
- Evaluate the antibacterial activity of the produced composite films against other types of microorganisms such as gram positive bacteria.
- Conducting antibacterial experiments over shorter periods of time would be very interesting perspective.
- Evaluate the performance of Ag-TiO_2-Fe antibacterial coatings in health care settings.

Appendix I

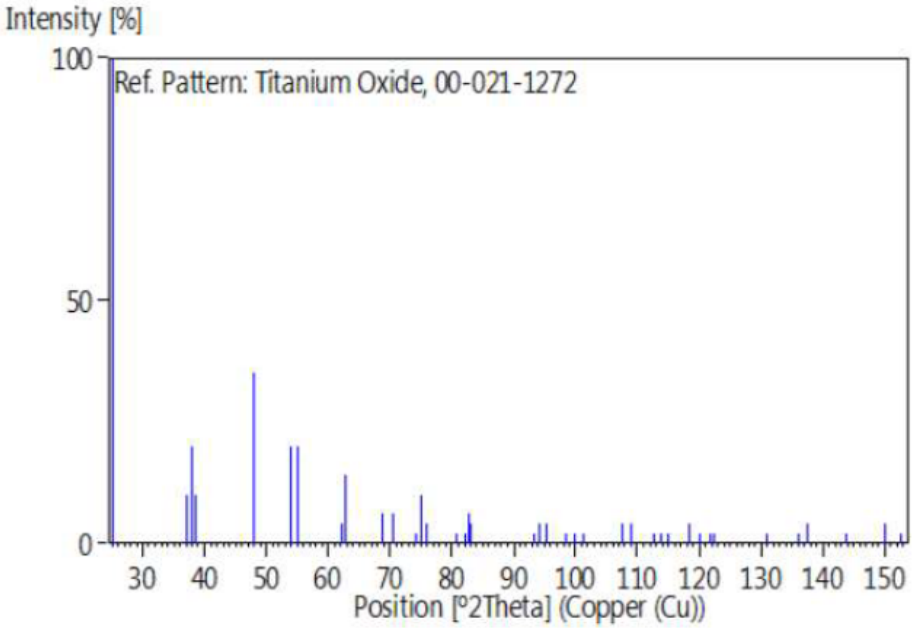

Figure 1: JCPDS card of TiO_2 anatase.

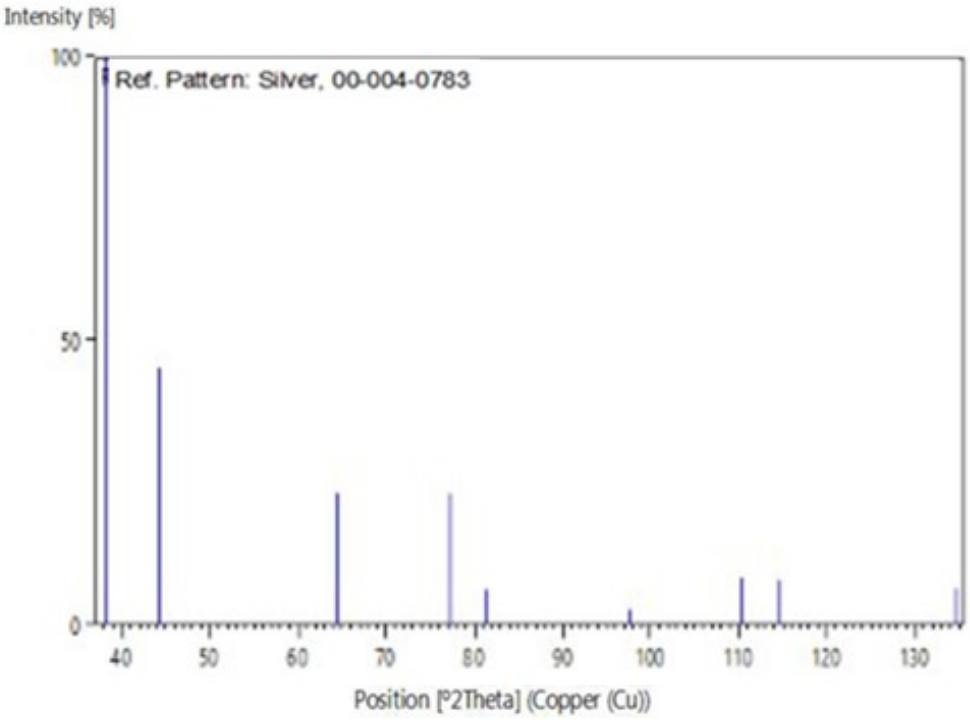

Figure 2: JCPDS card of Ag cubic.

Appendix II

Figure 1 presents the qualitative evaluation (zone of inhibition test), substrates coated with pure TiO_2, TiO_2-Fe and (5-20 wt%) Ag-TiO_2-Fe films were placed on the solidified agar gel containing the spread bacteria suspension in different Petri dishes without UV exposure. Then the plates were incubated at 37 ℃ for 24 h. The result demonstrates that no zone of inhibition is evident surrounding the pure and TiO_2-Fe coated substrate, whereas it is observed that 20% Ag-TiO_2-Fe sample prevented the growth of bacteria remarkably and formed well-defined inhibition zones around the samples (inhibition zones with diameter of 2.4 cm) indicates the better antibacterial efficiency of sample against the *E.coli* compared with other samples. The presence of small and no clear inhibition zones around 10 and 15% Ag-TiO_2-Fe coated substrates and no direct measurable zone of inhibition could be attributed to the no sufficient contact of the Ag diffused into the agar with the bacterial strains.

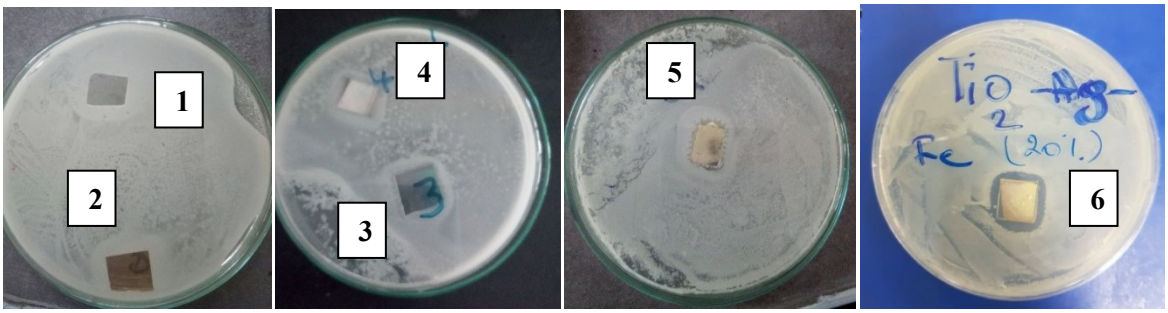

Figure 1: Zone of inhibition test results of the prepared films: (1) pure TiO_2, (2) TiO_2-Fe, and (3-6) Ag-TiO_2-Fe composite thin films at different Ag contents (5-20 wt%).

Conferences and Publications

1. Conferences

International conference

- **D.Grine**, T.Mekhalif and H.Akkari. «*Elaboration of Ag based thin layers for the detection of biomolecules*». Participation in: the 3rd International Symposium on Materials and Sustainable Development ISMSD2017, Novembre 07 & 08, 2017 Boumerdes , Algeria
- **D.Grine**, F.Lekoui and H.Akkari. «*Synthesis and characterization of iron oxides doped TiO_2/Ag thin film composites*». Participation in: International Conference on Nanomaterials and Renewable Energies ICNRE 2018, October 15-17, 2018 Skikda, Algeria
- **D.Grine**, H.Akkari and F.Lekoui. «*Deposition of TiO_2/Fe_2O_3 composite thin films by vacuum thermal evaporation*». Participation in: the 2nd International Workshop on Magnetic Materials and Nanomaterials–MMN' 2018, October 01-04, 2018 Boumerdes, Algeria.
- **D.Grine**, T.Mekhalif, H.Akkari and S.Hassani. «*Elaboration of TiO_2/Ag thin layers for the immobilization of glucose oxidase enzyme*». Participation in: the VIIème Congrès international de Biotechnologie et Valorisation des Bio-Ressources Mars, 20-23 , 2019 Tabarka, Tunisie.

2. Publications

International journals

Synthesis, characterization and antibacterial activity of Ag-TiO_2-Fe composite thin films.
Djihad Grine, Hocine Akkari, Paloma Fernández, Tahar Mekhalif, Salim Hassani, and Fouaz Lekoui.
Journal of Physica Status Solidi (A) applications and materials science. DOI: 10.1002/pssa.202200036.

physica status solidi a
www.pss-a.com

Synthesis, Characterization, and Antibacterial Activity of Ag–TiO_2–Fe Composite Thin Films

Djihad Grine, Hocine Akkari, Paloma Fernández, Tahar Mekhalif, Salim Hassani, and Fouaz Lekoui*

Ag–TiO_2–Fe composite thin films with different Ag contents are deposited onto a glass substrate by a thermal evaporation method. TiO_2, TiO_2–Fe, and Ag–TiO_2–Fe thin films are characterized by X-ray diffraction (XRD), Raman spectroscopy, scanning electron microscopy (SEM), UV–vis–NIR spectroscopy, and photoluminescence (PL) to study the relation between their structural, morphological, optical, and luminescent properties with their antibacterial activities. XRD and Raman measurements show the formation of the anatase phase with increasing silver content in Ag–TiO_2–Fe composite thin films. SEM images show the presence of silver in the metallic form. Optical measurements display a redshift in the optical absorption edge of TiO_2–Fe and Ag–TiO_2–Fe composite films with a decrease in the energy bandgap compared to pure TiO_2. The antibacterial activity of the films against *Escherichia coli* is investigated both in the dark and under UV light. It is found that Ag plays a major role on the antibacterial efficiency in the dark. Ag–TiO_2–Fe composite thin films exhibit a synergistic antibacterial effect under UV light, resulting an excellent antibacterial coating.

1. Introduction

Antibacterial coatings are one of the major topics of interest for applications in many different fields. They have attracted researchers due to their importance as inhibitors of microbial adhesion and reducing biofilm formation. Antibacterial coatings are used in medicine to protect medical devices against infections and for environmental surfaces in hospitals improving the quality of healthcare.[1] Titanium dioxide (TiO_2) is the most widely investigated semiconductor as effective photocatalyst because of its strong oxidizing power,[2] nontoxicity,[3] and good chemical stability.[4] It has been widely used in air and wastewater purification,[5,6] and been applied in various biomedical applications as well.[7] Anatase TiO_2 is a well-known photocatalytic material under UV irradiation.[8] After exposure to UV light, the photon energy excites electrons from the valence band to the conduction band, leaving positive charge holes (h^+). The electrons (e^-) in conduction band and holes (h^+) in valence band react with water and oxygen to generate reactive oxygen species (ROS) such as hydroxyl radicals ($HO^\bullet$) and superoxide anions ($O_2^{\bullet-}$); these reactive oxygen species would be responsible for deactivation of microbial organisms such as cancer cells, viruses, and bacteria.[9,10]

A variety of attempts have been made to improve photocatalytic efficiency and antibacterial activity of TiO_2 thin films. Recently, researchers reported that modification of TiO_2 by introducing various metals into the TiO_2 matrix such as Fe, Co, Ag, Pt, and Cr is a promising process to reduce the recombination rate of the electron/hole pairs.[11–15] Furthermore, they could enhance the photocatalytic activity in the visible light region and increase the antibacterial performance.[6,16,17] Ag is one of

D. Grine
Groupe des Matériaux Fonctionnels
Laboratoire LGMM
Faculté des Sciences
Université 20 Août 1955-Skikda
BP 26, 21000 Skikda, Algeria
E-mail: d.grine@univ-skikda.dz

D. Grine
Laboratoire de Recherche sur la Physico-Chimie des Surfaces et Interfaces
Université 20 Août 1955-Skikda
BP 26, 21000 Skikda, Algeria

H. Akkari
Département de Génie Industriel
Faculté de Technologie
Université Batna 2 Chahid Mostefa Ben Boulaid
05001 Batna, Algeria

The ORCID identification number(s) for the author(s) of this article can be found under https://doi.org/10.1002/pssa.202200036.

DOI: 10.1002/pssa.202200036

P. Fernández
Department of Materials Physics
Faculty of Physics
Complutense University of Madrid
28040 Madrid, Spain

T. Mekhalif
Laboratoire de Biochimie Appliquée
Faculté des Sciences de la Nature et de la Vie
Université de Sétif 1
19000 Sétif, Algeria

S. Hassani, F. Lekoui
Division des Milieux Ionisés & Laser
Centre de Développement des Technologies Avancées
Cité 20 Août 1956, Baba Hassen, 16081 Alger, Algeria

the most interesting materials due to their excellent physical and chemical properties, catalytic activity, and low toxicity.[18,19] It is well known as antibacterial agent from ancient time.[20] Several researches demonstrated that Ag played a significant role in enhancing the antibacterial properties of TiO_2.[21–23] Wahyuni and Roto reported the inactivation of *Escherichia coli* (*E. coli*) bacteria by Ag nanoparticles incorporated in TiO_2 matrix.[24] Several articles have enlightened the inhibition mechanism of silver on bacteria,[25–27] either by direct contact or by the action of released silver ions (Ag^+).[28] Materials based on metals and metal oxides are one of the best candidates for reducing bacterial growth which has been studied by several authors.[29–32] A significant improvement in the antibacterial properties can be achieved by introducing Fe into TiO_2 matrix under UV irradiation.[3,33,34] Trapalis et al. reported that Fe-doped TiO_2 films show high antibacterial activity eliminating the *E. coli* after 2 h illumination under UV radiation.[34] Modified TiO_2 in the form of thin films finds greater technological importance because of their variety of advantages and their role in different applications.[35] Many methods have been employed to grow TiO_2-based thin films such as chemical vapor deposition,[36] electron beam evaporation,[37] spray pyrolysis,[38] sol–gel,[39] and sputtering method.[40]

The aim of this study was to prepare Ag–TiO_2–Fe composite thin films as effective antibacterial coatings using thermal evaporation method. The antibacterial activity of pure TiO_2 and modified TiO_2 thin films was tested against *E. coli* bacteria. The influence of the incorporation of Fe and Ag on the TiO_2 thin film was explored. Furthermore, different Ag contents were used to observe their effect on antibacterial performance of composite films especially in the dark. The Ag–TiO_2–Fe composite film is more beneficial and has shown excellent antibacterial ability under UV irradiation due to the synergistic effect that arises between the Ag- and Fe-modified TiO_2. In addition, the structural, morphological, and optical properties of the prepared films were also analyzed and discussed.

2. Experimental Section

2.1. Sample Preparation

TiO_2 film and TiO_2 composite thin films were deposited by thermal evaporation method,[41] on glass substrates (microscope slides) with dimensions of $25 \times 75 \times 1.0$ mm using titanium dioxide powder (TiO_2; 99.5%, Sigma-Aldrich), iron powder (Fe; 99%, Biochem), and different amounts of silver (Ag lump; 99.99%, GoodFellow). Before deposition, the glass substrates were ultrasonically cleaned for 10 min with acetone and ethanol solution. The thermal evaporation unit is a homemade s ystem, developed at our institution. The vacuum chamber was first evacuated at low pressure of 6.2×10^{-5} mbar and the deposition process was carried out by heating a crucible containing only pure TiO_2 or a mixture of TiO_2–Fe or Ag–TiO_2–Fe with Fe fixed at 5.0 wt% and different Ag mass ratio (0, 5, 10, 15, and 20 wt%). The mixtures were thermally evaporated to form a gaseous atmosphere, which condense to form our thin films. Finally, the prepared samples were annealed in air at 400 °C for 1 h.

2.2. Materials Characterization

The X-ray diffraction (XRD) analysis was carried out for structural properties by PANalytical X'Pert PRO MRD diffractometer with a monochromator using Cu Kα source ($K\alpha_1$: 1.5406 Å) operated at 45 kV with 40 mA emission current. The scanning range was from 20° to 80°. Optical transmittance and spectral absorption were measured in the wavelength range of 300–1100 nm using UV–vis–NIR spectrophotometer (Shimadzu UV-1700). The morphology of the films was investigated with a FEI Inspect scanning electron microscope (SEM). Microphotoluminescence (μ-PL) and Raman measurements were performed at room temperature in a Horiba Jobin-Yvon LabRAM HR800 confocal microscope. In PL measurements the He–Cd laser ($\lambda_{ex} = 325$ nm) was employed as excitation source, while Raman spectra were recorded under excitation at 633 nm line of a He–Ne laser.

2.3. Antibacterial Test

The antibacterial activity of all the thin films was investigated using the so-called antibacterial drop test. The test was carried out against *Escherichia coli* (*E. coli*) as a model for the Gram-negative bacteria. The samples were examined under similar conditions in dark and under UV irradiation. All glassware and samples were sterilized by autoclaving at 120 °C for 15 min. The thin films (size of 15×10 mm) were placed in a sterilized Petri dish. Then, 100 μL of bacteria suspension (10^5 CFU mL^{-1}) was dropped onto the surface of the control sample and the coated thin films; the samples were then irradiated using UV light (8 W, 365 nm wavelength, Philips) for 60 min at 37 °C incubation. The process was also done in dark. After that, the bacteria were washed from the surface of the samples using 5 mL sterile physiological saline. Then, 50 μL of each diluted solution was spread on a nutrient agar plates. The numbers of surviving bacteria colonies on the agar plates were counted after incubation for 24 h at 37 °C. The reported values are averages of three similar independent experiments. The bacteria killing percentage "BK" was calculated by using Equation (1) as follows

$$\mathrm{BK} = \frac{A - B}{A} \times 100\% \tag{1}$$

where A and B are the number of bacteria colonies grown in the culture medium corresponding to the control sample and coated films, respectively.

3. Results and Discussion

3.1. XRD Analysis

Figure 1 shows the XRD patterns of TiO_2, TiO_2–Fe and Ag–TiO_2–Fe composite films with different Ag content. The XRD pattern of pure TiO_2 and TiO_2–Fe thin films does not show any diffraction peaks, which confirms that the films are amorphous. As Ag was introduced in TiO_2–Fe films, the films exhibited crystallization to anatase phase and the intensity of diffraction peaks was found to increase with increasing Ag content. This increase is particularly remarkable for Ag content at 15%

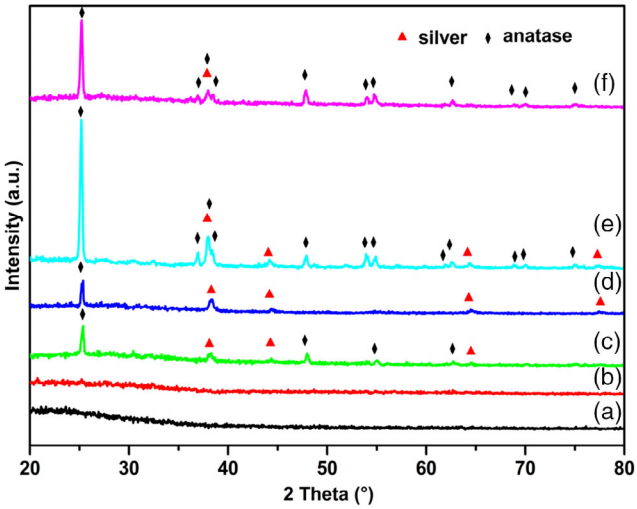

Figure 1. XRD patterns of a) pure TiO_2, b) TiO_2–Fe, c) 5%Ag–TiO_2–Fe, d) 10%Ag–TiO_2–Fe, e) 15%Ag–TiO_2–Fe, and f) 20%Ag–TiO_2–Fe composite thin films.

and would be indicative of a better film crystallinity.[42] For Ag–TiO_2–Fe composite films, a series of characteristic peak at 25.3°, 37.0°, 38.0°, 38.5°, 48.0°, 54.0°, 55.0°, 62.0°, 62.7°, 68.0°, 70.1°, and 75.1° are observed that are assigned to the (101), (103), (004), (112), (200), (102), (211), (213), (204), (116), (220), and (215) crystallographic planes of TiO_2 anatase phase (JCPDS no. 21-1272), without any other TiO_2 phases detected. The other peaks of the XRD pattern at 38.1°, 44.2°, 64.5° and 77.5° are indexed to (111), (200), (220), and (311) crystal planes related to face-centered cubic (fcc) structure of metallic silver (JCPDS card no. 04-0783). The diffraction peak corresponding to (004) of TiO_2 and (111) of Ag is very close to one another. Thus, it is difficult to differentiate the Ag signals from the TiO_2 signals. No peaks related to iron species were observed; this may be attributed to the small amount of Fe into titanium oxide matrix. There are no obvious differences in TiO_2 crystallite size in all Ag–TiO_2–Fe composite thin films with the increase of silver content, and these findings are in good agreement with the literature.[2,43] The crystallite size of TiO_2 determined using the Scherrer's formula[44] on (101) diffraction peak was estimated about 33 nm.

3.2. Raman Analysis

The Raman spectra of prepared samples are displayed in **Figure 2**. It is clear that pure TiO_2 and TiO_2–Fe thin films exhibit the amorphous characteristic in their Raman spectra, which is in agreement with the result of XRD analysis. The Ag–TiO_2–Fe composite films show a main characteristic peak slightly above 151 cm^{-1} corresponding to the $E_g(1)$ mode of anatase TiO_2, as long as some additional peaks, with a much lower intensity, in fact only appreciated for the highest Ag content (Figure 2e and f). They are located at 640 cm^{-1} $E_g(3)$ corresponding to the Raman active modes of anatase phase,[45] and at 328 cm^{-1}, due to the Ag–O stretching vibration.[46–48] Resulting from the oxidation of a few Ag nanoparticles on irregularities such as pits or bumps

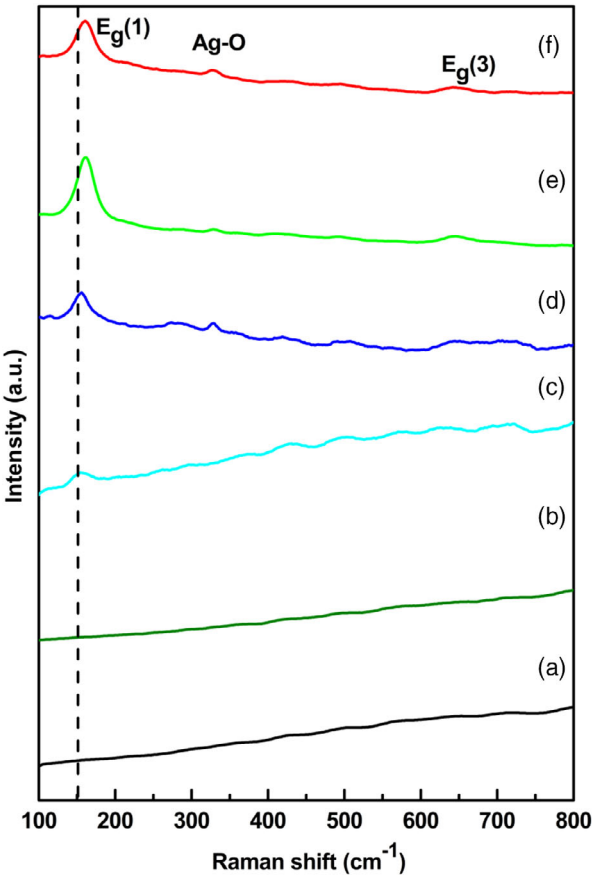

Figure 2. Raman spectra of a) pure TiO_2, b) TiO_2–Fe, c) 5%Ag–TiO_2–Fe, d) 10%Ag–TiO_2–Fe, e) 15%Ag–TiO_2–Fe, and f) 20%Ag–TiO_2–Fe composite thin films.

appeared on the surface of the composite thin films, where the Ag atoms might preferentially locate. However, no crystalline phases for the Fe or its oxides were detected for the samples because of the low amount of Fe. When silver is introduced into TiO_2–Fe thin films, the $E_g(1)$ Raman intensities of Ag–TiO_2–Fe composite thin films are enhanced especially at 15 wt% Ag. This enhancement in the intensity of Raman can be also attributed to the surface-enhanced Raman spectra (SERS) properties of Ag.

Similar results have been reported by Xu et al.[49] Moreover, the $E_g(1)$ peak position exhibits a large shift from 151 to 158 cm^{-1} according to the increase of Ag content (5–20 wt%) compared to typical TiO_2 bonding modes.[50] In general, the shift in Raman peak occurs due to the nonstoichiometry structure defects and surface interaction between metal and TiO_2.[51,52]

3.3. Surface Morphology

The SEM images of the pure TiO_2, TiO_2–Fe, and Ag–TiO_2–Fe composite thin films with different Ag content annealed at 400 °C are presented in **Figure 3**a–f. It could be seen that the pure TiO_2 film shows a uniform bubble distribution (Figure 3a). The surface morphology of the deposited TiO_2 film became smoother

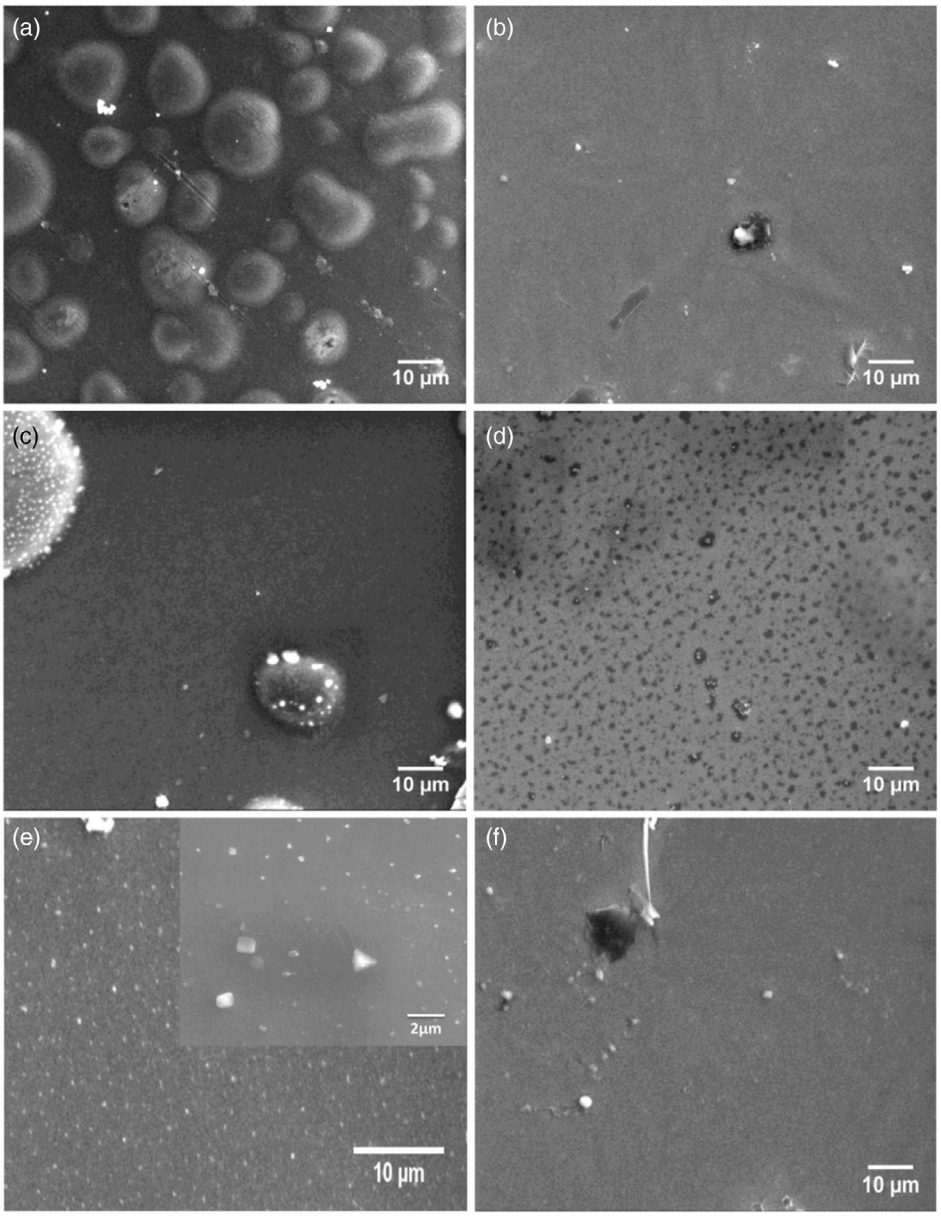

Figure 3. SEM images of a) pure TiO_2, b) TiO_2–Fe, c) 5%Ag–TiO_2–Fe, d) 10%Ag–TiO_2–Fe, e) 15%Ag–TiO_2–Fe, and f) 20%Ag–TiO_2–Fe composite thin films.

after the addition of Fe, which resulted in the disappearance of the bubbles (Figure 3b).

The surface morphology of composite thin films seems to change significantly as a function of Ag content. At 5 wt% Ag–TiO_2–Fe showed a random distribution of particles contained a bright spots of varying sizes of metallic silver distributed upon the smooth surface of TiO_2 (Figure 3c). While at 10 wt% Ag the film had flat morphology with some voids on the surface (Figure 3d). With increasing Ag content from 15 to 20 wt% images showed a uniform distribution of Ag nanoparticles (inset of Figure 3e) with varying sizes (from 70 to 400 nm), and the films structure becomes smoother and more homogeneous (Figure 3f).

3.4. Optical Properties

The optical transmittance spectra of prepared samples in the wavelength range of 300–1100 nm are shown in **Figure 4**. It can be seen that pure TiO_2 film has the highest transparency ≈83.02% in the visible region compared to the other samples.

It is clear that there is a slight decrease ≈76.84% in the transmittance in the infrared region with the presence of Fe. However, the addition of silver decreases the transmittance rapidly and significantly in the Ag–TiO_2–Fe composite thin films in the visible region. The oscillation observed in the transmittance spectra is attributed to the interference effect between air-film and film-substrate interface.[53]

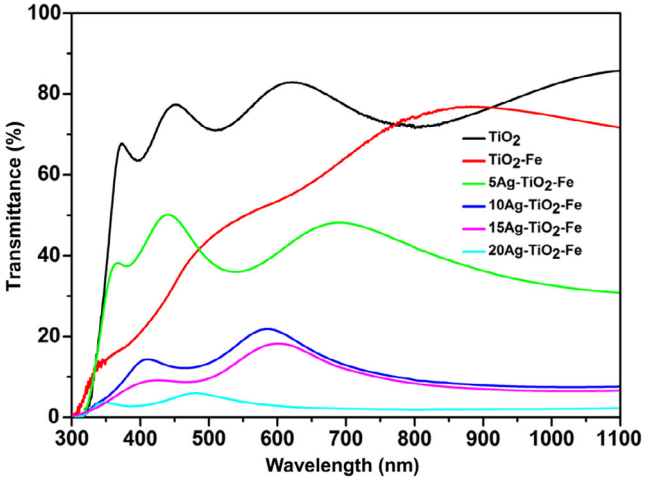

Figure 4. Transmission spectra of pure TiO_2, TiO_2–Fe, and Ag–TiO_2–Fe composite thin films at different Ag contents.

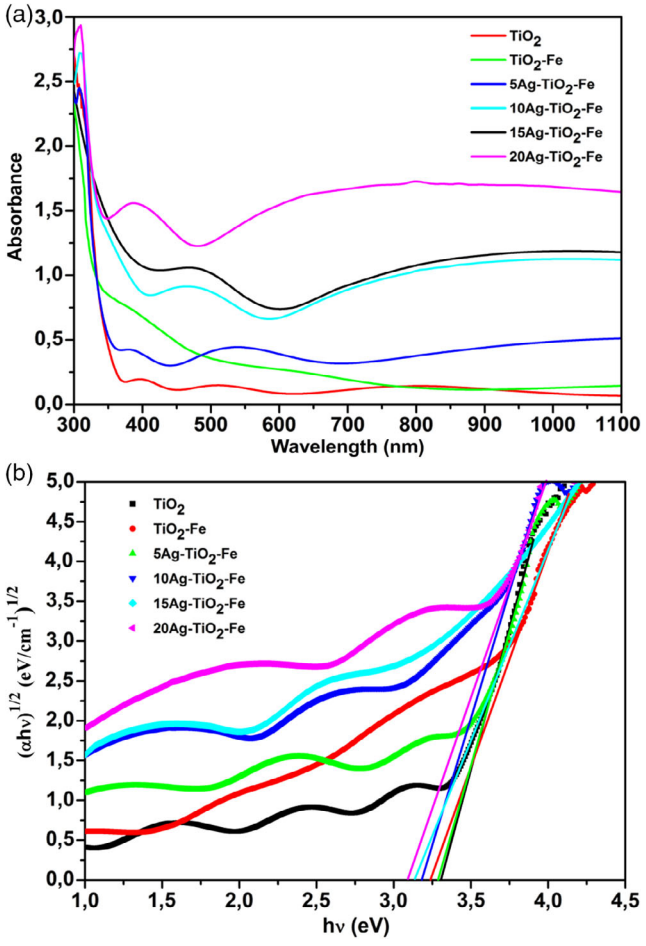

Figure 5. a) UV–vis absorption spectra of pure TiO_2, TiO_2–Fe, and Ag–TiO_2–Fe composite thin films at different Ag contents. b) Plots of $(\alpha h\nu)^{1/2}$ versus $h\nu$ to determine bandgap of each samples.

Figure 5a shows UV–vis absorption spectra of the prepared samples. It can be seen that the absorption edge of prepared

Table 1. Bandgap energy of all samples.

Samples	Bandgap [eV]
TiO_2	3.31
TiO_2–Fe	3.24
5Ag–TiO_2–Fe	3.29
10Ag–TiO_2–Fe	3.18
15Ag–TiO_2–Fe	3.13
20Ag–TiO_2–Fe	3.09

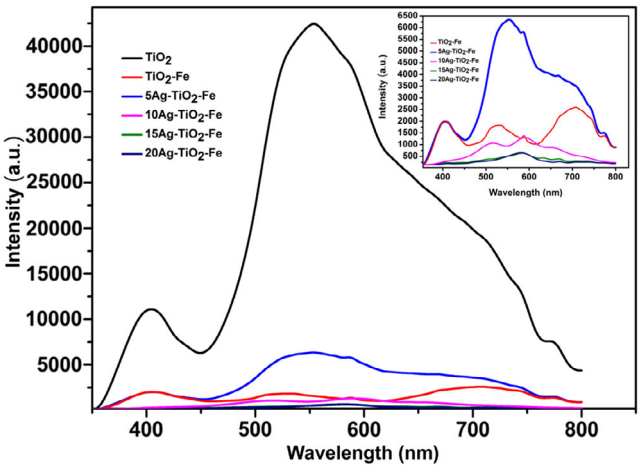

Figure 6. PL spectra of pure TiO_2, TiO_2–Fe, and Ag–TiO_2–Fe composite thin films at different Ag contents.

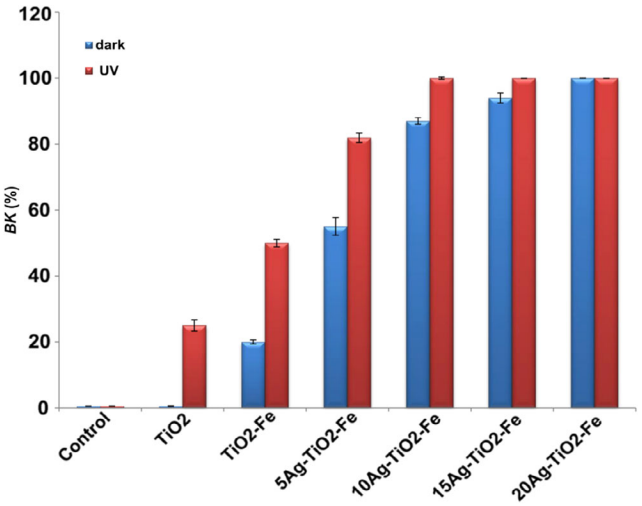

Figure 7. Bacteria killing percentage of pure TiO_2, TiO_2–Fe, and Ag–TiO_2–Fe composite thin films at different Ag contents in dark and under UV irradiation.

TiO_2–Fe and Ag–TiO_2–Fe composite thin films was shifted toward longer wavelengths (redshifted) compared with that of pure TiO_2. The level of redshift increases with higher Ag content, which indicates a reduction in the bandgap energy. The addition

of Fe and Ag metals into TiO_2 matrix enhances the absorption in the visible region.

Additionally, it is clear that 10%, 15%, and 20% Ag–TiO_2–Fe composite films exhibit a broad absorption bands at 467, 474, and 389 nm, respectively, which can be attributed to the surface plasmon absorption (SPA) of Ag nanoparticles.[54,55] The position of SPA band of silver nanoparticles could be influenced by many factors such as size, shape, and surface charge chemistry of particle.[54]

The optical bandgap of all prepared samples can be determined from the Tauc plots using the following Equation (2)[56]

$$\alpha h\nu = A(h\nu - E_g)^{1/2} \quad (2)$$

where $h\nu$ is the photon energy, α is the absorption coefficient, A is the proportionality constant, and E_g is the optical bandgap.

Figure 5b represents the graph of $(\alpha h\nu)^{1/2}$ versus $h\nu$; the bandgap energy values for prepared samples are shown in **Table 1**. It is clear that E_g values reduce with the presence of Fe and Ag. However, when the Ag content was increased to (10, 15, and 20 wt%) in the composite films, the E_g was further decreased. The reduction in optical bandgap by introducing Fe or

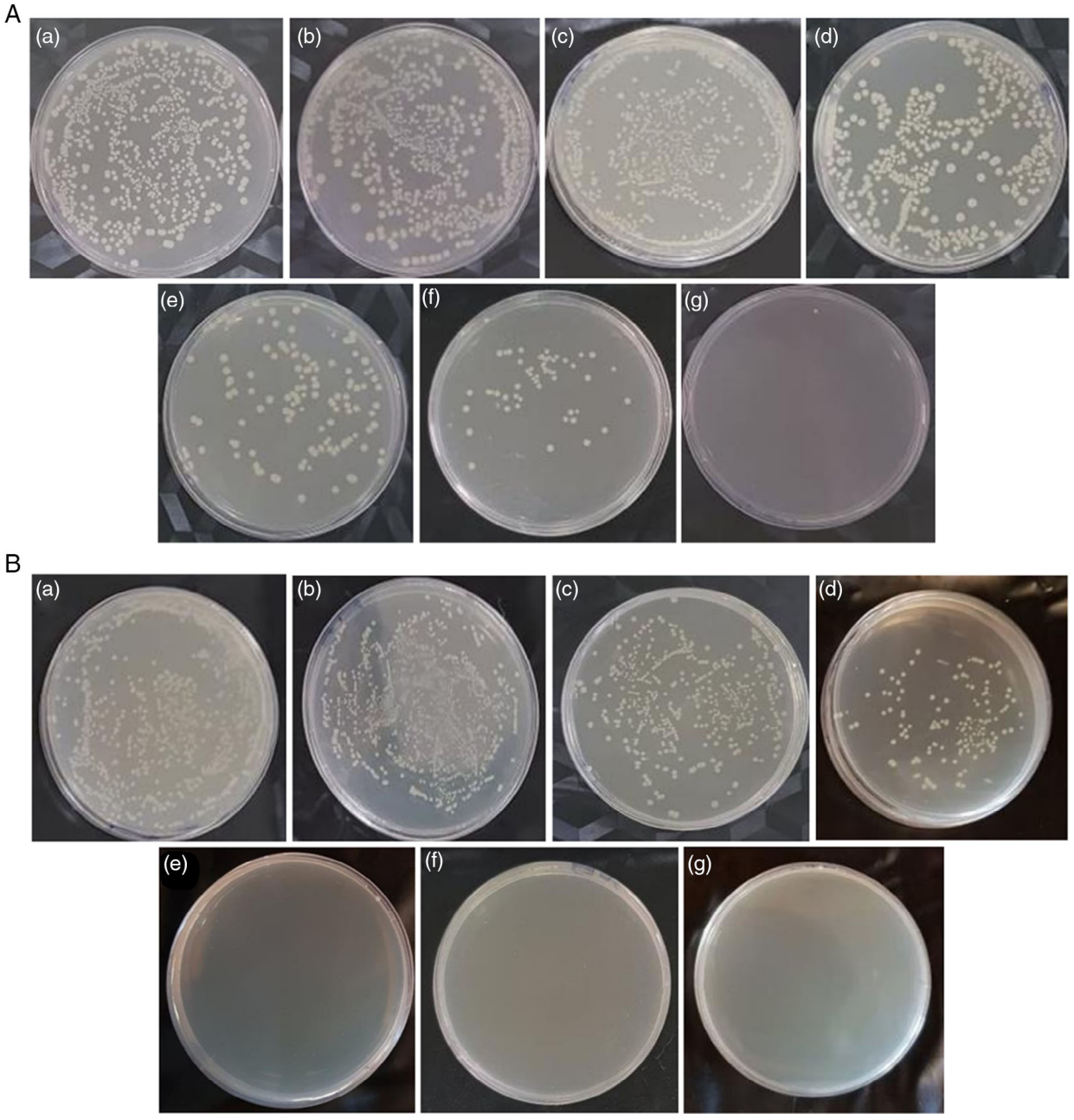

Figure 8. Photographs of the viable *E. coli* colonies after 1 h at 37 °C: A) in the dark, B) under UV irradiation for a) control, b) pure TiO_2, c) TiO_2–Fe, d) 5%Ag–TiO_2–Fe, e) 10%Ag–TiO_2–Fe, f) 15%Ag–TiO_2–Fe, and g) 20%Ag–TiO_2–Fe composite thin films.

Ag metals is reported in other studies.[12,51,57] This decrease in the optical bandgap energies leads to enhance the photocatalytic activity.

Figure 6 shows the PL spectra of TiO_2, TiO_2–Fe, and Ag–TiO_2–Fe films at different Ag content (5, 10, 15, and 20 wt%) in the wavelength range from 350 to 800 nm with excitation wavelength of 325 nm. All the samples have an emission peaks at 404–410 nm, which could be due to free exciton recombination.[58,59] It can also be seen a visible emission peak centered at 516–707 nm, which is usually attributed to the structural defects and oxygen vacancy levels.[59] The pure TiO_2 showed a higher PL intensity, while PL intensity is reduced when Fe and Ag introduced to the TiO_2 matrix. We noted that the PL peaks shift toward higher wavelengths in Ag–TiO_2–Fe composite thin films with higher Ag content and their intensities further decreased. Ag could act as trap to capture photogenerated electrons from TiO_2 conduction band, inhibiting recombination of electron–hole pairs. Therefore, electron–holes separation is promoted,[60,61] resulting in improved photocatalytic efficiency as well as antibacterial properties of the composite thin films.

3.5. Antibacterial Activity

The BK percentage (Equation (1)) of the prepared samples in the dark and under UV irradiation after 1 h interaction is shown in **Figure 7**. The results of dark reactions show that pure TiO_2 thin film has no antibacterial activity. TiO_2–Fe sample showed bacterial reduction of 20%, and the addition of silver in TiO_2–Fe structure led to enhance the antibacterial activity of the films. It is clear that the Ag–TiO_2–Fe composite film with 20 wt% Ag has a high antibacterial effect in the dark with a bacteria killing percentage of 100%, while those of 5, 10, and 15 wt% are 55%, 87%, and 94%, respectively. This indicates that the presence of silver was responsible for the antibacterial effect of the composite films in dark. The bacteria inhibition effect of silver itself has been widely reported.[62,63,26] Under UV light or in dark the control sample did not show any bacterial reduction.

Under UV irradiation, the pure TiO_2 thin film showed low antibacterial activity (25%), which could be due to the amorphous structure of the film. However, the antibacterial activity of TiO_2–Fe film is improved (≈50%) under UV irradiation due to the extremely small size of metallic iron. Fe^0 reacts with oxygen and water, hence producing iron species (especially at the top of the highest peaks of the rough surface which shows local increased reactivity) which participate in the photo-Fenton reaction by generating hydroxyl radicals ($HO^{\bullet}$). As a result, it causes oxidative damage to bacteria cell.[64,65] The Ag–TiO_2–Fe composite thin films showed excellent antibacterial activity under UV irradiation: up to 81% at 5 wt%, and 100% at each of 10, 15, and 20 wt% Ag–TiO_2–Fe samples due to the synergistic antibacterial effects of TiO_2 photocatalytic anatase phase. It is well known that TiO_2 in anatase phase is the most powerful form of TiO_2 to produce ROS under UV light such as superoxide radicals and hydroxyl radicals which damage organisms.[66] Moreover, the presence of Fe and the addition of Ag with different content in the TiO_2 matrix strongly influenced the photocatalytic and antibacterial efficiency of TiO_2 by reducing the e^-–h^+ recombination rate. Indeed, it is due to more effective charge separation between the electrons and holes, hence improving the formation of ROS.[6,13] On the other hand, the strong bactericidal effect of AgNps plays an important role in enhancing the antibacterial performance of composite films. The AgNps antibacterial action remains unclear until now. Previous studies have shown that both Ag nanoparticles and released Ag^+ ions possess antibacterial properties.[9,67] The three most common mechanisms of AgNps toxicity in bacteria suggested by several researchers are as follows.[26,27,62]

First, the AgNps can adhere to the bacterial cell wall and consequently penetrate it. This action will alter the membrane properties, which can lead to damage of the cell membrane and bacteria death. Second, silver nanoparticles and the released Ag^+ inside the bacterial cell may interact with biological components such as proteins, respiratory enzymes, lipids, and DNA; this can result to bacterial dysfunction. Third, high levels of ROS generated by silver nanoparticles and Ag^+, causing to bacteria death.

Figure 8 illustrates the spread plate technique of the test samples A (in the dark) and B (under UV irradiation) employed for the purpose of counting the viable number of *E. coli* colonies.

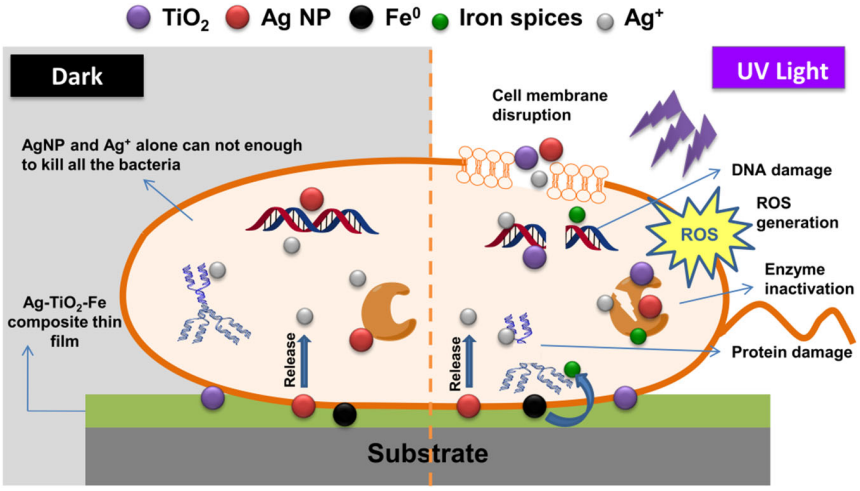

Figure 9. Schematic diagram of the antibacterial killing mechanism of the Ag–TiO_2–Fe composite thin film in the dark and under UV light.

The spread plate results revealed that there was a significant decrease in viable number of bacteria in the case of Ag–TiO_2–Fe composite films compared to pure TiO_2 and TiO_2–Fe films in dark. While it was observed that the antibacterial activity of all samples was improved under UV irradiation, especially the Ag–TiO_2–Fe composite films with high silver content that showed a complete inhibition of bacteria colonies within 1 h. The possible mechanism of antibacterial performance of Ag–TiO_2–Fe composite thin films in dark and under UV light is illustrated in **Figure 9**.

4. Conclusions

In this work, pure TiO_2 and Ag-modified TiO_2–Fe composite thin films have been prepared on glass substrates by thermal evaporation method. An increase in silver content results in a formation of anatase crystalline phase in the Ag–TiO_2–Fe composite films, and the enhancement in Raman intensity was also partly due to the surface plasmon response of Ag NPs. It was found that the addition of Fe and Ag reduces the bandgap and helps to shift the optical absorbance toward the visible region. Antibacterial activity was evaluated by the inactivation of *E. coli* bacteria in the dark and under UV light. Ag–TiO_2–Fe composite films displayed an enhancement in the antibacterial activity depending on the Ag content in dark. However, strong antibacterial efficacy observed under UV irradiation is due to a synergistic action in the ingredients of the Ag–TiO_2–Fe composite films. These coatings are promising candidate as antibacterial materials for medical devices, environmental surfaces disinfection, and water treatment field.

Acknowledgements

The authors are grateful to the University of 20 Août 1955 Skikda for financial support. The authors acknowledge Dr. Bouzrara Moufida and all the staff in laboratory of microbiology at Abderrezak Bouhara Hospital, Skikda. The authors are also thankful to the Complutense University of Madrid and Banco Santander for support via the project UCM-Santander 2019 (PR87/19-22613) and the Spanish Ministry of Science, Innovation and Universities for support via the project MINECO/FEDER-MAT2015-65274-R.

Conflict of Interest

The authors declare no conflict of interest.

Data availability statement

Research data are not shared.

Keywords

antibacterial activity, photocatalytic materials, thermal evaporation, thin films, TiO_2

Received: January 18, 2022
Revised: March 30, 2022
Published online:

[1] T. Vladkova, O. Angelov, D. Stoyanova, D. Gospodinova, L. Gomes, A. Soares, F. Mergulhao, I. Ivanova, *Surf. Coat. Technol.* **2020**, *384*, 125322.
[2] B. Yu, K. M. Leung, Q. Guo, W. M. Lau, J. Yang, *Nanotechnology* **2011**, *22*, 115603.
[3] S. M. H. AL Jawad, A. A. Taha, M. M. Salim, *Optik* **2017**, *142*, 42.
[4] S. Veziroglu, M. Z. Ghori, A. Obermann, K. Röder, O. Polonskyi, T. Strunskus, F. Faupel, O. C. Aktas, *Phys. Status Solidi A* **2019**, *216*, 1800898.
[5] X. Yuan, S. Liang, H. Ke, Q. Wei, Z. Huang, D. Chen, *Vacuum* **2020**, *172*, 109103.
[6] Y. Liu, X. Wang, F. Yang, X. Yang, *Microporous Mesoporous Mater.* **2008**, *114*, 431.
[7] N. Abbas, G. N. Shao, M. S. Haider, S. M. Imran, S. S. Park, S. J. Jeon, H. T. Kim, *Mater. Sci. Eng. C* **2016**, *68*, 780.
[8] J. Mungkalasiri, L. Bedel, F. Emieux, J. Doré, F. N. R. Renaud, C. Sarantopoulos, F. Maury, *Chem. Vap. Deposition* **2010**, *16*, 35.
[9] M. S. Wong, C. W. Chen, C. C. Hsieh, S. C. Hung, D. S. Sun, H. H. Chang, *Sci. Rep.* **2015**, *5*, 11978.
[10] M. Ahamed, M. A. M. Khan, M. J. Akhtar, H. A. Alhadlaq, A. Alshamsan, *Sci. Rep.* **2017**, *7*, 17662.
[11] J. Choi, H. Park, M. R. Hoffmann, *J. Mater. Res.* **2010**, *25*, 149.
[12] U. Arellano, M. Asomoza, F. Ramírez, *J. Photochem. Photobiol. Chem.* **2011**, *222*, 159.
[13] Md. A. Hossain, Md. Elias, D. R. Sarker, Z. R. Diba, J. M. Mithun, M. A. K. Azad, I. A. Siddiquey, M. M. Rahman, J. Uddin, Md. N. Uddin, *Res. Chem. Intermed.* **2018**, *44*, 2667.
[14] V. Diesen, C. W. Dunnill, E. Österberg, I. P. Parkin, M. Jonsson, *Dalton Trans.* **2014**, *43*, 344.
[15] N. E. Méndez, M. Apátiga Castro, A. Manzano Ramírez, E. M. Rivera Muñoz, R. Velázquez Castillo, C. Alberto González, M. A. Zamora Antuñano, *Results Phys.* **2020**, *16*, 102891.
[16] A. Aouina, F. Bensouici, M. Bououdina, R. Tala Ighil, M. Toubane, F. Kezzoula, K. Chebout, *Mater. Res. Express.* **2018**, *6*, 016406.
[17] K. Sunada, T. Watanabe, K. Hashimoto, *Environ. Sci. Technol.* **2003**, *37*, 4785.
[18] F. Bensouici, T. Souier, A. A. Dakhel, A. Iratni, R. Tala Ighil, M. Bououdina, *Superlattices Microstruct.* **2015**, *85*, 255.
[19] M. G. Méndez Medrano, E. Kowalska, A. Lehoux, A. Herissan, B. Ohtani, D. Bahena, V. Briois, C. Colbeau Justin, J. L. Rodríguez López, H. Remita, *J. Phys. Chem. C* **2016**, *120*, 5143.
[20] V. A. Ponomarev, I. V. Sukhorukova, A. N. Sheveyko, E. S. Permyakova, A. M. Manakhov, S. G. Ignatov, N. A. Gloushankova, I. Y. Zhitnyak, O. I. Lebedev, J. Polčak, A. M. Kozmin, D. V. Shtansky, *ACS Appl. Mater. Interfaces* **2018**, *10*, 24406.
[21] X. Hou, H. Ma, F. Liu, J. Deng, Y. Ai, X. Zhao, D. Mao, D. Li, B. Liao, *J. Hazard. Mater.* **2015**, *299*, 59.
[22] X. Wang, X. Hou, W. Luan, D. Li, K. Yao, *Appl. Surf. Sci.* **2012**, *258*, 8241.
[23] T. D. Pham, B. K. Lee, *J. Colloid Interface Sci.* **2014**, *428*, 24.
[24] E. T. Wahyuni, R. Roto, *in Titanium Dioxide - Material for a Sustainable Environment*(Ed.:D. Yang), IntechOpen, London, UK **2018**, p. 331.
[25] J. S. Kim, E. Kuk, K. N. Yu, J. H. Kim, S. J. Park, H. J. Lee, S. H. Kim, Y. K. Park, Y. H. Park, C. Y. Hwang, Y. K. Kim, Y. S. Lee, D. H. Jeong, M. H. Cho, *Nanomed.: Nanotechnol. Biol. Med.* **2007**, *3*, 95.
[26] N. Durán, M. Durán, M. B. de Jesus, A. B. Seabra, W. J. Fávaro, G. Nakazato, *Nanomed.: Nanotechnol. Biol. Med.* **2016**, *12*, 789.
[27] Y. Qing, L. Cheng, R. Li, G. Liu, Y. Zhang, X. Tang, J. Wang, H. Liu, Y. Qin, *Int. J. Nanomed.* **2018**, *13*, 3311.
[28] K. Zawadzka, A. Kisielewska, I. Piwoński, K. Kądzioła, A. Felczak, S. Różalska, N. Wrońska, K. Lisowska, *Bull. Mater. Sci.* **2016**, *39*, 57.

[29] Y. Miao, X. Xu, K. Liu, N. Wang, *Ceram. Int.* **2017**, *43*, 9658.
[30] M. A. Tartanson, L. Soussan, M. Rivallin, S. Pecastaings, C. V. Chis, D. Penaranda, C. Roques, C. Faur, *Appl. Environ. Microbiol.* **2015**, *81*, 7135.
[31] N. Mahmoudi Khatir, Z. Abdul Malek, A. K. Zak, A. Akbari, F. Sabbagh, *J. Sol-Gel Sci. Technol.* **2016**, *78*, 91.
[32] P. Korshed, L. Li, Z. Liu, A. Mironov, T. Wang, *Int. J. Nanomed.* **2017**, *13*, 89.
[33] S. Naghibi, S. Vahed, O. Torabi, A. Jamshidi, M. H. Golabgir, *Appl. Surf. Sci.* **2015**, *327*, 371.
[34] C. C. Trapalis, P. Keivanidis, G. Kordas, M. Zaharescu, M. Crisan, A. Szatvanyi, M. Gartner, *Thin Solid Films* **2003**, *433*, 186.
[35] N. D. S. Mohallem, M. M. Viana, M. A. M. L. de Jesus, G. H. de Magalhães Gomes, L. F. de Sousa Lima, E. D. L. Alves, *in Titanium Dioxide - Material for a Sustainable Environment* (Ed.: D. Yang), IntechOpen, London, UK **2018**, 81.
[36] A. M. Alotaibi, S. Sathasivam, B. A. D. Williamson, A. Kafizas, C. Sotelo Vazquez, A. Taylor, D. O. Scanlon, I. P. Parkin, *Chem. Mater.* **2018**, *30*, 1353.
[37] C. Garlisi, G. Palmisano, *Appl. Surf. Sci.* **2017**, *420*, 83.
[38] T. C. Paul, J. Podder, M. H. Babu, *Surf. Interfaces.* **2020**, *21*, 100725.
[39] A. Fouzia, B. Rabah, *Mater. Sci. Eng., B* **2021**, *265*, 114982.
[40] M. Sreedhar, I. Neelakanta Reddy, Ch. V. Reddy, J. Shim, J. Brijitta, *Mater. Sci. Semicond. Process* **2018**, *85*, 113.
[41] F. Lekoui, R. Amrani, W. Filali, E. Garoudja, L. Sebih, I. E. Bakouk, H. Akkari, S. Hassani, N. Saoula, S. Oussalah, H. Albalawi, N. Alwadai, M. Henini, *Opt. Mater.* **2021**, *118*, 111236.
[42] B. A. Akgun, C. Durucan, N. P. Mellott, *J. Sol-Gel Sci. Technol.* **2011**, *58*, 277.
[43] S. Demirci, T. Dikici, M. Yurddaskal, S. Gultekin, M. Toparli, E. Celik, *Appl. Surf. Sci.* **2016**, *390*, 591.
[44] M. A. Majeed Khan, S. Kumar, M. Naziruddin Khan, M. Ahamed, A. S. Al Dwayyan, *J. Lumin.* **2014**, *155*, 275.
[45] T. Ohsaka, F. Izumi, Y. Fujiki, *J. Raman Spectrosc.* **1978**, *7*, 321.
[46] N. Iwasaki, Y. Sasaki, Y. Nishina, *Surf. Sci.* **1988**, *198*, 524.
[47] G. I. N. Waterhouse, G. A. Bowmaker, J. B. Metson, *Phys. Chem. Chem. Phys.* **2001**, *3*, 3838.
[48] X. D. Wang, R. G. Greenler, *Phys. Rev. B* **1991**, *43*, 6808.
[49] J. Xu, X. Xiao, F. Ren, W. Wu, Z. Dai, G. Cai, S. Zhang, J. Zhou, F. Mei, C. Jiang, *Nanoscale Res. Lett.* **2012**, *7*, 239.
[50] J. M. Walls, J. S. Sagu, K. G. Upul Wijayantha, *RSC Adv.* **2019**, *9*, 6387.
[51] T. Sun, E. Liu, X. Liang, X. Hu, J. Fan, *Appl. Surf. Sci.* **2015**, *347*, 696.
[52] K. Baba, S. Bulou, M. Quesada Gonzalez, S. Bonot, D. Collard, N. D. Boscher, P. Choquet, *ACS Appl. Mater. Interfaces.* **2017**, *9*, 41200.
[53] D. Komaraiah, E. Radha, J. Sivakumar, M. V. Ramana Reddy, R. Sayanna, *Surf. Interfaces.* **2019**, *17*, 100368.
[54] J. Yu, J. Xiong, B. Cheng, S. Liu, *Appl. Catal. B Environ.* **2005**, *60*, 211.
[55] J. Xu, Z. Wang, W. Li, X. Zhang, D. He, X. Xiao, *Nanoscale Res. Lett.* **2017**, *12*, 54.
[56] J. Tauc, *Amorphous and Liquid Semiconductors*, Plenum, London and New york **1974**,1785.
[57] S. Khan, M. ul Haq, Y. Ma, M. Nisar, Y. Li, R. Khan, G. Han, Y. Liu, *J. Sol-Gel Sci. Technol.* **2020**, *93*, 273.
[58] Y. X. Zhang, G. H. Li, Y. X. Jin, Y. Zhang, J. Zhang, L. D. Zhang, *Chem. Phys. Lett.* **2002**, *365*, 300.
[59] J. Dhanalakshmi, S. Iyyapushpam, S. T. Nishanthi, M. Malligavathy, D. Pathinettam Padiyan, *Adv. Nat. Sci.: Nanosci. Nanotechnol.* **2017**, *8*, 015015.
[60] O. Akhavan, E. Ghaderi, *Surf. Coat. Technol.* **2010**, *204*, 3676.
[61] S. P. Lim, A. Pandikumar, H. N. Lim, R. Ramaraj, N. M. Huang, *Sci. Rep.* **2015**, *5*, 11922.
[62] B. Le Ouay, F. Stellacci, *Nano Today* **2015**, *10*, 339.
[63] S. D. Ponja, S. K. Sehmi, E. Allan, A. J. MacRobert, I. P. Parkin, C. J. Carmalt, *ACS Appl. Mater. Interfaces* **2015**, *7*, 28616.
[64] C. Lee, J. Y. Kim, W. I. Lee, K. L. Nelson, J. Yoon, D. L. Sedlak, *Environ. Sci. Technol.* **2008**, *42*, 4927.
[65] Q. Chen, J. Li, Y. Wu, F. Shen, M. Yao, *RSC Adv.* **2013**, *3*, 13835.
[66] U. Joost, K. Juganson, M. Visnapuu, M. Mortimer, A. Kahru, E. Nõmmiste, U. Joost, V. Kisand, A. Ivask, *J. Photochem. Photobiol. B* **2015**, *142*, 178.
[67] I. Sondi, B. Salopek Sondi, *J. Colloid Interface Sci.* **2004**, *275*, 177.

ملخص

تعد تكنولوجيا الطبقات الرقيقة المضادة للبكتيريا ابتكارا متطورا يلعب دورًا مهما في الحد من مخاطر انتقال البكتيريا والعدوى الناتجة عنها, مما يعزز الصحة العامة والسلامة. في هذا السياق , يهدف هذا العمل إلى إنشاء طبقة جديدة مضادة للبكتيريا تعتمد على نظام Ag-TiO_2-Fe. تم تحضير طبقات رقيقة مختلفة من TiO_2 , TiO_2-Fe و Ag-TiO_2-Fe طبقات رقيقة مركبة ذات محتويات مختلفة من الفضة وذلك عن طريق استخدام تقنية التبخر الحراري. لقد تمت دراسة مدى تأثير إضافة الحديد بنسبة كتلية تقدرب 5% وكذا الفضة بنسب مختلفة تتراوح من (5 إلى 20%) على الخصائص الهيكلية, البنيوية ,البصرية والضيائية لطبقة TiO_2 و كيفية تأثيرها على الأداء المضاد للبكتيريا. تم توصيف الأفلام باستخدام تقنيات مختلفة كحيود الأشعة السينية (XRD) ، ومطيافية رامان , المجهر الإلكتروني الماسح (SEM) , مطيافية الأشعة الفوق البنفسجية المرئية والقريبة من الأشعة تحت الحمراء (UV-Visible-NIR), والضيائية الفوتونية (PL). كما تم فحص الفعالية المضادة للبكتيريا للطبقات الرقيقة المحضرة ضد الإشريكية القولونية في الظلام وتحت ضوء الأشعة فوق البنفسجية. أظهرت النتائج أن إضافة الفضة للطبقة الرقيقة TiO_2-Fe يؤدي إلى تكوين الطور البلوري (Anatase). كما أكدت صور الفحص المجهري الإلكتروني وجود الفضة في حالتها المعدنية كجسيمات بأحجام مختلفة تتراوح بين 70 و 400 نانومتر في الطبقات الرقيقة المركبة. لقد وجد أن طاقة الفجوة الالكترونية للطبقات TiO_2-Fe و Ag-TiO_2-Fe بمحتويات مختلفة من الفضة (5-20%) منخفضة مقارنة بطبقة TiO_2 النقية. لاحظنا أيضًا انخفاضًا في كثافات الضيائية الفوتونية (PL) مع إضافة الحديد والفضة إلى مصفوفة TiO_2 , وكان الانخفاض ملحوظًا بشكل كبير في محتويات الفضة الأعلى , مما يشير إلى انخفاض معدل إعادة تركيب زوج ثقب – الإلكترون , وبالتالي تعزيز فصل الشحنات, مما يؤدي إلى تعزيز نشاط الكفاءة المضادة للبكتيريا. أظهرت الاختبارات المضادة لبكتيريا ا*لإشريكية القولونية* أن الفضة حسنت بشكل كبير من الكفاءة المضادة للبكتيريا للطبقات المركبة Ag-TiO_2-Fe في الظلام (بنسب تصل إلى 87% و 94% و 100% لمحتويات الفضة 10% و 15% و 20% على التوالي). تحت ضوء الأشعة فوق البنفسجية, أظهرت الطبقات المركبة Ag-TiO_2-Fe نشاطًا ضوئيا ممتازًا في قتل بكتيريا ا*لإشريكية القولونية* بالمقارنة مع طبقة TiO_2 النقية وطبقة TiO_2-Fe بنسب تصل إلى 81% بالنسبة ل 5% من الفضة, و100% للطبقات الرقيقة المركبة Ag-TiO_2-Fe بنسب 10% و 15% و 20% من محتوى الفضة بسبب التأثير التآزري الناجم عن تعديل TiO_2 بواسطة الفضة والحديد. تشير هذه النتائج إلى فعالية نظام-Ag TiO_2-Fe كطبقة رقيقة مضادة للبكتيريا واعدة للاستخدام في مختلف التطبيقات الطبية والبيئية.

الكلمات الرئيسية: طبقة مضاد للبكتيريا، محفز ضوئي, طريقة التبخر الحراري, TiO_2-Fe طبقة رقيقة , Ag-TiO_2طبقة رقيقة , *الإشريكية القولونية*.

Résumé

La technologie des revêtements antibactériens est une innovation de pointe qui joue un rôle essentiel dans la réduction du risque de transmission et de contamination bactérienne, améliorant ainsi la santé publique et la sécurité. Dans ce contexte, ce travail vise à créer un nouveau revêtement antibactérien basé sur le système Ag-TiO_2-Fe. Divers couches minces de TiO_2, TiO_2-Fe et Ag-TiO_2-Fe des couches composites avec des teneurs en argent variables, ont été préparés par la méthode d'évaporation thermique. L'effet de l'incorporation de Fe avec un pourcentage massique de (5 %) et d'Ag avec différentes teneurs (de 5 à 20 %) sur les propriétés structurales, morphologiques, optiques et luminescentes des couches minces de TiO_2, et comment ils affectent les performances antibactériennes, a été étudié. Les couches ont été caractérisées à l'aide de la diffraction des rayons X (DRX), la spectroscopie Raman, la microscopie électronique à balayage (MEB), la spectroscopie UV-Visible proche infrarouge (UV-Visible-NIR) et de la photoluminescence (PL). L'efficacité antibactérienne des couches préparées contre *Escherichia coli* a été examinée à la fois dans l'obscurité et sous lumière UV. Les résultats montrent que l'ajout d'argent dans TiO_2-Fe conduit à la formation de la phase cristalline d'anatase. Les images MEB ont confirmé la présence d'argent à l'état métallique avec des tailles de particules différentes allant de 70 à 400 nm dans les couches composites. On constate que l'énergie de la bande interdite des couches composites TiO_2-Fe et Ag-TiO_2-Fe avec différentes teneurs en Ag (5-20 %) a diminué par rapport au couche TiO_2 pur, et on a également noté une réduction des intensités de photoluminescence avec l'ajout de Fe et Ag à la matrice de TiO_2, la réduction étant significative à des teneurs en argent plus élevées, ce qui indique un faible taux de recombinaison des paires électron-trou. Par conséquent, la séparation des charges est favorisée, ce qui entraîne une amélioration de l'activité de photokiling. Les tests antibactériens contre *E. coli* ont montré que l'argent améliorait significativement l'efficacité antibactérienne des couches composites Ag-TiO_2-Fe dans l'obscurité (87, 94 et 100 % pour 10, 15 et 20 %, respectivement). Sous lumière UV, les couches composites Ag-TiO_2-Fe ont montré une excellente activité de photokilling d'*E. coli* par rapport aux couches TiO_2 pur et TiO_2-Fe, jusqu'à 81 % pour 5 % d'Ag et 100 % pour 10, 15 et 20 % de couches composites Ag-TiO_2-Fe, en raison de l'effet synergique qui se produit entre TiO_2 modifié par Ag et Fe. Ces résultats indiquent l'efficacité du système Ag-TiO_2-Fe en tant que revêtement antibactérien prometteur pour une utilisation dans les applications médicales et environnementales.

Mots-clés : Revêtement antibactérien, photocatalyseur, évaporation thermique, TiO_2-Fe couche mince, Ag-TiO_2 couche mince, *Escherichia coli.*

Abstract

Antibacterial coating technology is a cutting-edge innovation that plays a vital role in reducing the risk of bacterial transmission and contamination, thereby enhancing public health and safety. In this context, this work aims to create a novel antibacterial coating based on the Ag-TiO_2-Fe system. Various films of TiO_2, TiO_2-Fe, and Ag-TiO_2-Fe composites thin films with varying silver contents were prepared via thermal evaporation method. The effect of the incorporation of Fe (5 wt%) and Ag with different content (from 5 to 20 wt%) on the structural, morphological, optical, and luminescent properties of TiO_2 thin film and how they affect the antibacterial performance was investigated. The films were characterized using X-ray diffraction (XRD), Raman spectroscopy, scanning electron microscopy (SEM), UV–vis–NIR spectroscopy, and photoluminescence (PL). The antibacterial efficiency of the prepared films against *Escherichia coli* is examined both in the dark and under UV light. The results demonstrate that the addition of silver in TiO_2-Fe lead the formation of the anatase crystalline phase. SEM images confirmed the presence of silver in its metallic state with different particles sizes ranging from 70 to 400 nm in the composite films. It is found that the band gap energy of TiO_2-Fe and Ag-TiO_2-Fe composite films with different Ag content (5-20 wt%) decreased compared to pure TiO_2 film, we also noted a reduction in photoluminescence intensities with the addition of Fe and Ag to TiO_2 matrix and the reduction was significant at higher silver content, this indicates a low rate of electron-hole pair recombination, therefore charge separation is promoted, resulting in enhancement in the photokilling activity. Antibacterial tests against *E.coli* showed that silver significantly improved antibacterial efficiency of the Ag-TiO_2-Fe composite films in the dark (87, 94, and 100% for 10, 15, and 20 wt%), respectively. Under UV light, Ag-TiO_2-Fe composite films exhibited excellent photokilling activity of *E.coli* compared to pure TiO_2 and TiO_2-Fe films up to 81% for 5 wt% Ag, and 100% for 10, 15, and 20 wt% Ag-TiO_2-Fe composite films due to the synergistic effect that arises between Ag- and Fe-modified TiO_2. These results indicate the effectiveness of the Ag-TiO_2-Fe system as a promising antibacterial coating for use in medical and environmental applications.

Keywords: Antibacterial coating, photocatalyst, thermal evaporation, TiO_2-Fe film, Ag-TiO_2 film, *Escherichia coli*.